Physics – Uspekhi **54** (8) 799 – 828 (2011)

REVIEWS OF TOPICAL PROBLEMS PACS numbers: **12.39. – x**, **13.40. – f**, 13.60.Le, 13.75.Lb

Light scalar mesons in photon–photon collisions

N N Achasov, G N Shestakov

DOI: 10.3367/UFNe.0181.201108b.0827

Contents

Abstract. Discovered more than forty years ago and from the very start a stumbling block for the naive quark–antiquark model, light scalar mesons are virtually universally believed to be nontrivial in nature today. A major contribution to understanding the nature of light scalar mesons has come from the physics of photon–photon collisions, a field which has recently entered the era of high-precision statistics. In this paper, conclusions from current experimental data concerning the mechanisms of the two-photon creation of light scalar mesons are reviewed.

1. Introduction

Hadron scalar channels in an energy range of up to 1 GeV became a stumbling block in quantum chromodynamics (QCD) because neither perturbation theory nor sum rules work in these channels.[1] At the same time, knowledge of the nature of light scalar mesons $\sigma(600)$, $\kappa(800)$, $a_0(980)$, and $f_0(980)$ [10, 11] is paramount to understanding the mechanism behind chiral symmetry resulting from the confinement, and therefore to understanding the confinement itself.

Searching for light σ- and κ-mesons began away back in the 1960s and preliminary information about them appeared at approximately that time in the reviews of the Particle Data Group (PDG) [12–14]. The theoretical basis of the search for scalar mesons was provided by the linear σ model (LSM) [15–17] that takes into account the spontaneous break of chiral symmetry and considers pseudoscalar mesons as Goldstone bosons. Surprisingly, it turned out that this model can be one of the efficient realizations of QCD at low energies. In the late sixties and early seventies [13, 18, 19], narrow scalar resonances [isovector $a_0(980)$ and isoscalar $f_0(980)$ resonances] were discovered.[2]

As far as σ- and κ-mesons are concerned, numerous unsuccessful attempts to conclusively prove their existence led to general disappointment, and information on these

[1] In this energy range, scalar channels, unlike classical vector channels, contain no solitary resonances, i.e., resonances unaccompanied by a large background inseparable from them. Specifically, in the case of solitary $a_0(980)$ and $f_0(980)$ resonances, the resonance peaks in $\phi \to \gamma a_0(980) \to \gamma\pi\eta$ and $\phi \to \gamma f_0(980) \to \gamma\pi\pi$ decays would be not observed at all because the differential probabilities of these decays in the soft photon region decrease in proportion to the cube of the photon energy by virtue of gauge invariance [1–5] (see Section 2). The key role of the chiral background in the 'fate' of the $\sigma(600)$ resonance was demonstrated in the linear σ model [6–9]. The solitary resonance approximation in the case of light scalar mesons is nothing more than an academic exercise.

[2] In 1977, R L Jaffe described a nonet of light four-quark scalar states in the MIT bag model that phenomenologically incorporates confinement [20]. He also suggested that $a_0(980)$ and $f_0(980)$ might be such states with symbolic quark structures in the form $a_0^+(980) = u\bar{d}s\bar{s}$, $a_0^0(980) = (u\bar{u} - d\bar{d})s\bar{s}/\sqrt{2}$, $a_0^-(980) = d\bar{u}s\bar{s}$, and $f_0(980) = (u\bar{u} + d\bar{d})s\bar{s}/\sqrt{2}$. Since that time, $a_0(980)$ and $f_0(980)$ resonances have become true 'beloved children' of light quark spectroscopy.

N N Achasov, G N Shestakov Sobolev Institute of Mathematics, Siberian Branch of the Russian Academy of Sciences,
prosp. Akad. Koptyuga 4, 630090 Novosibirsk, Russian Federation
E-mail: achasov@math.nsc.ru, shestako@math.nsc.ru

Received 15 September 2010, revised 19 October 2010
Uspekhi Fizicheskikh Nauk **181** (8) 827 – 857 (2011)
DOI: 10.3367/UFNr.0181.201108b.0827
Translated by Yu V Morozov; edited by A Radzig

states disappeared from PDG reviews. One of the principal arguments against σ- and κ-mesons was the fact that the *S*-wave scattering phase shifts, both ππ and Kπ, fail to pass through 90° in expected masses of resonance. Nevertheless, experimental and theoretical investigations of the processes in which the σ- and κ-states could manifest themselves continued.

The situation changed drastically after it had been shown that the *S*-wave amplitude of ππ scattering with isospin $I = 0$ in the linear σ model contains a negative background phase [6] that hides the σ-meson, making it impossible for the ππ scattering phase shift to pass through 90° at an expected mass of the resonance. It became clear that shielding the wide lightest scalar resonances (by the background) is quite natural in chiral dynamics. This idea was picked up and triggered a new wave of theoretical and experimental searches for σ- and κ-mesons (see, for example, Refs [21–28]). As a result, the light σ-resonance and the light κ-resonance have again appeared in PDG reviews (since 1996 and 2004, respectively) [29, 30].

There is now an impressive wealth of data about light scalar mesons [10, 11, 31, 32]. The nontrivial nature of these states is almost universally recognized. In particular, there is much evidence in favor of their four-quark structure, widely discussed in the literature [1, 4, 31–84] (see Sections 2–6 below).

One such piece of evidence is the suppression of production of $a_0(980)$ and $f_0(980)$ resonances in $\gamma\gamma \to \pi^0\eta$ and $\gamma\gamma \to \pi\pi$ reactions, respectively, predicted in 1982 [85, 86] and confirmed in later experiments [10, 11]. There is a close relationship between mechanisms of $\sigma(600)$, $f_0(980)$, and $a_0(980)$ resonances production in $\gamma\gamma$ collisions and their quark structure. That is why investigations into two-photon processes is an important part of light scalar meson physics.

It should be noted that reactions of hadron production in photon–photon collisions are measured in electron–positron colliders; in other words, information about $\gamma\gamma \to$ *hadron* transitions is extracted from the data on $e^+e^- \to (e^+e^-,$ *hadrons*) processes (Fig. 1). The biggest amount of statistics is obtained by the 'nontag' method that detects hadrons, but not scattered electrons. In this case, the main contribution to the cross section of $e^+e^- \to (e^+e^-,$ *hadrons*) process is made by photons with very small virtualities, which yields data on hadron production in collisions between almost real photons. It is by this method that the majority of data on exclusive $\gamma\gamma \to$ *hadron* channels were obtained. Recording scattered electrons (with the loss of some statistics) makes it possible to additionally study the dependence of the hadron production cross section in $\gamma\gamma^*(Q^2)$ collisions on virtuality;[3] here, γ is the real photon, and $\gamma^*(Q^2)$ is the virtual photon with virtuality $Q^2 = (p_1 - p_1')^2$.

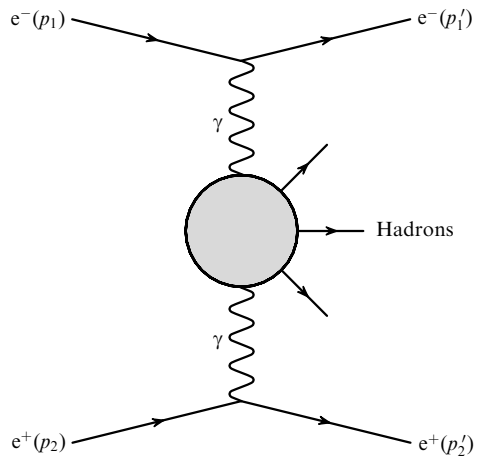

Figure 1. The process of hadron production in photon–photon collisions in electron–positron colliders; p_1, p_1' and p_2, p_2' are the 4-momenta of electrons and positrons.

Recently, a qualitative leap has been made in experimental investigations of $\gamma\gamma \to \pi\pi$ and $\gamma\gamma \to \pi^0\eta$ processes [89–93], which confirmed theoretical predictions based on the four-quark nature of light scalar mesons [85, 86]. The Belle Collaboration published new data on the cross sections of $\gamma\gamma \to \pi^+\pi^-$ [90, 91], $\gamma\gamma \to \pi^0\pi^0$ [92], and $\gamma\gamma \to \pi^0\eta$ [93] reactions the statistics on which are hundreds of times larger than those of all previous experiments. The Belle Collaboration also observed for the first time clear signals of $f_0(980)$ resonance in $\gamma\gamma \to \pi^+\pi^-$ and $\gamma\gamma \to \pi^0\pi^0$ channels. The previous indications of $f_0(980)$ production in $\gamma\gamma$ collisions [94–100] were very uncertain.

The review outline is as follows. In Sections 3–5, we present the results of investigations into the mechanisms of $\gamma\gamma \to \pi^+\pi^-$, $\gamma\gamma \to \pi^0\pi^0$, and $\gamma\gamma \to \pi^0\eta$ reactions based on an analysis of the Belle data [89–93] and our previous research on scalar meson physics in $\gamma\gamma$ collisions [9, 48, 85, 86, 101–110]. We also briefly (sometimes critically) discuss the analyses of other authors.

A combined analysis of the high-statistics Belle data on $\gamma\gamma \to \pi^+\pi^-$ and $\gamma\gamma \to \pi^0\pi^0$ reactions is presented, and the principal dynamic mechanisms of these processes are elucidated in an energy range up to 1.5 GeV. Also, the analysis of the high-statistics Belle data on the $\gamma\gamma \to \pi^0\eta$ cross section is also presented. It is shown that the $\sigma(600) \to \gamma\gamma$, $f_0(980) \to \gamma\gamma$, and $a_0(980) \to \gamma\gamma$ decays of the lightest scalar resonances are largely governed by rescattering mechanisms

$$\sigma \to \pi^+\pi^- \to \gamma\gamma\,,$$

$$f_0(980) \to (K^+K^- + \pi^+\pi^-) \to \gamma\gamma\,,$$

$$a_0(980) \to (K\bar{K} + \pi^0\eta + \pi^0\eta') \to \gamma\gamma\,,$$

i.e., they are four-quark transitions, in contrast to two-photon decays of classical *P*-wave tensor $q\bar{q}$-mesons $a_2(1320)$, $f_2(1270)$, and $f_2'(1525)$ that primarily occur as a consequence of the direct two-quark transition $q\bar{q} \to \gamma\gamma$. Direct coupling constants between $\sigma(600)$, $f_0(980)$, and $a_0(980)$ resonances and the $\gamma\gamma$ system are rather small. The following estimates are obtained for the two-photon widths averaged over resonance mass distributions: $\langle\Gamma_{f_0\to\gamma\gamma}\rangle_{\pi\pi} \approx 0.19$ keV, $\langle\Gamma_{a_0\to\gamma\gamma}\rangle_{\pi\eta} \approx 0.4$ keV, and $\langle\Gamma_{\sigma\to\gamma\gamma}\rangle_{\pi\pi} \approx 0.45$ keV.

Section 7 draws reader's attention to the additional possibilities for studying the properties of $a_0(980)$ and $f_0(980)$ resonances associated with $\gamma\gamma \to K^+K^-$ and $\gamma\gamma \to K^0\bar{K}^0$ reactions, thus far unexplored experimentally, and to the highly promising research on $\sigma(600)$, $f_0(980)$, and $a_0(980)$ resonances in $\gamma\gamma^*(Q^2)$ collisions.

[3] Detailed formulas for experimental studies of $e^+e^- \to (e^+e^-,$ *hadrons*) reactions can be found in the reviews [87, 88].

2. The special place of light scalar mesons in the realm of hadron physics. Evidence of their four-quark structure

Even a cursory examination of PDG reviews suggests the $q^2\bar{q}^2$-structure of the nonet of light scalar mesons $\sigma(600)$, $\kappa(800)$, $a_0(980)$, and $f_0(980)$.[4]

Indeed, this nonet is found to be inverted [49]:

$$\begin{array}{ccccc} a_0^- & & a_0^0/f_0 & & a_0^+ \\ & \{\kappa\} & & \{\kappa\} & \\ & & \sigma & & \end{array}, \qquad (1)$$

with respect to the classical *P*-wave $q\bar{q}$-nonet of tensor mesons $a_2(1320)$, $f_2(1270)$, $K_2^*(1420)$, and $f_2'(1525)$:

$$\begin{array}{ccccc} & & f_2' & & \\ & \{K_2^*\} & & \{K_2^*\} & \\ a_2^- & & a_2^0/f_2 & & a_2^+ \end{array}, \qquad (2)$$

and the classical *S*-wave $q\bar{q}$-nonet of vector mesons $\rho(770)$, $\omega(782)$, $K^*(892)$, and $\phi(1020)$.[5] In the naive quark model, such a scalar nonet cannot be interpreted as a *P*-wave nonet of $q\bar{q}$-mesons, but it can be readily understood as a $q^2\bar{q}^2$-nonet in which $\sigma(600)$ contains no strange quarks, $\kappa(800)$ has the s-quark, and $a_0(980)$ and $f_0(980)$ each have the $s\bar{s}$-pair.

Scalar mesons $f_0(980)$ and $a_0(980)$ discovered about forty years ago became a difficult problem from the very beginning for the naive $q\bar{q}$ model.[6] Indeed, almost exact degeneration of the masses of the isovector, $a_0(980)$, and isoscalar, $f_0(980)$, states seems, on the one hand, to be consistent with the quark structure $a_0^+(980) = u\bar{d}$, $a_0^0(980) = (u\bar{u} - d\bar{d})/\sqrt{2}$, $a_0^-(980) = d\bar{u}$, and $f_0(980) = (u\bar{u} + d\bar{d})/\sqrt{2}$, similar to the structure of vector ρ- and ω-mesons or tensor $a_2(1320)$- and $f_2(1270)$-mesons. On the other hand, however, the strong coupling of $f_0(980)$ with $K\bar{K}$ suggests the presence of a significant $s\bar{s}$-component in the wave function of $f_0(980)$.

In the early 1980s, it was demonstrated in a series of papers [34, 123, 132–136] that the data on $f_0(980)$ and $a_0(980)$ resonances can be interpreted in favor of the $q^2\bar{q}^2$ model, i.e., can be explained assuming the $f_0(980)$ and $a_0(980)$ states exhibit Okubo–Zweig–Iizuka (OZI)-super-allowed coupling to the pairs of pseudoscalar mesons and using for the corresponding coupling constants relations predicted by the $q^2\bar{q}^2$ model. In particular, the authors of the above papers obtained and specified formulas for scalar resonance propagators, taking into account corrections for the finite width in the case of strong coupling with two-particle decay channels. Later on, these formulas were applied to fitting the data of a series of experiments on $f_0(980)$ and $a_0(980)$ resonance production (see, e.g., Refs [90–92, 137–151]). Recently, it has been shown that the aforementioned scalar resonance propagators satisfy the Kaellen–Lehmann representation in the domain of usually used values of coupling constants [152].

In the late 1980s, it was shown that the study of radiative decays $\phi \to \gamma a_0(980) \to \gamma\pi^0\eta$ and $\phi \to \gamma f_0(980) \to \gamma\pi\pi$ can shed light on the problem of $a_0(980)$- and $f_0(980)$-mesons [1]. Over the next ten years preceding the first experiments (1998), the question was considered from different standpoints [153–165].

To date, these decays have been studied not only theoretically but also in experiments with the help of the Spherical Neutral Detector (SND) [137–140] and the Calorimetric Magnetic Detector (CMD-2) [141, 142] at the Institute of Nuclear Physics (Novosibirsk), and the KLOE detector (K LOng experiment) at the Fraskati ϕ-factory (Italy) [143, 144, 146–148, 151, 166–168].

Experimental findings gave impetus to a number of theoretical studies [2–5, 49, 169–172] that yielded evidence in support of the four-quark nature of the $f_0(980)$ and $a_0(980)$ states. Here is clear qualitative proof of this fact. The isovector $a_0(980)$ resonance is produced in the radiative decay of the ϕ-meson as intensely as the isoscalar $\eta'(958)$-meson that is roughly 66% composed of the $s\bar{s}$ contribution responsible for the $\phi \approx s\bar{s} \to \gamma s\bar{s} \to \gamma\eta'(958)$ decay. In the case of the two-quark model, $a_0^0(980) = (u\bar{u} - d\bar{d})/\sqrt{2}$, the $\phi \approx s\bar{s} \to \gamma a_0(980)$ decay would be suppressed in accordance with the OZI rule. It appears that the available experimental data point to the presence of an $s\bar{s}$-pair in the wave function of the isovector $a_0(980)$ state, i.e., suggest its four-quark nature.

When justifying experimental investigations [1], a kaon-loop model $\phi \to K^+K^- \to \gamma a_0(980) \to \gamma\pi^0\eta$ and $\phi \to K^+K^- \to \gamma f_0(980) \to \gamma\pi\pi$ was proposed for radiative decays (Fig. 2). This model, used in data processing, has been validated by experiment [137–144, 146–148, 151, 166–168, 173–175] (Fig. 3). Its main advantage is a new nontrivial threshold phenomenon (Fig. 4). Indeed, experimental mass distributions

$$\frac{\mathrm{dBR}(\phi \to \gamma R \to \gamma ab; m)}{\mathrm{d}m} \sim |g(m)|^2 \omega(m)$$

can be described if the function $|g(m)|^2$ is smooth for $m \leqslant 0.99$ GeV. (Here, m is the invariant mass of the ab-state, $R = a_0(980)$, $f_0(980)$, $ab = \pi^0\eta, \pi^0\pi^0$, and function $g(m)$ describes the vertex of $\phi \to \gamma[a_0(m)/f_0(m)]$ transition.) But gauge invariance requires that $g(m)$ be proportional to

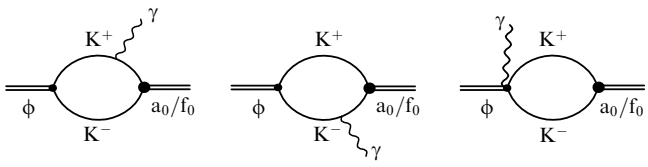

Figure 2. K^+K^--loop mechanism of radiative $\phi(1020) \to \gamma(a_0(980)/f_0(980))$ decays.

[4] To recall, LSM does not contradict the non-$q\bar{q}$-nature of light scalar mesons, because quantum fields may contain different virtual particles in different regions of virtuality.

[5] In diagrams (1) and (2), the mass and the third component of the isotopic spin of the states grow from bottom to top and from left to right, respectively.

[6] Worthy of mention is a series of important experiments performed in the 1970s, in which $f_0(980)$ and $a_0(980)$ resonances were investigated [111–116], as well as a few theoretical analyses of scalar meson properties dating to the same period [20, 117–122]. Reference [122] reports the theoretical discovery of a beautiful threshold phenomenon, $f_0(980)-a_0(980)$ mixing, that breaks isotopic invariance (see also paper [123]). Recently, interest in the $f_0(980)-a_0(980)$ mixing revived, as appears from new suggestions for the search for this phenomenon (see papers [124–127] and references cited therein), along with the first evidence of its manifestation in the $f_1(1285) \to \pi^+\pi^-\pi^0$ decay measured with the VES detector at the Institute of High Energy Physics (Protvino) [128–130], in $J/\psi \to \phi f_0(980) \to \phi a_0(980) \to \phi\eta\pi$ and $\chi_{c1} \to \pi^0 a_0(980) \to \pi^0 f_0(980) \to \pi^+\pi^-\pi^0$ decays studied at BES III (China) [131].

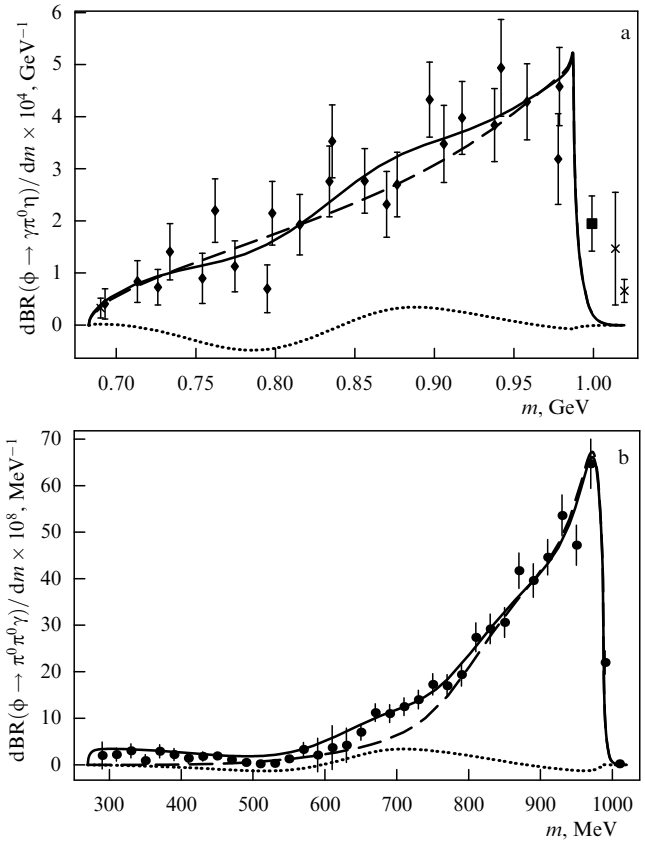

Figure 3. The fit to the KLOE data for the $\pi^0\eta$ and $\pi^0\pi^0$ mass spectra in (a) $\phi \to \gamma\pi^0\eta$ [143] and (b) $\phi \to \gamma\pi^0\pi^0$ [144] decays. (See Refs [169–172] for details.)

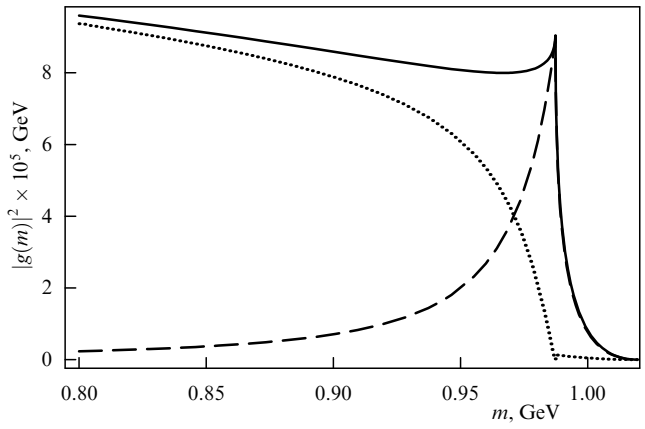

Figure 4. A new threshold phenomenon in the $\phi \to K^+K^- \to \gamma R$ decay. Function $|g(m)|^2 = |g_R(m)/g_{RK^+K^-}|^2$, universal in the K^+K^--loop model, is shown by the solid line. The dashed and dotted lines indicate contributions of the imaginary and real parts of $g(m)$, respectively.

the photon energy $\omega(m)$. The key moment is cessation of $[\omega(m)]^3$ growth in mass distributions at $\omega(990\,\text{MeV}) = 29$ MeV. Figure 4 illustrates how the K^+K^--loop model resolves this problem in an elegant manner [2–5, 39, 49]. In truth, it means that $a_0(980)$ and $f_0(980)$ resonances are seen in radiative decays of the $\phi(1020)$-meson owing to the K^+K^- intermediate state. Thus, the mechanism of $a_0(980)$ and $f_0(980)$ production in radiative $\phi(1020)$ decays is established at least at the physical level of proof.

Both real and imaginary parts of the $\phi \to \gamma R$ transition amplitude are determined by the K^+K^- intermediate state. The imaginary part is due to the real K^+K^- intermediate state, while the real part is due to the virtual compact K^+K^- intermediate state; in other words, we are dealing here with a four-quark transition [4, 5, 39, 40]. Needless to say, radiative four-quark transitions may occur both between two $q\bar{q}$-states and between $q\bar{q}$- and $q^2\bar{q}^2$-states, but their intensities strongly depend on the type of transition. A radiative four-quark transition between two $q\bar{q}$-states requires the creation and annihilation of an additional $q\bar{q}$ pair, i.e., such a transition is forbidden according to the OZI rule, whereas a radiative four-quark transition between the $q\bar{q}$- and $q^2\bar{q}^2$-states requires only the creation of an additional $q\bar{q}$-pair, i.e., it is allowed by the OZI rule. The consideration of this question from the standpoint of large N_c expansion [4, 5] confirms the suppression of radiative four-quark transition between two $q\bar{q}$-states in comparison with the radiative four-quark transition between the $q\bar{q}$ and $q^2\bar{q}^2$ states. Thus, both the intensity and the mechanism of $a_0(980)$ and $f_0(980)$ production in radiative decays of the $\phi(1020)$-meson point to their four-quark nature.

Note also the intriguing absence of $J/\psi \to \gamma f_0(980)$, $J/\psi \to a_0(980)\rho$, and $J/\psi \to f_0(980)\omega$ decays in the presence of rather intensive $J/\psi \to \gamma f_2(1270)$ (or even $J/\psi \to \gamma f_2'(1525)$), $J/\psi \to a_2(1320)\rho$, $J/\psi \to f_2(1270)\omega$ decays involving the corresponding classical *P*-wave tensor $q\bar{q}$-resonances; this testifies to the $q^2\bar{q}^2$-structure of the $a_0(980)$- and $f_0(980)$-states and against their *P*-wave $q\bar{q}$-structure [36–38, 41].

3. Light scalar mesons in view of photon–photon collisions

3.1 The history of investigations

Experimental investigations of light scalar mesons in $\gamma\gamma \to \pi^+\pi^-$, $\gamma\gamma \to \pi^0\pi^0$, and $\gamma\gamma \to \pi^0\eta$ reactions in e^+e^--colliders began in the 1980s and have continued since then. In the first decade, a then-record number of groups (DM1, DM1/2, PLUTO, TASSO, CELLO, JADE, Crystal Ball, MARK II, DELCO, and TPC/2γ) participated in them. Only Crystal Ball and JADE could study both $\pi^0\pi^0$ and $\pi^0\eta$ channels, while all the others (and JADE) confined themselves to the $\pi^+\pi^-$ channel. Those wishing to read more widely on this interesting period in scalar mesons physics are referred to Refs [48, 85, 86, 88, 101, 102, 176–197].

The very first data on $f_0(980)$-resonance production are presented in Tables 1 and 2.

Naturally, the first conclusions had a qualitative character and the data on the $f_0(980) \to \gamma\gamma$ decay width either had large errors or were upper bounds. Note for the reference point that the TASSO and Crystal Ball measurement results (Table 2)

Table 1. First conclusions on the production of $f_0(980)$ in $\gamma\gamma \to \pi\pi$ (see reviews [176–178]).

Experiments	Conclusions
Crystal Ball	No significant $f_0(980)$ signal
CELLO	Hint of $f_0(980)$
JADE	No evidence of $f_0(980)$
TASSO	Good fit to PDG parameters for $f_2(1270)$ includes $f_0(980)$ (3σ-effect)
MARK II	No significant $f_0(980)$ signal

Table 2. Early data on the $f_0(980) \to \gamma\gamma$ decay width (see reviews [88, 176, 177, 179, 180, 184]).

Experiments	$\Gamma_{f_0\to\gamma\gamma}$, keV
TASSO	$(1.3 \pm 0.4 \pm 0.6)/B(f_0 \to \pi^+\pi^-)$
Crystal Ball	$< 0.8/B(f_0 \to \pi\pi)$ (95 % CL)
JADE	< 0.8 (95 % CL)
Kolanoski (1988) [184]	0.27 ± 0.12 (average value)

were based on an integral luminosity of 9.24 and 21 pb^{-1}, respectively.

As for the $a_0(980)$ resonance, it was observed in the $\gamma\gamma \to \pi^0\eta$ reaction only in three experiments. The Crystal Ball group [189], having collected during two years an integrated luminosity of 110 pb^{-1} and selected 336 events relevant to the $\gamma\gamma \to \pi^0\eta$ reaction in the $a_0(980)$ and $a_2(1320)$ resonance regions (Fig. 5), published the following result in 1986:

$$\Gamma_{a_0\to\gamma\gamma}B(a_0 \to \pi^0\eta) = (0.19 \pm 0.07^{+0.10}_{-0.07})\ \text{keV}\,,$$

where $\Gamma_{a_0\to\gamma\gamma}$ is the $a_0(980) \to \gamma\gamma$ decay width, and $B(a_0 \to \pi^0\eta)$ is the relative fraction or probability of the $a_0(980) \to \pi^0\eta$ decay. The measured product $\Gamma_{a_0\to\gamma\gamma}B(a_0 \to \pi^0\eta)$ characterizes the intensity of $a_0(980)$ resonance production in the $\gamma\gamma \to a_0(980) \to \pi^0\eta$ channel. (See Refs [179, 185, 186] for the prehistory of this result). In 1990, the JADE group added the result for $\Gamma_{a_0\to\gamma\gamma}B(a_0 \to \pi^0\eta) = (0.28 \pm 0.04 \pm 0.10)$ keV [96] (see also paper [184]) based on the integrated luminosity of 149 pb^{-1} and 291 events for $\gamma\gamma \to \pi^0\eta$. The Crystal Ball and JADE data on the $a_0(980) \to \gamma\gamma$ decay have aroused great interest (see, for example, Refs [102, 182–184, 187, 192, 195, 196, 198, 199]). Thereafter, the need for statistically more significant data naturally arose. However, no new experiments on the $\gamma\gamma \to \pi^0\eta$ reaction have been undertaken until recently. The mean value of $\Gamma_{a_0\to\gamma\gamma}B(a_0 \to \pi^0\eta) = (0.24^{+0.8}_{-0.7})$ keV deduced from the first two experiments was cited in PDG reviews for 18 consecutive years [10, 196]. Only in 2009 was the third experiment on the $\gamma\gamma \to \pi^0\eta$-reaction [93], with statistics three orders of magnitude more than those of the Crystal Ball and JADE experiments, conducted at the B-factory, KEK, using the Belle detector. These data will be analyzed in more detail in Section 5. Here, only the estimate of

$$\Gamma_{a_0\to\gamma\gamma}B(a_0 \to \pi^0\eta) = (0.128^{+0.003+0.502}_{-0.002-0.043})\ \text{keV}$$

reported by the authors of the experiment [93] is presented along with the average value of

$$\langle\Gamma_{a_0\to\gamma\gamma}B(a_0 \to \pi^0\eta)\rangle = (0.21^{+0.8}_{-0.4})\ \text{keV}$$

taken from the last PDG review [11].

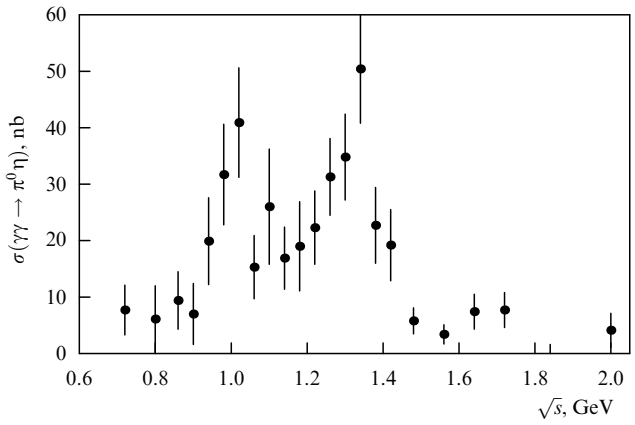

Figure 5. Cross section of the $\gamma\gamma \to \pi^0\eta$ reaction as a function of $\sqrt{s}$ in the $|\cos\theta| \leqslant 0.9$ region; $\sqrt{s}$ is the invariant mass of the $\pi^0\eta$ system, θ is the polar take-off angle of π^0-meson in the $\gamma\gamma$ center-of-mass system. (Crystal Ball data [189].)

The JADE group measured not only the $\gamma\gamma \to \pi^0\eta$ cross section but also the $\gamma\gamma \to \pi^0\pi^0$ cross section [96]; observing (60 ± 8) events in the $f_0(980)$ resonance region [to compare, there were (2177 ± 47) events in the $f_2(1270)$ region], it obtained $\Gamma_{f_0\to\gamma\gamma} = (0.42 \pm 0.06^{+0.08}_{-0.18})$ keV for the $f_0 \to \gamma\gamma$ decay width (which corresponds to $\Gamma_{f_0\to\gamma\gamma} < 0.6$ keV at 95% CL). What is more, similar results for $\Gamma_{f_0\to\gamma\gamma}$ were obtained in 1990 by the MARK II group in an experiment on the $\gamma\gamma \to \pi^+\pi^-$ reaction with an integrated luminosity of 209 pb^{-1} [95], and in 1990–1992 by the Crystal Ball group in experiments on the $\gamma\gamma \to \pi^0\pi^0$ reaction with integrated luminosities of 97 pb^{-1} [94] and 255 pb^{-1} [98, 200]. These data are given in Table 3. Figure 6 illustrates manifestations of $f_0(980)$ and $f_2(1270)$ resonances in the cross sections of $\gamma\gamma \to \pi\pi$ reactions observed by MARK II and Crystal Ball. Although the statistical significance of the $f_0(980)$-signal in the cross sections and invariant $\pi\pi$ mass resolutions left much to be desired, the existence of a 'shoulder' in the region of $f_0(980)$ resonance during $\gamma\gamma$ collisions was beyond question (see Fig. 6).

Table 3. 1990–1992 data on the $f_0(980) \to \gamma\gamma$ decay width (see the text).

Experiments	$\Gamma_{f_0\to\gamma\gamma}$, keV
Crystal Ball (1990)	$0.31 \pm 0.14 \pm 0.09$
MARK II (1990)	$0.29 \pm 0.07 \pm 0.12$
JADE (1990)	$0.42 \pm 0.06^{+0.08}_{-0.18}$
Karch (1991)	0.25 ± 0.10
Bienlein (1992)	$0.20 \pm 0.07 \pm 0.04$
	$\leqslant 0.31$ (90 % CL)

Experiments of the 1980s and early 1990s showed that the two-photon widths of scalar $f_0(980)$ and $a_0(980)$ resonances were smaller than the two-photon widths of tensor $f_2(1270)$ and $a_2(1320)$ resonances for which $\Gamma_{f_2\to\gamma\gamma} \approx 2.6-3$ keV ([94–97] (see also Refs [10, 11]) and $\Gamma_{a_2\to\gamma\gamma} \approx 1$ keV [96, 189] (see also Refs [10, 11]). This fact pointed to the four-quark nature of the $f_0(980)$ and $a_0(980)$ states [94, 96, 182–184, 187, 189, 192, 195, 196, 199, 201, 202].

As mentioned, it was predicted in the early 1980s [85, 86] that, given the four-quark structure of $a_0(980)$- and $f_0(980)$-mesons, the intensity of their production in photon–photon collisions must be suppressed by a factor of ten in comparison with mesons having the two-quark structure. The estimate of

$$\Gamma_{a_0\to\gamma\gamma} \sim \Gamma_{f_0\to\gamma\gamma} \sim 0.27\ \text{keV}\,, \tag{3}$$

obtained in the four-quark model [85, 86], was confirmed in experiment. As regards the $q\bar{q}$ model, it predicted that

$$\frac{\Gamma_{0^{++}\to\gamma\gamma}}{\Gamma_{2^{++}\to\gamma\gamma}} = \frac{15}{4} \times \text{corrections} \approx 1.3-5.5 \tag{4}$$

for the states with $J^{PC} = 0^{++}$ and 2^{++} pertaining to the same P-wave family (see, for example, Refs [36, 94, 102, 187, 192,

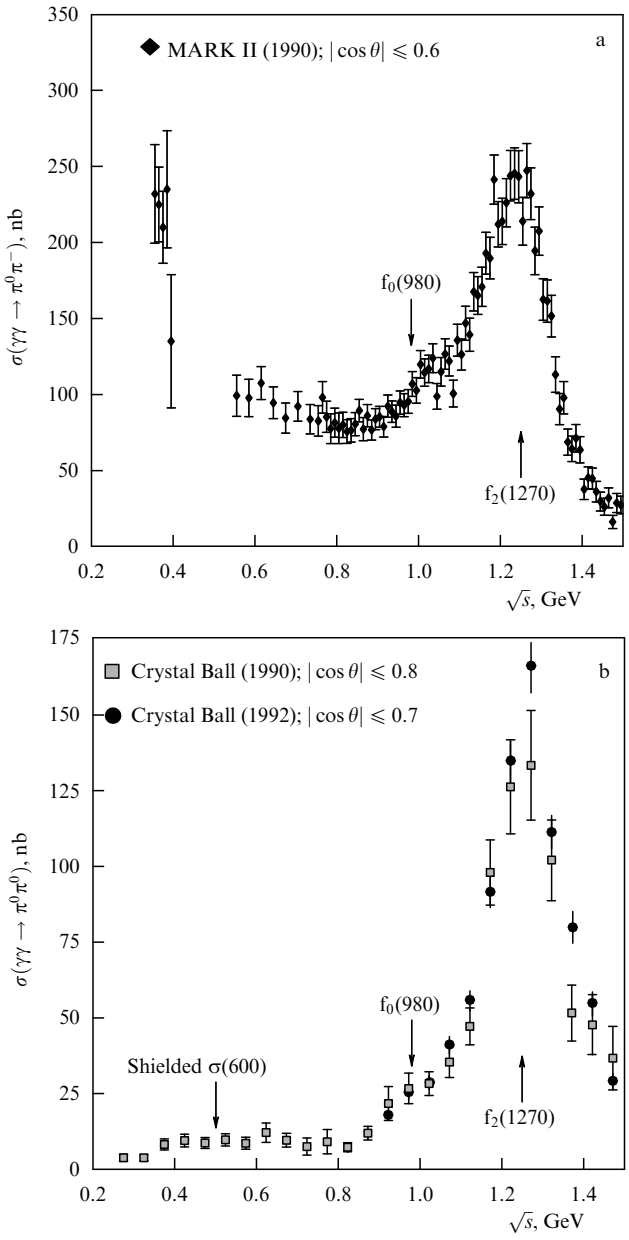

Figure 6. Cross sections of $\gamma\gamma \to \pi^+\pi^-$ (a) and $\gamma\gamma \to \pi^0\pi^0$ (b) as functions of $\sqrt{s}$ ($\pi\pi$ invariant mass). Restrictions on θ (the polar take-off angle of final pions in the $\gamma\gamma$ center-of-mass system) related to the conditions of recording two-photon events are indicated in the figure.

195, 198, 199, 203–211]. Coefficient 15/4 was obtained in a nonrelativistic quark model, according to which

$$\Gamma_{0^{++}\to\gamma\gamma} = \frac{256}{3}\,\frac{\alpha^2|R'(0)|^2}{M^4}\,,$$

$$\Gamma_{2^{++}\to\gamma\gamma} = \frac{1024}{45}\,\frac{\alpha^2|R'(0)|^2}{M^4}\,,$$

where $R'(0)$ is the derivative of the radial wave function of the P-wave state with a mass M at the zero point. $\Gamma_{2^{++}\to\gamma\gamma}$ differs from $\Gamma_{0^{++}\to\gamma\gamma}$ by the product of the square of the Clebsch–Gordan spin–orbit coefficient (1/2) and the quantity $\sin^4\vartheta$ averaged over the solid angle (8/15) (see report [205] for details of the derivation). Hence, $\Gamma_{f_0\to\gamma\gamma} \geqslant 3.4$ keV and $\Gamma_{a_0\to\gamma\gamma} \geqslant 1.3$ keV could be expected.

Let us consider in addition predictions of the molecular model in which $a_0(980)$- and $f_0(980)$-mesons are bound states of the $K\bar{K}$ system [212, 213]. Similar to the $q^2\bar{q}^2$ model, the molecular model explains mass degeneration of the states and their strong coupling with the $K\bar{K}$-channel; moreover, there are no problems with the small values of the $B[J/\psi \to a_0(980)\rho]/B[J/\psi \to a_2(1320)\rho]$ and $B[J/\psi \to f_0(980)\omega]/B[J/\psi \to f_2(1270)\omega]$ ratios (see Refs [36, 38] for details). However, the predictions of this model for two-photon widths [187, 198]

$$\Gamma_{a_0(K\bar{K})\to\gamma\gamma} = \Gamma_{f_0(K\bar{K})\to\gamma\gamma} \approx 0.6 \text{ keV} \qquad (5)$$

are at variance with the experimental data in Table 3 within two standard deviations. Moreover, the hadron widths of $K\bar{K}$ molecules must be smaller (strictly speaking, much smaller) than the binding energy $\epsilon \approx 10$ MeV. But recent data [11] are in conflict with this requirement: $\Gamma_{a_0} \sim (50-100)$ MeV and $\Gamma_{f_0} \sim (40-100)$ MeV. Also, the $K\bar{K}$ model predicts [157, 162] that $B[\phi \to \gamma a_0(980)] \approx B[\phi \to \gamma f_0(980)] \sim 10^{-5}$, which disagrees with experimental findings [11]. Besides, as shown recently [214, 215], the kaon-loop model verified in experiment describes the production of a compact state rather than a loose molecule. Finally, experiments in which $a_0(980)$- and $f_0(980)$-mesons were produced in reactions $\pi^-p \to \pi^0\eta n$ and $\pi^-p \to \pi^0\pi^0 n$ [216–220] within a broad range of the transferred 4-momentum squared, $0 < -t < 1$ GeV^2, showed that these states are compact, e.g., like two-quark mesons ρ, ω, $a_2(1320)$, $f_2(1270)$, etc., rather than loose $K\bar{K}$-state molecules with form factors attributed to wave functions. These experiments leave no chances for the $K\bar{K}$ model.[7] As far as four-quark states are concerned, they are as compact as two-quark ones. (An additional argument against the molecular model for the $a_0(980)$ resonance is put forward in Section 5.)

The Particle Data Group has provided information on the average value of $\Gamma_{f_0\to\gamma\gamma}$ since 1992. Note that no new experimental data on $\Gamma_{f_0\to\gamma\gamma}$ were reported between 1992 and 2006; nevertheless, its average value in PDG reviews evolved substantially during this period. Based on the data in Table 3, the current average $\Gamma_{f_0\to\gamma\gamma}$ value would be (0.26 ± 0.08) keV. In 1992, PDG [196] derived the average value of $\Gamma_{f_0\to\gamma\gamma} = (0.56 \pm 0.11)$ keV by combining the JADE (1990) result [96] (see Table 3) with the value of $\Gamma_{f_0\to\gamma\gamma} = (0.63 \pm 0.14)$ keV found by Morgan and Pennington (1990) [208] from theoretical analysis of the MARK II (1990) [95] and Crystal Ball (1990) [94] data. In 1999, Boglione and Pennington [222] carried out a new theoretical analysis of the situation and halved the desired value: $\Gamma_{f_0\to\gamma\gamma} = (0.28^{+0.09}_{-0.13})$ keV (see also paper [223]). The Particle Data Group noted that the Boglione and Pennington (1999) result replaces that of Morgan and Pennington (1990), but utilized both together with the JADE (1990) data for the calculation of the average $f_0 \to \gamma\gamma$ decay width. In this way, the value of $\Gamma_{f_0\to\gamma\gamma} = (0.39^{+0.10}_{-0.13})$ keV emerged in the PDG (2000) review [224].

In 2003, preliminary unprecedentedly high-statistics Belle data on the $\gamma\gamma \to \pi^+\pi^-$ reaction were reported. They contained a well-apparent signal from the $f_0(980)$ resonance

[7] A $K\bar{K}$ structure of unknown origin with the average relativistic Euclidean momentum squared, $\langle k^2\rangle \approx 2$ GeV^2, has recently been considered in Ref. [221] and called the '$K\bar{K}$ molecule'. Such liberal interpretation of the term molecule can be misleading for those readers who consider molecules to be extended nonrelativistic weakly bound systems.

[89]. In 2005, the first comments on these data appeared in paper [105]. It became clear that $\Gamma_{f_0\to\gamma\gamma}$ cannot be large. In 2006, PDG excluded the Morgan and Pennington (1990) result [$\Gamma_{f_0\to\gamma\gamma} = (0.63 \pm 0.14)$ keV] from its sample and suggested a new value of $\Gamma_{f_0\to\gamma\gamma} = (0.31^{+0.08}_{-0.11})$ keV [225] based only on the JADE (1990) data and the Boglione–Pennington (1999) result. We shall consider in Sections 3.2, 3.4 what happened with the average $\Gamma_{f_0\to\gamma\gamma}$ value afterward and trace its further fate.

3.2 Recent experimental results

In 2007, the Belle Collaboration published data on the cross section of reaction $\gamma\gamma \to \pi^+\pi^-$ in the region of the $\pi^+\pi^-$ invariant mass, $\sqrt{s}$, from 0.8 to 1.5 GeV, based on the integrated luminosity of 85.9 fb^{-1} [90, 91]. These data are presented in Fig. 7. Owing to the huge statistics and high energy resolution in the Belle experiment, a clear signal of the $f_0(980)$ resonance was detected for the first time. Its amplitude proved to be small, which agrees qualitatively with the four-quark model prediction [85, 86]. The visible height of the $f_0(980)$ peak was only 15 nb above a smooth background around 100 nb. Its visible (effective) width proved to be about 30–35 MeV (see Fig. 7).

Then, the Belle Collaboration published the data on the cross section of the $\gamma\gamma \to \pi^0\pi^0$ reaction mainly for the energy interval in the center-of-mass system, $\sqrt{s}$, from 0.6 to 1.6 GeV, based on the integrated luminosity of 95 fb^{-1} [92] (see also Refs [226–228]). Here, the clear signal of the $f_0(980)$ resonance was detected for the first time, too. Note that the background conditions for the manifestation of $f_0(980)$ resonance in the $\gamma\gamma \to \pi^0\pi^0$ channel are more favorable than in $\gamma\gamma \to \pi^+\pi^-$.

Figure 8 illustrates the overall picture of the data on cross sections of $\pi^+\pi^-$ and $\pi^0\pi^0$ production in $\gamma\gamma$ collisions in the $\sqrt{s}$ region from the $\pi\pi$ threshold up to 1.5 GeV after the Belle experiments. It is worth comparing this figure with Fig. 6 illustrating the situation in the preceding period.

Current information about $\Gamma_{f_0\to\gamma\gamma}$ decay widths is presented in Table 4. The Belle Collaboration determined $\Gamma_{f_0\to\gamma\gamma}$ (see Table 4) by fitting mass distributions (Figs 7b and 8b), taking into account the contributions from $f_0(980)$ and $f_2(1270)$ resonances and smooth nonresonant background

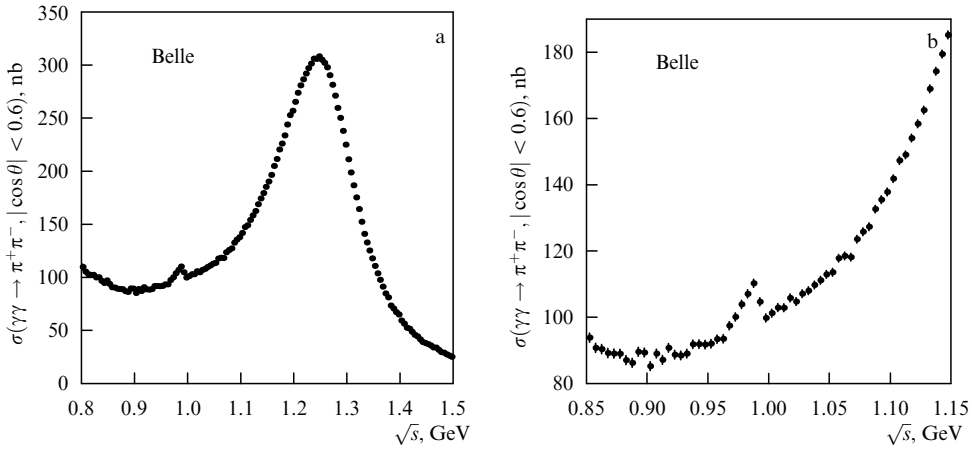

Figure 7. (a) High-statistics Belle data on the $\gamma\gamma \to \pi^+\pi^-$ reaction cross section for $|\cos\theta| \leqslant 0.6$ [91]. Plot (b) depicts the $f_0(980)$ peak region. Only relative values of statistical errors ranging from 0.5% to 1.5% are shown. The step in $\sqrt{s}$ is equal to 5 MeV (experimental invariant mass resolution reaches ≈ 2 MeV).

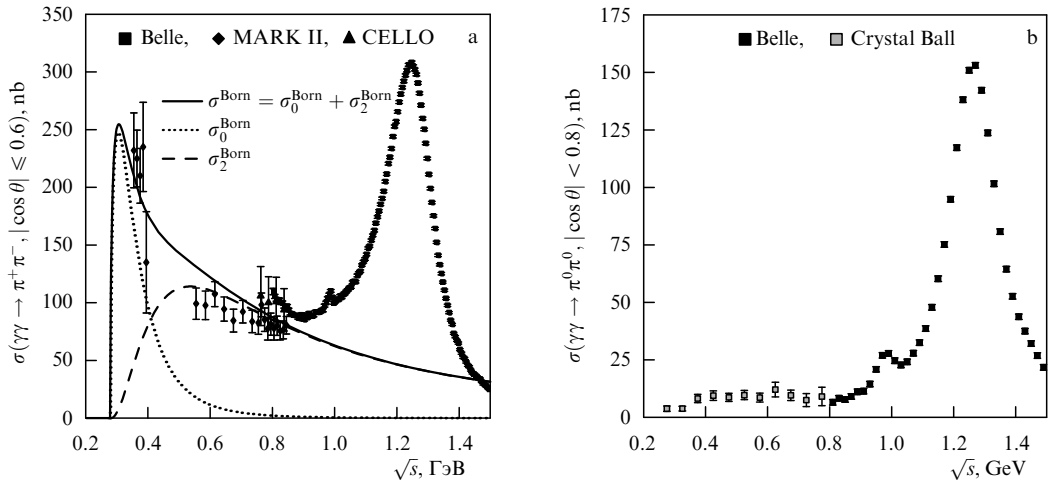

Figure 8. (a) MARK II [94] and CELLO [97] data for $\sqrt{s} \leqslant 0.85$ GeV and Belle [91] data for $0.8 \leqslant \sqrt{s} \leqslant 1.5$ GeV on the $\gamma\gamma \to \pi^+\pi^-$ reaction cross section. (b) Crystal Ball data [95] for $\sqrt{s} < 0.8$ GeV and Belle data [92] for $0.8 \leqslant \sqrt{s} \leqslant 1.5$ GeV on the $\gamma\gamma \to \pi^0\pi^0$ reaction cross section. Plots (a) for $\sqrt{s} > 0.85$ GeV and (b) for $\sqrt{s} > 0.8$ GeV show only the Belle data to better expose the detected weak signals from the $f_0(980)$ resonance. The theoretical curves shown on plot (a) indicate the cross sections of the $\gamma\gamma \to \pi^+\pi^-$ reaction for $|\cos\theta| \leqslant 0.6$ (the total integrated cross section $\sigma^{Born} = \sigma_0^{Born} + \sigma_2^{Born}$ and integrated cross sections σ_λ^{Born} with the helicity $\lambda = 2$ and 0) corresponding to the Born mechanism of the elementary one-pion exchange.

Table 4. Current data on the $f_0(980) \to \gamma\gamma$ decay width.

Experiments	$\Gamma_{f_0\to\gamma\gamma}$, keV
$\gamma\gamma \to \pi^+\pi^-$, Belle (2007) [90]	$0.205^{+0.095+0.147}_{-0.083-0.117}$
$\gamma\gamma \to \pi^0\pi^0$, Belle (2008) [92]	$0.286 \pm 0.017^{+0.211}_{-0.070}$
PDG [10, 11], average value	$0.29^{+0.07}_{-0.06}$

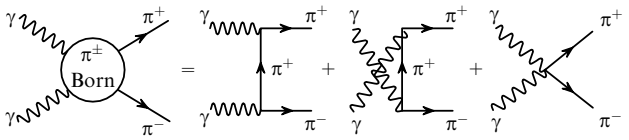

Figure 9. The Born diagrams of the $\gamma\gamma \to \pi^+\pi^-$ process.

contributions that play an important role in the fitting and simultaneously are a source of large model-spawned uncertainties in $\Gamma_{f_0\to\gamma\gamma}$ (see Refs [90–92] for details).

3.3 Dynamics of $\gamma\gamma \to \pi\pi$ reactions: Born contributions and angular distributions

The magnitudes of experimental cross sections can be explained by referring to Fig. 8a which displays as the guiding line the curves corresponding to the purely Born cross section of the $\gamma\gamma \to \pi^+\pi^-$ process, $\sigma^{\rm Born} = \sigma_0^{\rm Born} + \sigma_2^{\rm Born}$, and its constituent cross sections, $\sigma_\lambda^{\rm Born}$, where $\lambda = 2$ and 0 are the absolute values of the difference between initial photon helicities. These cross sections are determined by the elementary charged one-pion exchange mechanism (Fig. 9). By virtue of the Low theorem [8] and chiral symmetry,[9] the Born contributions should dominate in the near-threshold region of the $\gamma\gamma \to \pi^+\pi^-$ reaction. As shown in Fig. 8a, this expectation does not contradict the current data obtained near the threshold, although rather large errors still exist. Moreover, in the entire resonance region including $f_2(1270)$ resonance, the Born contributions can be regarded as a reasonable approximation of background (nonresonance) contributions to the $\gamma\gamma \to \pi^+\pi^-$ amplitudes. Also, the Born electromagnetic contributions provide a basis for the construction of amplitudes including final-state strong interactions [9, 105, 181, 190, 193, 194, 232–239].

The Born contributions have the following features. First, $\sigma^{\rm Born}$ has a maximum at $\sqrt{s} \approx 0.3$ GeV, where $\sigma^{\rm Born} \approx \sigma_0^{\rm Born}$; however, $\sigma_0^{\rm Born}$ quickly falls with increasing $\sqrt{s}$, so that $\sigma^{\rm Born}$ is totally dominated by the $\sigma_2^{\rm Born}$ contribution for $\sqrt{s} > 0.5$ GeV (Fig. 8a). Second, although roughly 80% of $\sigma_2^{\rm Born}$ is determined by the D-wave amplitude, its interference with the contributions from higher partial waves is considerable in the differential cross section $d\sigma^{\rm Born}(\gamma\gamma \to \pi^+\pi^-)/d|\cos\theta|$ (Fig. 10). The interference, being destructive in the first half of the experimentally accessible interval $|\cos\theta| \leqslant 0.6$ and constructive in the second one, flattens out the $|\cos\theta|$ distribution in this interval, so that this effect enhances with increasing $\sqrt{s}$ (see Fig. 10a).

Since the first resonance with $I^G(J^{PC}) = 0^+(4^{++})$ has a mass near 2 GeV [10,11], the contributions from S- and D-waves alone must supposedly dominate for $\sqrt{s} \leqslant 1.5$ GeV, and the differential cross section of the $\gamma\gamma \to \pi^+\pi^-$ process can be represented as [91]

$$\frac{d\sigma(\gamma\gamma \to \pi^+\pi^-)}{d\Omega} = |S + D_0 Y_2^0|^2 + |D_2 Y_2^2|^2, \qquad (6)$$

where S, D_0, and D_2 are S- and D_λ-wave amplitudes with helicity $\lambda = 0$ and 2, and Y_J^m are the usual spherical harmonics.[10] However, the above discussion shows that the smooth background in the $\gamma\gamma \to \pi^+\pi^-$ cross section contains higher partial waves due to the one-pion exchange mechanism, so it can imitate a large S-wave contribution in the $|\cos\theta| \leqslant 0.6$ region.

The one-pion exchange makes no contribution in the $\gamma\gamma \to \pi^0\pi^0$ channel and the representation of the cross section of this reaction in the form similar to Eqn (6) is a

[8] According to the Low theorem [229–231], the Born contributions give the exact physical amplitude of the crossing-reaction $\gamma\pi^\pm \to \gamma\pi^\pm$ near its threshold.

[9] Chiral symmetry guarantees weakness of $\pi\pi$ interaction at low energies.

[10] Equation (6) corresponds to the 'untagged' situation (taking place in all experiments under discussion) in which the dependence on the pion azimuth take-off angle φ is not measured.

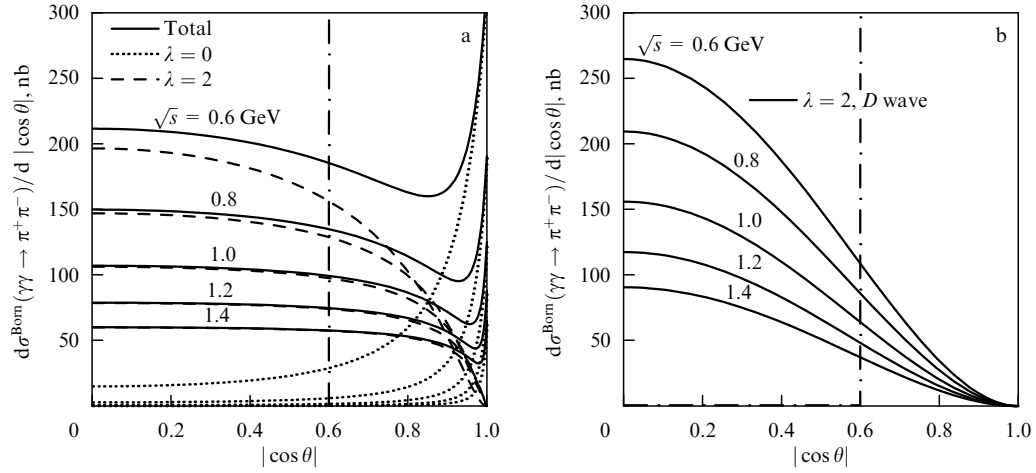

Figure 10. The Born differential cross section of $\gamma\gamma \to \pi^+\pi^-$ and its components for different $\sqrt{s}$ values. The vertical straight lines $|\cos\theta| = 0.6$ show the upper boundary of the region accessible for measurements.

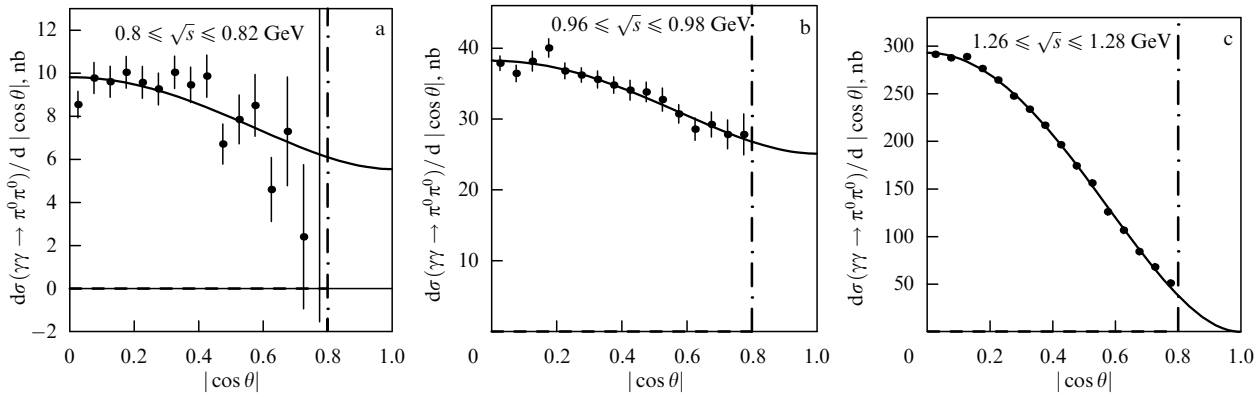

Figure 11. Belle data on the angular distributions for $\gamma\gamma \to \pi^0\pi^0$ events [92]. The solid lines exhibit their approximations. The vertical straight lines $|\cos\theta| = 0.8$ show the upper boundary of the region accessible for measurements.

good approximation for $\sqrt{s} \leqslant 1.5$ GeV:

$$\frac{\mathrm{d}\sigma(\gamma\gamma \to \pi^0\pi^0)}{\mathrm{d}\Omega} = |\tilde{S} + \tilde{D}_0 Y_2^0|^2 + |\tilde{D}_2 Y_2^2|^2 , \qquad (7)$$

where $\tilde{S}$, $\tilde{D}_0$, and $\tilde{D}_2$ are the corresponding S- and D_λ-wave amplitudes with helicities $\lambda = 0$ and 2. However, the partial wave analysis of $\gamma\gamma \to \pi^0\pi^0$ events based on Eqn (7) encounters difficulties because the existing relation $\sqrt{6}\,|Y_2^2| = \sqrt{5}\,Y_0^0 - Y_2^0$ between spherical harmonics does not permit separating the partial waves using the data on differential cross section alone [91, 92, 96]. With this relation, it is always possible to represent the contribution of the amplitude with helicity 2 as a combination of contributions of the amplitudes with helicity 0. Therefore, additional assumptions are needed for their separation, such as the assumption of the predominance of $f_2(1270)$-resonance production in a wave with $\lambda = 2$ [209, 240–242]. The observed angular distributions are in excellent agreement with this expectation, which usually serves as a guide to their proper interpretation.

Formally, the $\mathrm{d}\sigma(\gamma\gamma \to \pi^0\pi^0)/\mathrm{d}\Omega$ cross section in formula (7) is a polynomial of the second power in $z = \cos^2\theta$ that can be expressed in terms of its roots z_1 and z_1^*:[11]

$$\frac{\mathrm{d}\sigma(\gamma\gamma \to \pi^0\pi^0)}{\mathrm{d}\Omega} = C(z - z_1)(z - z_1^*) , \qquad (8)$$

where C is the real constant. Thus, only three independent parameters, viz. C, $\mathrm{Re}\,z_1$, and $\mathrm{Im}\,z_1$ (up to the sign), can be found from fitting experimental data on the differential cross section, rather than four — $|\tilde{S}|$, $|\tilde{D}_0|$, $|\tilde{D}_2|$, and $\cos\delta$ — as one would like (here, δ is the relative phase of $\tilde{S}$ and $\tilde{D}_0$ amplitudes).

Figure 11 depicts the Belle data on the angular distributions in $\gamma\gamma \to \pi^0\pi^0$ events at three $\sqrt{s}$ values. All of them are fairly well described by the simple two-parameter expression $|a|^2 + |b\,Y_2^2|^2$ [107]. Therefore, it can be assumed that the cross section of $\gamma\gamma \to \pi^0\pi^0$ for $\sqrt{s} < 1.5$ GeV is saturated with contributions only from the partial $\tilde{S}$- and $\tilde{D}_2$-waves.

3.4 Mechanisms for the production of scalar resonances

The anticipation of new Belle data and their advent have given rise to a series of theoretical papers studying the dynamics of $f_0(980)$, $\sigma(600)$, and $a_0(980)$ resonance production in the $\gamma\gamma \to \pi\pi$ and $\gamma\gamma \to \pi^0\eta$ processes by various methods and discussing the nature of these states [9, 45, 46, 65, 73, 77, 78, 105–109, 211, 239, 246–258].

The main physically meaningful contention that can be made from the analysis of the production mechanisms of light scalars in $\gamma\gamma$ collisions is as follows [45].

The classical P-wave tensor $q\bar{q}$-mesons $f_2(1270)$, $a_2(1320)$, and $f_2'(1525)$ are produced in $\gamma\gamma$ collisions largely due to direct $\gamma\gamma \to q\bar{q}$ transitions, whereas light scalar $\sigma(600)$-, $f_0(980)$-, and $a_0(980)$-mesons are mainly produced by rescatterings $\gamma\gamma \to \pi^+\pi^- \to \sigma$, $\gamma\gamma \to K^+K^- \to f_0$, $\gamma\gamma \to (K^+K^-, \pi^0\eta) \to a_0$, etc., i.e., due to four-quark transitions. The direct $\gamma\gamma \to \sigma$, $\gamma\gamma \to f_0$, and $\gamma\gamma \to a_0$ transitions are strongly suppressed, in agreement with the four-quark model.

This contention introduces a new seminal view of $\gamma\gamma \to \pi\pi$ and $\gamma\gamma \to \pi^0\eta$ reaction dynamics at low energies. Let us consider it in more detail.

To begin with, here are a few elementary facts about interactions of C-even mesons with photons based on the quark model [11, 88, 183, 184]. Coupling of the $\gamma\gamma$ system with classical $q\bar{q}$-states, including the lightest pseudoscalar ($J^{PC} = 0^{-+}$) and tensor (2^{++}) mesons, is proportional to the fourth power of the charges of constituent quarks.

As it is, only the probability of a π^0-meson production in $\gamma\gamma$ collisions (or the $\pi^0 \to \gamma\gamma$ decay width) is purely evaluated from the first principles [259–262]. $\Gamma_{\pi^0\to\gamma\gamma}$ is determined completely by the Adler–Bell–Jackiw axial anomaly, and in this case the theory (QCD) is in excellent agreement with the experiment [263, 264]. The relations between the widths of $\pi^0 \to \gamma\gamma$, $\eta \to \gamma\gamma$, and $\eta' \to \gamma\gamma$ decays are obtained in the $q\bar{q}$-model, taking into account the mixing and SU(3) symmetry breaking effects [183, 262, 265].

As far as tensor mesons are concerned, in the case of ideal mixing [i.e., when $f_2 = (u\bar{u} + d\bar{d})/\sqrt{2}$ and $f_2' = s\bar{s}$], the quark model predicts the following ratios for the coupling constant squared:

$$g^2_{f_2\gamma\gamma} : g^2_{a_2\gamma\gamma} : g^2_{f_2'\gamma\gamma} = 25:9:2 . \qquad (9)$$

Although absolute values of two-photon widths of light tensor meson decays cannot be obtained from the first principles [88, 183, 192, 203, 206, 266–268] as in the case of pseudoscalars, the prediction (9) of the $q\bar{q}$ model underlies the relations actually used between the widths of $f_2(1270) \to \gamma\gamma$, $a_2(1320) \to \gamma\gamma$, and $f_2'(1525) \to \gamma\gamma$ decays that take account of the deviations from the ideal mixing and SU(3) symmetry breaking effects [11, 88, 183, 191, 269,

[11] Such a procedure is known to form the basis of the method for finding all possible solutions in partial wave analysis (see Refs [120, 218–220, 243–245]).

270]. Roughly speaking, the situation for light tensor mesons generally agrees with the prediction of the $q\bar{q}$ model (9). This implies that the contributions to $g^2_{f_2\gamma\gamma}$, $g^2_{a_2\gamma\gamma}$, and $g^2_{f_2'\gamma\gamma}$ taking account of the finiteness of the widths of $f_2(1270)$, $a_2(1320)$, and $f_2'(1525)$ resonance decays [i.e., contributions from $f_2(1270) \to \pi^+\pi^- \to \gamma\gamma$ type rescatterings, and so forth] are small compared with the contributions of direct annihilation $q\bar{q}(2^{++}) \to \gamma\gamma$ transitions.

The observed smallness of the two-photon widths of scalar $a_0(980)$- and $f_0(980)$-mesons in comparison with those of tensor mesons (and the resulting failure of the $q\bar{q}$ model prediction of relation (4) between the widths of direct 0^{++} and $2^{++} \to \gamma\gamma$ transitions) indicates that $a_0(980)$ and $f_0(980)$ resonances are not the quark and antiquark bound states. Once the $q\bar{q}$ component is absent in the wave functions of light scalars, and their $q^2\bar{q}^2$ component contains practically no white neutral vector mesons (as in the MIT-bag model [85, 86]), the $\sigma(600) \to \gamma\gamma$, $f_0(980) \to \gamma\gamma$, and $a_0(980) \to \gamma\gamma$ decays must be four-quark transitions caused by mechanisms of $\sigma(600) \to \pi^+\pi^- \to \gamma\gamma$, $f_0(980) \to K^+K^- \to \gamma\gamma$, and $a_0(980) \to (K^+K^-, \pi^0\eta) \to \gamma\gamma$ rescatterings. Such a scenario was for the first time hypothesized as early as 1988 based on an analysis of the Crystal Ball data [189] on the $a_0(980)$-resonance production in the $\gamma\gamma \to \pi^0\eta$ reaction [102] (see also the discussion of the mechanisms of $\gamma\gamma \to K\bar{K}$ reactions [103, 104]). Fifteen years later, when the preliminary high-statistics Belle data on $f_0(980)$ resonance in the $\gamma\gamma \to \pi^+\pi^-$ reaction were reported [89], we undertook a study on the role of rescattering mechanisms [specifically, the $\gamma\gamma \to K^+K^- \to f_0(980) \to \pi^+\pi^-$ mechanism] in the $f_0(980)$ production. As a result, we showed that it is this mechanism that plays very important, unless dominating, role and accounts for a natural and reasonable scale of $f_0(980)$ resonance manifestations in $\gamma\gamma \to \pi^+\pi^-$ and $\gamma\gamma \to \pi^0\pi^0$ cross sections [105].

Then, it was shown in the framework of the $SU(2)_L \times SU(2)_R$ for a linear σ model that the σ field is described by its four-quark component [at least in the energy (virtuality) range of σ-resonance] and that the $\sigma(600)$-meson decay in $\gamma\gamma$ collisions is the four-quark transition: $\sigma(600) \to \pi^+\pi^- \to \gamma\gamma$ [9]. It was emphasized that the σ-meson contribution to the $\gamma\gamma \to \pi\pi$ amplitudes is shielded due to its strong destructive interference with the background contributions[12] as in the $\pi\pi \to \pi\pi$ amplitudes. In other words, production of σ-mesons by rescattering in $\gamma\gamma$ collisions is always accompanied by a great chiral background: $\gamma\gamma \to \pi^+\pi^- \to (\sigma + \textit{background}) \to \pi\pi$. As a result, the $\gamma\gamma \to \pi^0\pi^0$ cross section in the σ-resonance region proves to be small and ranges (5–10) nb (see Fig. 8b and Section 4 for details).

The above considerations concerning the dynamics of $\sigma(600)$-, $f_0(980)$-, and $f_2(1270)$-resonance production were further developed in the combined analysis of final high-statistics Belle data on $\gamma\gamma \to \pi^+\pi^-$ and $\gamma\gamma \to \pi^0\pi^0$ reactions [106, 107] discussed in the next section.

4. Analysis of high-statistics Belle data on $\gamma\gamma \to \pi^+\pi^-$ and $\gamma\gamma \to \pi^0\pi^0$ reactions. Manifestations of $\sigma(600)$ and $f_0(980)$ resonances

In the region of interest with $\sqrt{s} < 1.5$ GeV, the partial S- and D_2 wave contributions dominate in the Born cross sections σ_0^{Born} and σ_2^{Born} for $\gamma\gamma \to \pi^+\pi^-$, respectively. Because the $\pi\pi$ interaction for $\sqrt{s} < 1.5$ GeV is strong only in S- and D-waves, it is these Born contributions to $\gamma\gamma \to \pi^+\pi^-$ processes that are essentially modified by the strong final-state interaction.[13] In addition, the contribution of inelastic $\gamma\gamma \to K^+K^- \to \pi\pi$ rescattering plays an important role in $\gamma\gamma \to \pi\pi$ processes, at least in the $f_0(980)$-resonance region (this fact was noticed for the first time in papers [85, 86]).

Thus, we shall use the model for helicity (M_λ) and partial ($M_{\lambda J}$) amplitudes of the $\gamma\gamma \to \pi\pi$ scattering taking account of Born electromagnetic contributions corresponding to charged π- and K-exchanges modified in S- and D_2-waves by strong final-state interactions, and contributions from direct resonance–photon interactions (see also Refs [9, 102–107, 164, 181, 247, 249, 253]):

$$M_0(\gamma\gamma \to \pi^+\pi^-; s, \theta) = M_0^{\text{Born}\,\pi^+}(s, \theta) + \\ + \tilde{I}^{\pi^+}_{\pi^+\pi^-}(s)\, T_{\pi^+\pi^- \to \pi^+\pi^-}(s) \\ + \tilde{I}^{K^+}_{K^+K^-}(s)\, T_{K^+K^- \to \pi^+\pi^-}(s) + M_{\text{res}}^{\text{direct}}(s)\,, \tag{10}$$

$$M_2(\gamma\gamma \to \pi^+\pi^-; s, \theta) = M_2^{\text{Born}\,\pi^+}(s, \theta) \\ + 80\pi d^2_{20}(\theta) M_{\gamma\gamma \to f_2(1270) \to \pi^+\pi^-}(s)\,, \tag{11}$$

$$M_0(\gamma\gamma \to \pi^0\pi^0; s, \theta) = M_{00}(\gamma\gamma \to \pi^0\pi^0; s) \\ = \tilde{I}^{\pi^+}_{\pi^+\pi^-}(s)\, T_{\pi^+\pi^- \to \pi^0\pi^0}(s) \\ + \tilde{I}^{K^+}_{K^+K^-}(s)\, T_{K^+K^- \to \pi^0\pi^0}(s) + M_{\text{res}}^{\text{direct}}(s)\,, \tag{12}$$

$$M_2(\gamma\gamma \to \pi^0\pi^0; s, \theta) = 5 d^2_{20}(\theta) M_{22}(\gamma\gamma \to \pi^0\pi^0; s) \\ = 80\pi d^2_{20}(\theta) M_{\gamma\gamma \to f_2(1270) \to \pi^0\pi^0}(s)\,, \tag{13}$$

where $d^2_{20}(\theta) = (\sqrt{6}/4)\sin^2\theta$. Figures 9, 12–14 are diagrammatic representations of these amplitudes. The first terms on the right-hand sides of Eqns (10) and (11) are the Born helicity amplitudes of the $\gamma\gamma \to \pi^+\pi^-$ scattering corresponding to the elementary one-pion exchange mechanism (see Fig. 9). Their explicit forms are presented in Appendix A.1. The terms in Eqns (10) and (12) containing the S-wave amplitudes of

[12] As mentioned in the Introduction, the large background shielding the σ-resonance in $\pi\pi \to \pi\pi$ events is a consequence of chiral symmetry.

[13] It is reliably established in experiment that S- and D-wave contributions dominate in the $\pi\pi$ scattering cross sections in the channels with isospin $I = 0$ and 2 for $\sqrt{s} < 1.5$ GeV (see, for example, Refs [112, 113, 115, 120, 217, 218, 220, 270, 271]). The partial amplitudes $T^I_J(s) = \{\eta^I_J(s)\exp[2i\delta^I_J(s)] - 1\}/[2i\rho_{\pi^+}(s)]$ of $\pi\pi$ scattering with $J = 0$, 2 and $I = 0$ [here, $\delta^I_J(s)$ and $\eta^I_J(s)$ are the phase and inelasticity of the J-wave $\pi\pi$ scattering in the channel with isospin I, and $\rho_{\pi^+}(s) = (1 - 4m^2_{\pi^+}/s)^{1/2}$] reach their unitarity limits at certain $\sqrt{s}$ values in the region of interest and demonstrate both smooth energy dependence and sharp resonance oscillations. The $T^0_2(s)$ amplitude is dominated by the $f_2(1270)$ resonance contribution, while the $T^0_0(s)$ amplitude contains $\sigma(600)$- and $f_0(980)$-resonance contributions. In the $\pi\pi$-threshold region, the $\sigma(600)$-resonance contribution is strongly compensated for by the chiral background, which ensures the observed smallness of the $\pi\pi$ scattering length a^0_0 and the presence of Adler zero in $T^0_0(s)$ at $s \approx m^2_\pi/2$ [6, 9, 171, 172]. $|T^0_0(s)|$ reaches the unitary limit in the energy region from 0.85 to 0.9 GeV and exhibits a narrow, deep (practically down to zero) dip caused by the destructive interference of the $f_0(980)$-resonance contribution with a large smooth background. Also, it is established that $\pi\pi$ scattering in the $I = 0$ channel is elastic in a very good approximation up to the $K\bar{K}$-channel threshold. However, inelasticity $\eta^0_0(s)$ shows a sharp jump just above the $K\bar{K}$ threshold due to the production of $f_0(980)$ resonance strongly coupled with the $K\bar{K}$ channel.

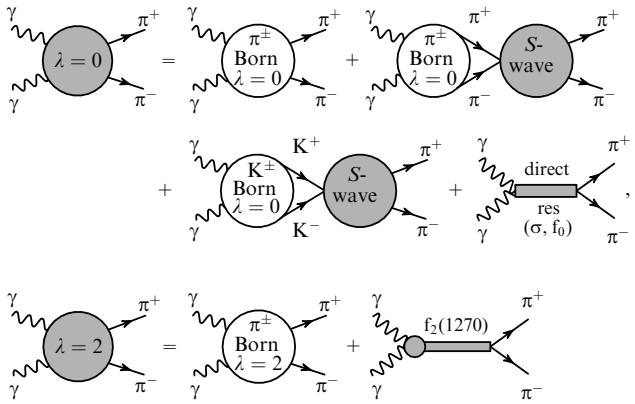

Figure 12. Diagrams corresponding to helicity amplitudes (10) and (11) for the $\gamma\gamma \to \pi^+\pi^-$ reaction.

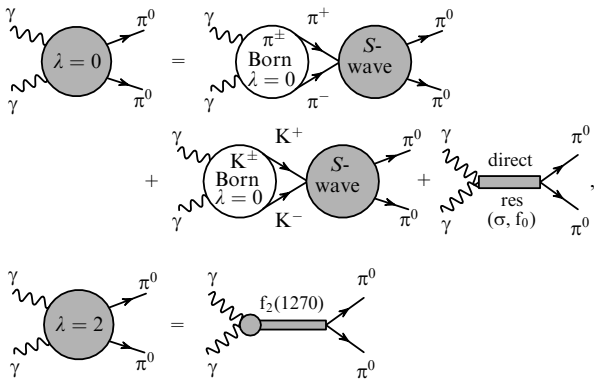

Figure 13. Diagrams corresponding to helicity amplitudes (12) and (13) for the $\gamma\gamma \to \pi^0\pi^0$ reaction.

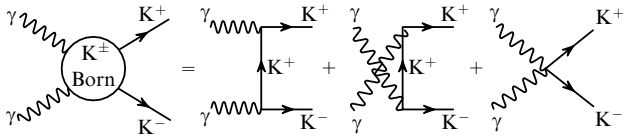

Figure 14. The Born diagrams of the $\gamma\gamma \to K^+K^-$ process.

hadron reactions, viz.

$$T_{\pi^+\pi^-\to\pi^+\pi^-}(s) = \frac{2T_0^0(s) + T_0^2(s)}{3}\,,$$

$$T_{\pi^+\pi^-\to\pi^0\pi^0}(s) = \frac{2\left[T_0^0(s) - T_0^2(s)\right]}{3}\,,$$

$$T_{K^+K^-\to\pi^+\pi^-}(s) = T_{K^+K^-\to\pi^0\pi^0}(s)\,,$$

take into account strong final-state interactions. Equations (10) and (12) imply that $T_{\pi^+\pi^-\to\pi\pi}(s)$ and $T_{K^+K^-\to\pi\pi}(s)$ amplitudes in the $\gamma\gamma \to \pi^+\pi^- \to \pi\pi$ and $\gamma\gamma \to K^+K^- \to \pi\pi$ rescattering loops (see Figs 12 and 13) are on the mass shell. Functions $\tilde{I}^{\pi^+}_{\pi^+\pi^-}(s)$ and $\tilde{I}^{K^+}_{K^+K^-}(s)$ are the amplitudes of the triangle loop diagrams describing $\gamma\gamma \to \pi^+\pi^- \to$ (*the scalar state with a mass equaling* $\sqrt{s}$) transitions and $\gamma\gamma \to K^+K^- \to$ (*the scalar state with a mass equaling* $\sqrt{s}$) transitions in which $\pi^+\pi^-$- and K^+K^--pairs are produced by electromagnetic Born sources (see Figs 9 and 14). Their explicit expressions are presented in Appendices A.1 and A.3. The amplitude $M^{\text{direct}}_{\text{res}}(s)$ entering into Eqns (10) and (12) and determined by direct coupling constants of $\sigma(600)$- and $f_0(980)$-resonances with photons and the $f_2(1270)$-production amplitudes in Eqns (11) and (13), $M_{\gamma\gamma\to f_2(1270)\to\pi^+\pi^-}(s) = M_{\gamma\gamma\to f_2(1270)\to\pi^0\pi^0}(s)$, are described at greater length below.

Let us demonstrate, using the example of S-wave amplitudes $M_{00}(\gamma\gamma \to \pi^+\pi^-;\, s)$ and $M_{00}(\gamma\gamma \to \pi^0\pi^0;\, s)$, that the requirements of the unitary condition or the Watson theorem of final-state interaction are fulfilled in the model under consideration [273]. First of all, note that the contribution of the inelastic 4π and 6π channels in $\pi\pi$ scattering for $\sqrt{s} < 1$ GeV is small [112–114]; therefore, in the entire $2m_\pi \leqslant \sqrt{s} \leqslant 2m_K$ region, we have [9, 105, 106, 171, 172]

$$T_{\pi^+\pi^-\to K^+K^-}(s) = \exp\left(i\delta_0^0(s)\right)\left|T_{\pi^+\pi^-\to K^+K^-}(s)\right|,$$

$$M^{\text{direct}}_{\text{res}}(s) = \pm\exp\left(i\delta_0^0(s)\right)\left|M^{\text{direct}}_{\text{res}}(s)\right|.$$

Taking into account that $\operatorname{Im}\tilde{I}^{\pi^+}_{\pi^+\pi^-}(s) = \rho_{\pi^+}(s)M_{00}^{\text{Born}\,\pi^+}(s)$, we arrive at

$$\begin{aligned} M_{00}(\gamma\gamma \to \pi^+\pi^-;\, s) &= M_{00}^{\text{Born}\,\pi^+}(s) \\ &+ \tilde{I}^{\pi^+}_{\pi^+\pi^-}(s)T_{\pi^+\pi^-\to\pi^+\pi^-}(s) + \\ &+ \tilde{I}^{K^+}_{K^+K^-}(s)T_{K^+K^-\to\pi^+\pi^-}(s) + M^{\text{direct}}_{\text{res}}(s)\,, \end{aligned} \tag{14a}$$

for $2m_\pi \leqslant \sqrt{s} \leqslant 2m_K$,

$$\begin{aligned} &M_{00}(\gamma\gamma \to \pi^+\pi^-;\, s) \\ &\quad = \frac{2}{3}\exp\left(i\delta_0^0(s)\right)A(s) + \frac{1}{3}\exp\left(i\delta_0^2(s)\right)B(s)\,; \end{aligned} \tag{14b}$$

$$\begin{aligned} M_{00}(\gamma\gamma \to \pi^0\pi^0;\, s) &= \tilde{I}^{\pi^+}_{\pi^+\pi^-}(s)T_{\pi^+\pi^-\to\pi^0\pi^0}(s) \\ &+ \tilde{I}^{K^+}_{K^+K^-}(s)T_{K^+K^-\to\pi^0\pi^0}(s) + M^{\text{direct}}_{\text{res}}(s)\,, \end{aligned} \tag{15a}$$

and for $2m_\pi \leqslant \sqrt{s} \leqslant 2m_K$,

$$\begin{aligned} &M_{00}(\gamma\gamma \to \pi^0\pi^0;\, s) \\ &\quad = \frac{2}{3}\exp\left(i\delta_0^0(s)\right)A(s) - \frac{2}{3}\exp\left(i\delta_0^2(s)\right)B(s)\,, \end{aligned} \tag{15b}$$

where $A(s)$ and $B(s)$ are the real functions:

$$\begin{aligned} A(s) &= M_{00}^{\text{Born}\,\pi^+}(s)\cos\delta_0^0(s) + \frac{1}{\rho_{\pi^+}(s)}\operatorname{Re}\left[\tilde{I}^{\pi^+}_{\pi^+\pi^-}(s)\right]\sin\delta_0^0(s) \\ &+ \frac{3}{2}\,\tilde{I}^{K^+}_{K^+K^-}(s)\left|T_{K^+K^-\to\pi^+\pi^-}(s)\right| \pm \frac{3}{2}\left|M^{\text{direct}}_{\text{res}}(s)\right|, \end{aligned}$$

$$B(s) = M_{00}^{\text{Born}\,\pi^+}(s)\cos\delta_0^2(s) + \frac{1}{\rho_{\pi^+}(s)}\operatorname{Re}\left[\tilde{I}^{\pi^+}_{\pi^+\pi^-}(s)\right]\sin\delta_0^2(s)\,.$$

Expressions (14) and (15) indicate that, in accordance with the Watson theorem, the phases of S-wave amplitudes of $\gamma\gamma \to \pi\pi$ processes with $I = 0$ and 2 in the elastic region (below the $K\bar{K}$ threshold) coincide with the phases of $\pi\pi$ scattering, $\delta_0^0(s)$ and $\delta_0^2(s)$, respectively.

We use the following notation and normalizations for the $\gamma\gamma \to \pi\pi$ cross sections:

$$\sigma(\gamma\gamma \to \pi^+\pi^-;\, |\cos\theta| \leqslant 0.6) \equiv \sigma = \sigma_0 + \sigma_2\,, \tag{16}$$

$$\sigma(\gamma\gamma \to \pi^0\pi^0;\, |\cos\theta| \leqslant 0.8) \equiv \tilde{\sigma} = \tilde{\sigma}_0 + \tilde{\sigma}_2\,, \tag{17}$$

$$\sigma_\lambda = \frac{\rho_{\pi^+}(s)}{64\pi s}\int_{-0.6}^{0.6}\left|M_\lambda(\gamma\gamma \to \pi^+\pi^-;\, s,\theta)\right|^2 \mathrm{d}\cos\theta\,, \tag{18}$$

$$\tilde{\sigma}_\lambda = \frac{\rho_{\pi^+}(s)}{128\pi s}\int_{-0.8}^{0.8}\left|M_\lambda(\gamma\gamma \to \pi^0\pi^0;\, s,\theta)\right|^2 \mathrm{d}\cos\theta\,. \tag{19}$$

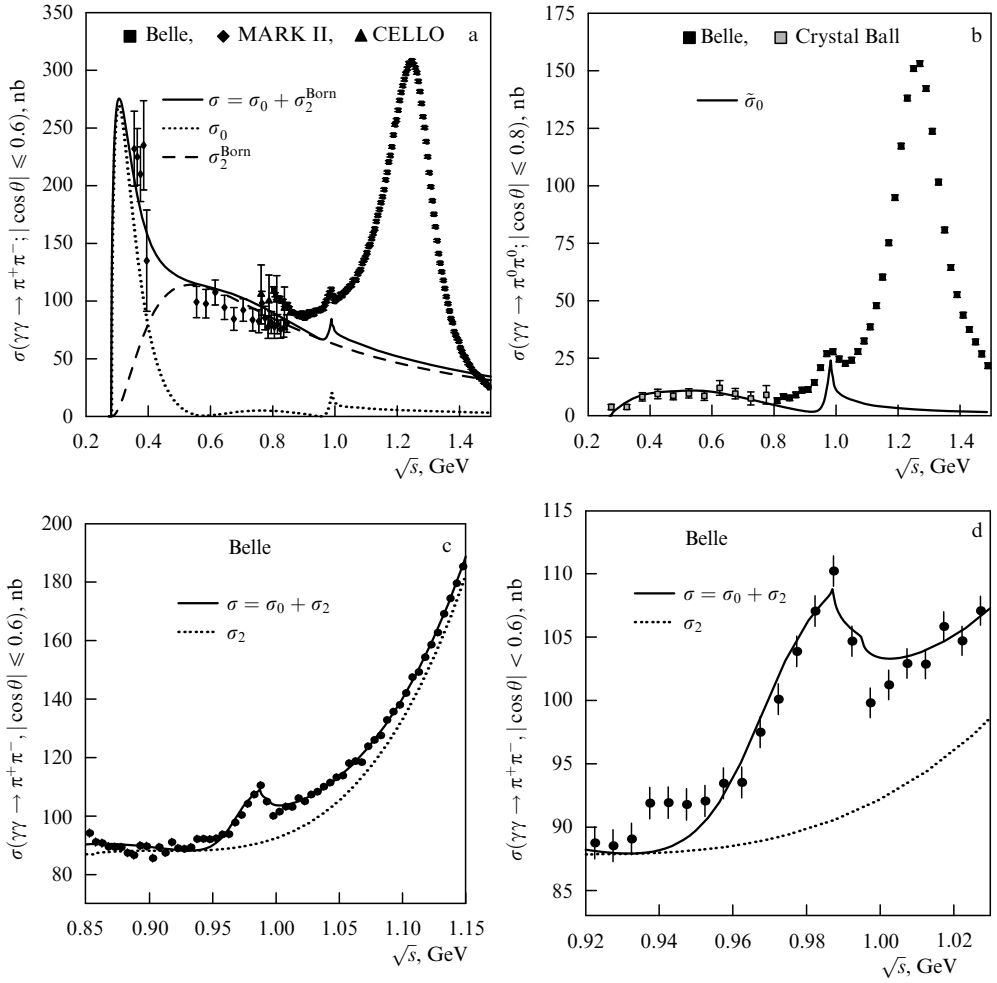

Figure 15. (a, b). Theoretical curves corresponding to the simplest model which incorporates only the Born contributions to $\gamma\gamma \to \pi^+\pi^-$ and $\gamma\gamma \to K^+K^-$ scatterings from π and K exchanges modified by strong final-state interactions in the *S*-wave. (c) Description of the Belle data in the $f_0(980)$-resonance region (see the text for details). (d) Blowup of the portion of figure (c).

In what follows, $\sigma_{\lambda J}$ and $\tilde{\sigma}_{\lambda J}$ denote the corresponding partial cross sections.

Before fitting the data with the use of the above model, it may be useful to consider in brief a somewhat simplified framework of their description.

Figure 15a borrowed from paper [106] displays theoretical curves for the $\gamma\gamma \to \pi^+\pi^-$ cross section $\sigma = \sigma_0 + \sigma_2^{\rm Born}$ and its components σ_0 and $\sigma_2^{\rm Born}$, corresponding to the simplest variant of the above model in which only the *S*-wave Born amplitudes of $\gamma\gamma \to \pi^+\pi^-$ and $\gamma\gamma \to K^+K^-$ events accompanied by π and K exchanges are taken into account in σ_0; they are modified by strong final-state interactions of charged pions and kaons, whereas all higher partial waves of $\gamma\gamma \to \pi^+\pi^-$ with $\lambda = 0$ and 2 are taken in the Born approximation [105, 106]. This modification results in appearing the $f_0(980)$-resonance signal in σ_0, the magnitude and the shape of which agree fairly well with the Belle data (Fig. 15a). It follows from comparison of the respective curves in Figs 8a and 15a that the S-wave contribution to $\sigma(\gamma\gamma \to \pi^+\pi^-; |\cos\theta| \leqslant 0.6)$ is small for $\sqrt{s} > 0.5$ GeV. It is clear that the contribution of $f_2(1270)$ resonance is the main missing element needed to describe the Belle data on $\gamma\gamma \to \pi^+\pi^-$ over the entire $\sqrt{s}$ range from 0.8 to 1.5 GeV. If the description is restricted to the data gathered in the vicinity of $f_0(980)$ resonance, the large incoherent background under it, caused by the σ_2 contribution, can be purely phenomenologically approximated by a polynomial in $\sqrt{s}$. The result of such a fit is shown in Fig. 15c, d [106].

Naturally, taking account of the final-state interactions in the *S*-wave Born amplitudes of $\gamma\gamma \to \pi^+\pi^-$ and $\gamma\gamma \to K^+K^-$ reactions eventually leads to the prediction of the $\gamma\gamma \to \pi^0\pi^0$ reaction for the S-wave amplitude [9, 105–107]. Figure 15b compares the $\gamma\gamma \to \pi^0\pi^0$ cross section estimated as described above with the Crystal Ball and Belle data. (Note that the step of $\sqrt{s}$ for the Crystal Ball and Belle data is 50 and 20 MeV, respectively.) The agreement with the data for $\sqrt{s} \leqslant 0.8$ GeV, i.e., in the $\sigma(600)$-resonance region, should be regarded as quite good since no fitting parameters were used to construct $\tilde{\sigma}_0$. Also, it is clear that the $f_2(1270)$-resonance responsibility region begins for $\sqrt{s} > 0.8$ GeV in both $\gamma\gamma \to \pi^0\pi^0$ and $\gamma\gamma \to \pi^+\pi^-$ channels.

Thus, two things become apparent even at this stage of data description: first, if the direct coupling constants of $\sigma(600)$ and $f_0(980)$ with $\gamma\gamma$ are included in the fittings, their role will be negligible in agreement with the prediction made in Refs [85, 86]; second, the $\sigma(600) \to \gamma\gamma$ and $f_0(980) \to \gamma\gamma$ decays are actually described in accordance with formulas (10) and (12) by the triangle loop rescattering diagrams, *resonance* $\to (\pi^+\pi^-, K^+K^-) \to \gamma\gamma$; this means that they represent four-quark transitions [9, 105–107].

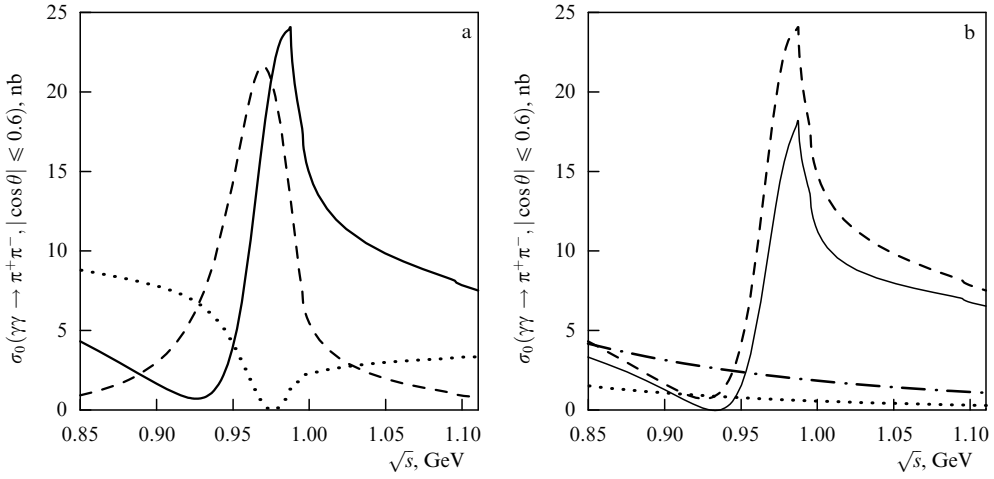

Figure 16. The structure of the $f_0(980)$ signal in σ_0. (a) Dashed, dotted and solid curves show the contributions from $\gamma\gamma \to K^+K^- \to \pi^+\pi^-$, $\gamma\gamma \to \pi^+\pi^- \to \pi^+\pi^-$ rescatterings, and their sum, respectively. (b) The dashed and solid lines in (a) are identical; the dotted and dashed-dot lines show the $\sigma_0^{\rm Born}$ and $\sigma_{00}^{\rm Born}$ cross sections, respectively ($\sigma_0^{\rm Born} < \sigma_{00}^{\rm Born}$ because of destructive interference between the S-wave and higher partial waves); the resulting $f_0(980)$ signal in σ_0 is plotted as the solid line.

An interesting and important feature of the $f_0(980)$ signal in $\gamma\gamma \to \pi^+\pi^-$ is its complicated 'internal' structure evidenced in Fig. 16. The $\gamma\gamma \to K^+K^- \to \pi\pi$ rescattering amplitude undoubtedly plays the defining role in the formation of this signal since it specifies the natural scale of $f_0(980)$-production cross section in $\gamma\gamma$ collisions [105].[14] Due to this amplitude, the $f_0(980)$ peak is transferred from $T_{K^+K^-\to\pi\pi}(s)$ to the $\gamma\gamma \to \pi\pi$ amplitude. In the $\gamma\gamma \to \pi^+\pi^- \to \pi^+\pi^-$ rescattering contribution, the $f_0(980)$ resonance is manifested as a dip. The resulting shape of the $f_0(980)$ signal strongly depends on the interference of the $\gamma\gamma \to K^+K^- \to \pi^+\pi^-$ resonance amplitude with the $\gamma\gamma \to \pi^+\pi^- \to \pi^+\pi^-$ amplitude (Fig. 16a),[15] the S-wave Born contribution, and Born contributions of higher partial waves with $\lambda = 0$ (Fig. 16b).

One more notable fact is that the amplitude of $f_0(980)$ production through $\gamma\gamma \to K^+K^- \to f_0(980)$ in the inelastic $\gamma\gamma \to K^+K^- \to \pi\pi$ rescattering mechanism changes drastically in the $f_0(980)$-peak region [105, 106] [just as the $\gamma\gamma \to K^+K^- \to a_0(980)$ amplitude in the $a_0(980)$ region]; see Section 5. Its contribution to the cross section is proportional to $|\tilde{I}^{K^+}_{K^+K^-}(s)|^2$ [see Eqns (10) and (12)]. Function $|\tilde{I}^{K^+}_{K^+K^-}(s)|^2$ is demonstrated in Fig. 17; evidently, it sharply decreases just under the K^+K^- threshold, i.e., directly in the $f_0(980)$-resonance region.[16] Such a behavior of the $f_0(980)$ two-photon production amplitude strongly suppresses the left wing of the $f_0(980)$ peak determined by the resonance amplitude $T_{K^+K^-\to\pi\pi}(s)$, making impossible approximation of the $f_0(980) \to \gamma\gamma$ decay width by a constant even in the $m_{f_0} - \Gamma_{f_0}/2 \leqslant \sqrt{s} \leqslant m_{f_0} + \Gamma_{f_0}/2$ region [105].

[14] The maximum of $\sigma(\gamma\gamma \to K^+K^- \to f_0(980) \to \pi^+\pi^-)$ is controlled by the product of the ratio of the squares of coupling constants $R_{f_0} = g^2_{f_0K^+K^-}/g^2_{f_0\pi^+\pi^-}$ and the quantity $|\tilde{I}^{K^+}_{K^+K^-}(4m^2_{K^+})|^2$. The estimation gives

$$\sigma(\gamma\gamma \to K^+K^- \to f_0(980) \to \pi^+\pi^-;\, |\cos\theta| \leqslant 0.6) \approx 0.6 \times 0.62\alpha^2 R_{f_0}/m^2_{f_0} \approx 8\ \text{nb} \times R_{f_0}\,,$$

where $\alpha = 1/137$, and m_{f_0} is the $f_0(980)$ mass.

[15] Note that the relative sign of these amplitudes, determining the character of interference, is inferred reliably [105, 106].

[16] Function $|\tilde{I}^{K^+}_{K^+K^-}(s)|^2$ decreases with respect to its maximum at $\sqrt{s} = 2m_{K^+} \approx 0.9873$ GeV by 1.66, 2.23, 2.75, 3.27, and 6.33 times at $\sqrt{s} = 0.98$, 0.97, 0.96, 0.95, and 0.9 GeV, respectively.

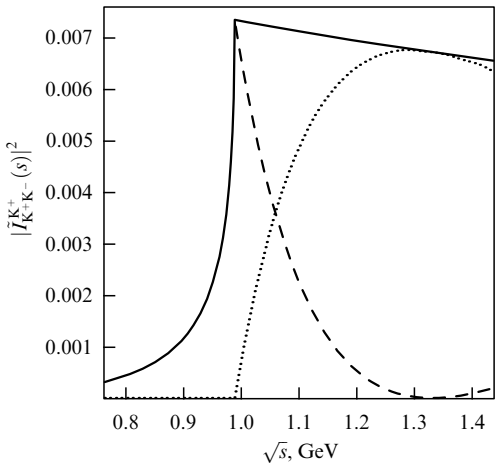

Figure 17. The solid curve depicts $|\tilde{I}^{K^+}_{K^+K^-}(s)|^2$ as a function of $\sqrt{s}$ (see Appendix A3); the dashed and dotted curves show the contributions above the K^+K^- threshold from the real and imaginary parts of $\tilde{I}^{K^+}_{K^+K^-}(s)$, respectively.

The following should be emphasized in connection with the aforesaid. The real situation is such that virtually any simplified form of the approximation of the $f_0(980)$ signal observed in $\gamma\gamma \to \pi^+\pi^-$ and $\gamma\gamma \to \pi^0\pi^0$ cross sections will provide only conventional information on the two-photon production mechanism of the $f_0(980)$-state and its parameters.

It is noteworthy that even current knowledge of dynamics of strong interaction amplitudes $T_{\pi\pi\to\pi\pi}(s)$ [or $T^0_0(s)$ and $T^2_0(s)$] and $T_{K^+K^-\to\pi\pi}(s)$ allows us to advance the understanding of the properties of light scalar mesons emerging from the data on the $\gamma\gamma \to \pi\pi$ reactions. In fitting these data, we utilize the model for $T^0_0(s)$ and $T_{K^+K^-\to\pi\pi}(s)$ amplitudes formulated in Ref. [171] and applied to the combined analysis of the data on the $\pi^0\pi^0$ mass spectrum in the $\phi \to \pi^0\pi^0\gamma$ decay, $\pi\pi$ scattering for $2m_\pi < \sqrt{s} < 1.6$ GeV, and the $\pi\pi \to K\bar{K}$ reaction [171, 172]. Parametrization used in this model for $T^0_0(s)$ takes into account the contributions from mixing $\sigma(600)$ and $f_0(980)$ resonances, and from the background (containing a large negative phase due to chiral

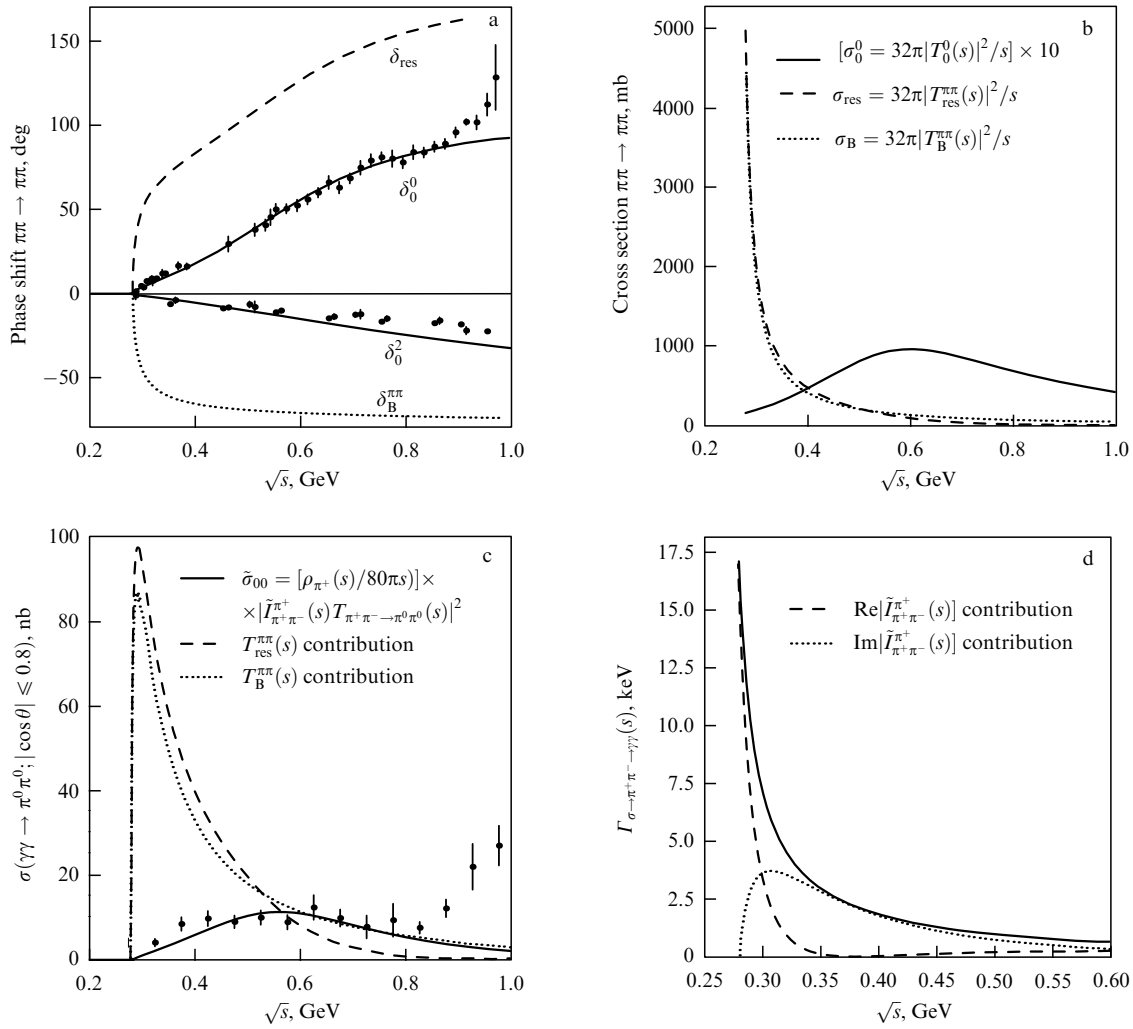

Figure 18. Illustration of the σ(600)-resonance chiral shielding effect in ππ → ππ and γγ → $\pi^0\pi^0$ reactions. Taken from Ref. [9] devoted to the lightest scalar in the $SU(2)_L \times SU(2)_R$-linear σ model.

symmetry) which shields (hides) the σ(600) resonance (see in addition Refs [6, 9, 45, 46]). Formulas (10) and (12) transfer the chiral shielding effect of the σ(600) resonance from the ππ scattering to the γγ → ππ amplitudes. This effect is illustrated in Fig. 18a by the example of ππ scattering phases $\delta_{res}(s)$, $\delta_B^{\pi\pi}(s)$, and $\delta_0^0(s)$ [see formulas (20)–(22) and (24)], and in Figs 18b and 18c with the corresponding cross sections of ππ → ππ and γγ → $\pi^0\pi^0$ reactions. As mentioned above and seen from Fig. 18c, the γγ → $\pi^0\pi^0$ cross section near the threshold in the absence of such shielding would be approximately 100 nb, not 5–10 nb, due to the $\pi^+\pi^-$ loop mechanism of σ(600) → γγ decay [9]. The decay width corresponding to this mechanism, $\Gamma_{\sigma \to \pi^+\pi^- \to \gamma\gamma}(s)$, is shown in Fig. 18d [see also formula (64) in Appendix A.1].

Let us write down following Ref. [171] the expressions for scattering amplitudes:

$$T_0^0(s) = T_B^{\pi\pi}(s) + \exp\left(2i\delta_B^{\pi\pi}(s)\right) T_{res}^{\pi\pi}(s)\,, \tag{20}$$

$$T_B^{\pi\pi}(s) = \frac{\exp\left(2i\delta_B^{\pi\pi}(s)\right) - 1}{2i\rho_{\pi^+}(s)}\,, \tag{21}$$

$$T_{res}^{\pi\pi}(s) = \frac{\eta_0^0(s)\exp\left(2i\delta_{res}(s)\right) - 1}{2i\rho_{\pi^+}(s)}\,, \tag{22}$$

$$T_{K^+K^- \to \pi^+\pi^-}(s) = \exp\left[i\left(\delta_B^{\pi\pi}(s) + \delta_B^{K\bar{K}}(s)\right)\right] T_{res}^{K\bar{K} \to \pi\pi}(s)\,, \tag{23}$$

where $\delta_B^{\pi\pi}(s)$ and $\delta_B^{K\bar{K}}(s)$ are the phases of the elastic S-wave background in ππ and $K\bar{K}$ channels with $I = 0$, and the ππ scattering phase is given by

$$\delta_0^0(s) = \delta_B^{\pi\pi}(s) + \delta_{res}(s)\,. \tag{24}$$

The amplitudes of the σ(600) – f_0(980) resonance complex in formulas (10), (12), (20), (22), and (23) have the form [171]

$$T_{res}^{\pi\pi}(s) = 3\,\frac{g_{\sigma\pi^+\pi^-}\Delta_{f_0}(s) + g_{f_0\pi^+\pi^-}\Delta_\sigma(s)}{32\pi\left[D_\sigma(s)D_{f_0}(s) - \Pi_{f_0\sigma}^2(s)\right]}\,, \tag{25}$$

$$T_{res}^{K\bar{K} \to \pi\pi}(s) = \frac{g_{\sigma K^+K^-}\Delta_{f_0}(s) + g_{f_0K^+K^-}\Delta_\sigma(s)}{16\pi[D_\sigma(s)D_{f_0}(s) - \Pi_{f_0\sigma}^2(s)]}\,, \tag{26}$$

$$M_{res}^{direct}(s) = s\exp\left(i\delta_B^{\pi\pi}(s)\right)\frac{g_{\sigma\gamma\gamma}^{(0)}\Delta_{f_0}(s) + g_{f_0\gamma\gamma}^{(0)}\Delta_\sigma(s)}{D_\sigma(s)D_{f_0}(s) - \Pi_{f_0\sigma}^2(s)}\,, \tag{27}$$

where

$$\Delta_{f_0}(s) = D_{f_0}(s)g_{\sigma\pi^+\pi^-} + \Pi_{f_0\sigma}(s)g_{f_0\pi^+\pi^-}\,,$$
$$\Delta_\sigma(s) = D_\sigma(s)g_{f_0\pi^+\pi^-} + \Pi_{f_0\sigma}(s)g_{\sigma\pi^+\pi^-}\,,$$

and $g_{\sigma\gamma\gamma}^{(0)}$ and $g_{f_0\gamma\gamma}^{(0)}$ are the direct coupling constants of σ- and f_0-resonances with photons, respectively. Here, we use the expressions from paper [171] (see also Appendices A.1–A.3)

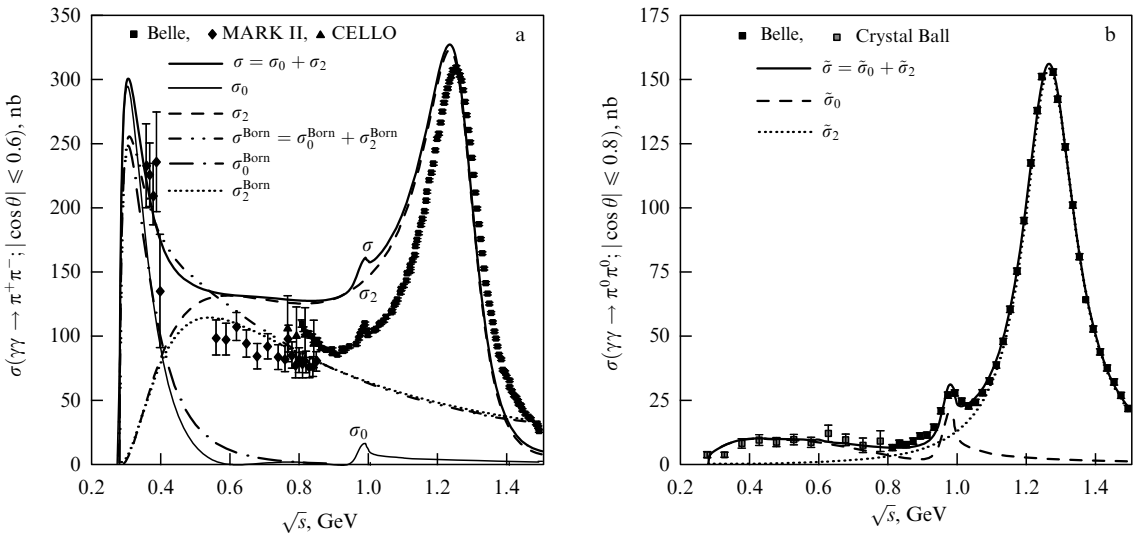

Figure 19. Cross sections of $\gamma\gamma \to \pi^+\pi^-$ and $\gamma\gamma \to \pi^0\pi^0$ reactions. Only statistical errors are shown for the Belle data [91, 92]. The curves in plot (a) are described in the text and in the figure. The curves in plot (b) are the result of fitting the data on the $\gamma\gamma \to \pi^0\pi^0$ reaction.

for the $\delta_{\rm B}^{\pi\pi}(s)$ and $\delta_{\rm B}^{\rm K\bar K}(s)$ phases, the propagators of $\sigma(600)$ and $f_0(980)$ resonances, $1/D_\sigma(s)$ and $1/D_{f_0}(s)$, and the polarization operator matrix element $\Pi_{f_0\sigma}(s)$. Mass m_{f_0} is a free parameter; the values of other parameters in the strong amplitudes (m_σ masses, $g_{\sigma\pi^+\pi^-}$ and $g_{f_0K^+K^-}$ coupling constants, etc.) correspond to variant 1 from Table 1 in the same paper.[17] In the $\pi\pi$ scattering amplitude with $J = 0$ and $I = 2$, we assume $\eta_0^2(s) = 1$ at all $\sqrt{s}$ values being considered and take $\delta_0^2(s)$ from Ref. [274].

The amplitudes of the $f_2(1270)$-resonance production in formulas (11) and (13) have the following form:

$$M_{\gamma\gamma\to f_2(1270)\to\pi^+\pi^-}(s) = M_{\gamma\gamma\to f_2(1270)\to\pi^0\pi^0}(s) = \frac{\sqrt{s}\,G_2(s)\sqrt{(2/3)\Gamma_{f_2\to\pi\pi}(s)/\rho_{\pi^+}(s)}}{m_{f_2}^2 - s - i\sqrt{s}\,\Gamma_{f_2}^{\rm tot}(s)}\,. \tag{28}$$

The main contribution to $\Gamma_{f_2}^{\rm tot}(s) = \Gamma_{f_2\to\pi\pi}(s) + \Gamma_{f_2\to K\bar K}(s) + \Gamma_{f_2\to 4\pi}(s)$ comes from the partial $f_2(1270) \to \pi\pi$ decay width

$$\Gamma_{f_2\to\pi\pi}(s) = \Gamma_{f_2}^{\rm tot}(m_{f_2}^2)\,B(f_2 \to \pi\pi) \times \frac{m_{f_2}^2}{s}\,\frac{q_{\pi^+}^5(s)}{q_{\pi^+}^5(m_{f_2}^2)}\,\frac{D_2\bigl(q_{\pi^+}(m_{f_2}^2)r_{f_2}\bigr)}{D_2\bigl(q_{\pi^+}(s)r_{f_2}\bigr)}\,, \tag{29}$$

where $B(f_2 \to \pi\pi) = 0.848$ [10], $q_{\pi^+}(s) = \sqrt{s}\,\rho_{\pi^+}(s)/2$, $D_2(x) = 9 + 3x^2 + x^4$, and r_{f_2} is the interaction radius. The small contributions from $\Gamma_{f_2\to K\bar K}(s)$ and $\Gamma_{f_2\to\pi\pi}(s)$ are the same as in Ref. [106]. The parameter r_{f_2} [90, 92, 94, 95, 97, 106, 107] controlling the shape of the $f_2(1270)$-resonance wings is important for fitting data with small errors.

The amplitude $G_2(s)$ in Eqn (28) describes the coupling of $f_2(1270)$ resonance with photons:

$$G_2(s) = \sqrt{\Gamma_{f_2\to\gamma\gamma}^{(0)}(s)} + i\,\frac{M_{22}^{{\rm Born}\,\pi^+}(s)}{16\pi}\sqrt{\frac{2}{3}\,\rho_{\pi^+}(s)\Gamma_{f_2\to\pi\pi}(s)}\,. \tag{30}$$

[17] Removing the misprint in the sign of constant $C \equiv C_{f_0\sigma}$ [171], we use $C_{f_0\sigma} = -0.047$ GeV^2. Note that our principal conclusions [the insignificance of the direct transition $\gamma\gamma \to$ *light scalar* and the predominant role of the four-quark transition $\gamma\gamma \to (\pi^+\pi^-, K^+K^-) \to$ *light scalar*] are independent of a concrete fitting variants presented in papers [171, 172].

The explicit form of the $M_{22}^{{\rm Born}\,\pi^+}(s)$ amplitude is presented in Appendix A.1 [see formula (53)]. By definition, the $f_2(1270) \to \gamma\gamma$ decay width is given by

$$\Gamma_{f_2\to\gamma\gamma}(s) = \bigl|G_2(s)\bigr|^2\,, \tag{31}$$

and

$$\Gamma_{f_2\to\gamma\gamma}^{(0)}(s) = \frac{m_{f_2}}{\sqrt{s}}\,\Gamma_{f_2\to\gamma\gamma}^{(0)}(m_{f_2}^2)\,\frac{s^2}{m_{f_2}^4} \tag{32}$$

[factor s^2 here and factor s in Eqn (27) arise from the requirement of gauge invariance]. The second term in $G_2(s)$ relates to the transition $f_2(1270) \to \pi^+\pi^- \to \gamma\gamma$ with real pions in the intermediate state, i.e., it corresponds to the imaginary part of the $f_2(1270) \to \pi^+\pi^- \to \gamma\gamma$ decay amplitude and ensures the fulfillment of the Watson theorem requirement for the $\gamma\gamma \to \pi\pi$ amplitude with $\lambda = J = 2$ and $I = 0$ in the region below the first inelastic threshold. This term makes a small contribution of less than 6% to $\Gamma_{f_2\to\gamma\gamma}(m_{f_2}^2)$. (According to different estimations, the absolute value of the real part of the $f_2(1270) \to \pi^+\pi^- \to \gamma\gamma$ amplitude is significantly smaller than that of the direct transition amplitude.) The simplest approximation (32) for $\Gamma_{f_2\to\gamma\gamma}^{(0)}(s)$ [the main contribution to the $f_2(1270) \to \gamma\gamma$ decay width] is consistent with the current state of the theory and phenomenological description of the data. The effective parameter $\Gamma_{f_2\to\gamma\gamma}^{(0)}(m_{f_2}^2) = (1/5)[g_{f_2\gamma\gamma}^2/(16\pi)]m_{f_2}^3$ in formula (32) reflects the lack of knowledge of absolute values of the amplitudes responsible for $f_2(1270) \to \gamma\gamma$ decay. For the above reasons (see Section 3), it is generally accepted that the $f_2(1270) \to \gamma\gamma$ decay is dominated by the direct quark–antiquark transition $q\bar q \to \gamma\gamma$ and its amplitude is characterized by constant $g_{f_2\gamma\gamma}$. As demonstrated in Refs [9, 102, 105–110] and as it gradually emerges here, the situation in the case of light scalar mesons is totally the opposite.

Now, we are prepared to discuss the general procedure of fitting the Belle experiment data on $\gamma\gamma \to \pi^+\pi^-$ and $\gamma\gamma \to \pi^0\pi^0$ cross sections, which was described in Refs [106, 107].

Let us first consider fitting the $\gamma\gamma \to \pi^0\pi^0$ reaction cross section (Fig. 19b), which has smaller background contributions beneath $f_0(980)$ and $f_2(1270)$ resonances than the $\gamma\gamma \to \pi^+\pi^-$ cross section, as follows from the comparison of

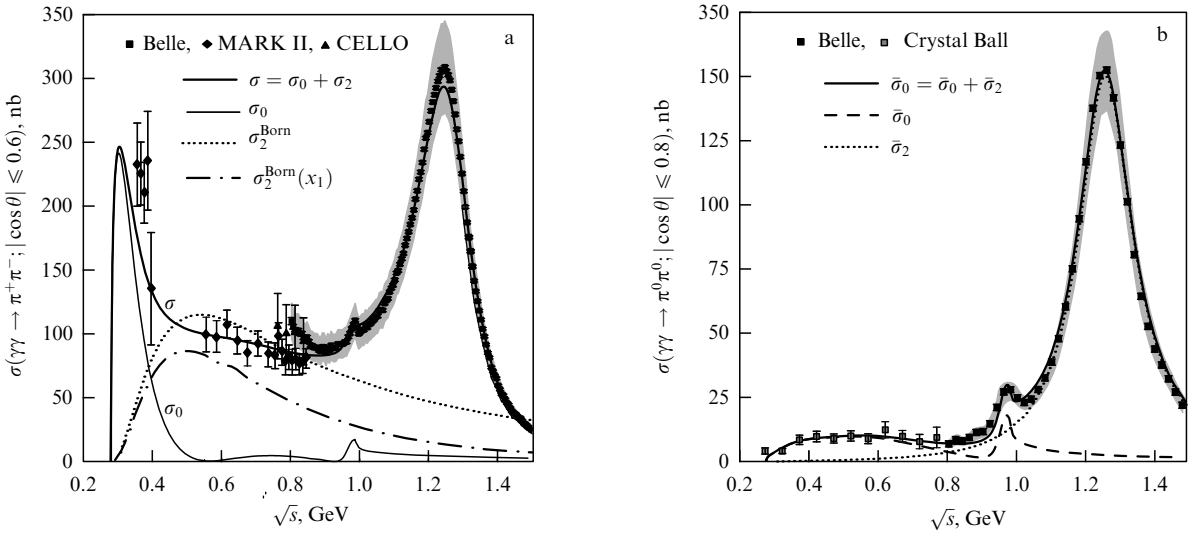

Figure 20. Combined description of the data on the cross sections of reactions $\gamma\gamma \to \pi^+\pi^-$ (a) and $\gamma\gamma \to \pi^0\pi^0$ (b). The shaded bands correspond to the Belle data [91, 92] with their statistical and systematic errors (added up quadratically). The curves are described in the text and in the figure; $\sigma_2^{\rm Born}(x_1)$ is the Born cross section of the $\gamma\gamma \to \pi^+\pi^-$ reaction, taking account of the form factor.

Figs 19a and 19b. The solid curve in Fig. 19b fairly well describes these data and corresponds to the following parameters of the model:[18] $m_{\rm f_2} = 1.269$ GeV, $\Gamma_{\rm f_2}^{\rm tot}(m_{\rm f_2}^2) = 0.182$ GeV, $r_{\rm f_2} = 8.2$ GeV^{-1}, $\Gamma_{\rm f_2\to\gamma\gamma}(m_{\rm f_2}) = 3.62$ keV [$\Gamma^{(0)}_{\rm f_2\to\gamma\gamma}(m_{\rm f_2}) = 3.43$ keV], $m_{\rm f_0} = 0.969$ GeV, $g^{(0)}_{\sigma\gamma\gamma} = 0.536$ GeV^{-1}, and $g^{(0)}_{\rm f_0\gamma\gamma} = 0.652$ GeV^{-1}. The results of the fitting suggest, in accordance with predictions [85, 86], the smallness of direct coupling constants $g^{(0)}_{\sigma\gamma\gamma}$ and $g^{(0)}_{\rm f_0\gamma\gamma}$:[19]

$$\Gamma^{(0)}_{\sigma\to\gamma\gamma}(m_\sigma^2) = \frac{|m_\sigma^2 g^{(0)}_{\sigma\gamma\gamma}|^2}{16\pi m_\sigma} = 0.012\ \text{keV}\,,$$

and

$$\Gamma^{(0)}_{\rm f_0\to\gamma\gamma}(m_{\rm f_0}^2) = \frac{|m_{\rm f_0}^2 g^{(0)}_{\rm f_0\gamma\gamma}|^2}{16\pi m_{\rm f_0}} = 0.008\ \text{keV}\,.$$

This, in turn, emphasizes the dominance of $\pi^+\pi^-$ and K^+K^- loop coupling mechanisms of $\sigma(600)$ and $f_0(980)$ resonances with photons. Indeed, the $\sigma(600) \to \pi^+\pi^- \to \gamma\gamma$ decay width due to the $\pi^+\pi^-$ loop mechanism is estimated at $\approx (1-1.75)$ keV over the range of $0.4 < \sqrt{s} < 0.5$ GeV [9] (Fig. 18d), whereas the resonance mass distribution average of the $f_0(980) \to K^+K^- \to \gamma\gamma$ decay width due to the K^+K^--loop mechanism is $\approx (0.15-0.2)$ keV [105].

However, such fitting of the $\gamma\gamma \to \pi^0\pi^0$ cross section comes into conflict with the data on $\gamma\gamma \to \pi^+\pi^-$ reaction (see the solid curve for $\sigma = \sigma_0 + \sigma_2$ in Fig. 19a) due to the large Born contribution to σ_2 and its strong constructive (destructive) interference with the $f_2(1270)$-resonance contribution for $\sqrt{s} < m_{\rm f_2}$ ($\sqrt{s} > m_{\rm f_2}$), absent in $\gamma\gamma \to \pi^0\pi^0$. The difficulty of the combined description of $\gamma\gamma \to \pi^+\pi^-$ and $\gamma\gamma \to \pi^0\pi^0$ cross sections after the publication of new Belle data was highlighted in paper [106] where a method to obviate it was proposed. The situation can be significantly improved by multiplying the Born $\gamma\gamma \to \pi^+\pi^-$ amplitudes corresponding to elementary one-pion exchange by the common suppressing form factor[20] $G_{\pi^+}(t,u)$ (where t and u are the Mandelstam variables for the $\gamma\gamma \to \pi^+\pi^-$ reaction). To show this, we use as an example the expression for $G_{\pi^+}(t,u)$ suggested in paper [191]:

$$G_{\pi^+}(t,u) = \frac{1}{s}\left[\frac{m_{\pi^+}^2 - t}{1-(u-m_{\pi^+}^2)/x_1^2} + \frac{m_{\pi^+}^2 - u}{1-(t-m_{\pi^+}^2)/x_1^2}\right], \quad (33)$$

where x_1 is the free parameter. Such an ansatz is quite acceptable in the physical region of the $\gamma\gamma \to \pi^+\pi^-$ reaction. Note that the introduction of the form factor by replacing the amplitudes $M_\lambda^{{\rm Born}\,\pi^+}(s,\theta)$ of elementary one-pion exchange by $M_\lambda^{{\rm Born}\,\pi^+}(s,\theta;x_1) = G_{\pi^+}(t,u)M_\lambda^{{\rm Born}\,\pi^+}(s,\theta)$ does not break the gauge invariance of the tree approximation [191]. The substitution $m_{\pi^+} \to m_{K^+}$, $x_1 \to x_2$ in formula (33) also yields the form factor $G_{K^+}(t,u)$ for the Born amplitudes of $\gamma\gamma \to K^+K^-$. The solid curves for the cross sections $\sigma = \sigma_0 + \sigma_2$ and $\tilde\sigma = \tilde\sigma_0 + \tilde\sigma_2$ in Figs 20a and 20b demonstrate combined fitting of the data on the $\gamma\gamma \to \pi^+\pi^-$ cross section in the $0.85 < \sqrt{s} < 1.5$ GeV region, and the data on the $\gamma\gamma \to \pi^0\pi^0$ cross section in the $2m_\pi < \sqrt{s} < 1.5$ GeV region, taking account of the form factors modifying the point-like Born contributions. The description thus obtained is more than satisfactory provided all, i.e., both statistical and systematic, errors of the Belle data shown in Fig. 20 by shaded bands are taken into consideration. We believe such fitting to

[18] Due to the high statistical accuracy of the Belle data, the formally calculated errors for the principal parameters of the model are negligibly small. In such situations, the model dependence of adjustable parameter values is the main source of their uncertainty.

[19] The small values of these coupling constants are 'grasped' in data fitting due to the interference of the $M_{\rm res}^{\rm direct}(s)$ amplitude [see formulas (10), (12), and (27)] with the contributions of the dominant rescattering mechanisms. Clearly, in this situation the values of $g^{(0)}_{\sigma\gamma\gamma}$ and $g^{(0)}_{\rm f_0\gamma\gamma}$ proper are not as important as the fact of their relative smallness, implying that direct $\Gamma^{(0)}_{\sigma\to\gamma\gamma}(m_\sigma^2)$ and $\Gamma^{(0)}_{\rm f_0\to\gamma\gamma}(m_{\rm f_0}^2)$ decay widths $\ll 0.1$ keV.

[20] Such a modification of point-like Born contributions is quite absolutely natural; in due time it was discussed in the literature in connection with the data on the $\gamma\gamma \to \pi^+\pi^-$ reaction [95, 97, 191, 193, 194] and the $\gamma\gamma \to K^+K^-$ and $\gamma\gamma \to K^0\bar K^0$ reactions near the threshold [103, 104]. However, it is the problem of the combined description of the new Belle data on $\gamma\gamma \to \pi^+\pi^-$ and $\gamma\gamma \to \pi^0\pi^0$ reactions that unambiguously points to the necessity of modification of the Born sector in the model for $\gamma\gamma \to \pi^+\pi^-$ [106, 107].

be totally justified, the statistical errors of both Belle measurements being so small that it is practically impossible to obtain a formally acceptable value of χ^2 in the combined fitting of the $\pi^+\pi^-$ and $\pi^0\pi^0$ data in a wide $\sqrt{s}$ region without taking the systematic errors into consideration.[21] The curves in Fig. 20 correspond to the following values of the parameters: $m_{f_2} = 1.272$ GeV, $\Gamma^{\rm tot}_{f_2}(m^2_{f_2}) = 0.196$ GeV, $r_{f_2} = 8.2$ GeV^{-1}, $\Gamma_{f_2\to\gamma\gamma}(m_{f_2}) = 3.83$ keV [$\Gamma^{(0)}_{f_2\to\gamma\gamma}(m_{f_2}) = 3.76$ keV], $m_{f_0} = 0.969$ GeV, $g^{(0)}_{\sigma\gamma\gamma} = -0.049$ GeV^{-1} [$\Gamma^{(0)}_{\sigma\to\gamma\gamma}(m^2_\sigma)$ is insignificantly small], $g^{(0)}_{f_0\gamma\gamma} = 0.718$ GeV^{-1} [$\Gamma^{(0)}_{f_0\to\gamma\gamma}(m^2_{f_0}) \approx 0.01$ keV], $x_1 = 0.9$ GeV, and $x_2 = 1.75$ GeV. It is clear from a comparison of Figs 19b and 20b that the influence of the form factors on the $\gamma\gamma \to \pi^0\pi^0$ cross section is weak in contrast to its effect on $\gamma\gamma \to \pi^+\pi^-$ (cf. Figs 19a and 20a), which most notably modifies the σ_2 contribution. It should be emphasized that all our conclusions about the mechanisms of the two-photon decays (productions) of the $\sigma(600)$ and $f_0(980)$ resonances remain in force.[22]

Thus, the physics of two-photon decays of light scalar mesons can be more clearly delineated. The mechanism of their decays into $\gamma\gamma$ differs from the decay mechanism of the classical tensor $q\bar{q}$-meson, i.e., direct $q\bar{q} \to \gamma\gamma$ annihilation. The decays of light scalar mesons into $\gamma\gamma$, suppressed in comparison with those of tensor mesons, are mediated through the rescattering mechanisms, i.e., four-quark transitions $\sigma(600) \to \pi^+\pi^- \to \gamma\gamma$, $f_0(980) \to K^+K^- \to \gamma\gamma$, $a_0(980) \to K^+K^- \to \gamma\gamma$, etc. Such a picture is consistent with available data and confirms the $q^2\bar{q}^2$-nature of light scalar mesons. Importantly, it is impossible for a number of reasons to comprehensively characterize the coupling between scalar mesons and photons (by analogy with tensor mesons) by the values of the $\Gamma_{0^{++}\to\gamma\gamma}(m^2_{0^{++}})$ constants.

Above all, it is clear that when we deal with resonances accompanied by an appreciable background, and when their two-photon decay widths change sharply over the resonance peak width due to the proximity of inelastic channel thresholds, there is no point in discussing the two-photon width at the resonance point.

In this context, it is interesting to consider the S-wave cross section of the $\gamma\gamma \to \pi^+\pi^-$ reaction determined by resonance contributions alone, namely

$$\sigma_{\rm res}(\gamma\gamma \to \pi^+\pi^-; s) = \frac{\rho_{\pi^+}(s)}{32\pi s}\left|\tilde{I}^{\pi^+}_{\pi^+\pi^-}(s; x_1)\exp\left(2i\delta^{\pi\pi}_{\rm B}(s)\right)T^{\pi\pi}_{\rm res}(s) + \tilde{I}^{K^+}_{K^+K^-}(s; x_2)\, T_{K^+K^-\to\pi^+\pi^-}(s) + M^{\rm direct}_{\rm res}(s)\right|^2 \qquad (34)$$

[21] The presence of large systematic errors, the sources of which are described at length in publications by the Belle Collaboration [90–92], do not diminish the role of high-statistics data that enabled the researchers to resolve small local effects associated with manifestations of the $f_0(980)$ resonance.

[22] Notice the absence of experimental evidences of elementary ω and $a_2(1320)$ exchanges in the $\gamma\gamma \to \pi^0\pi^0$ and $\gamma\gamma \to \pi^+\pi^-$ amplitudes, respectively, which make contributions (mostly S-wave contributions) to the cross sections that rapidly increase with energy and become comparable with the $f_2(1270)$-resonance contribution in the respective energy range. This observation was explained in Ref. [103] through the example of the $\gamma\gamma \to \pi^0\eta$ reaction (see Section 5 for details). The proper Reggeization of point-like exchanges with high spins significantly reduces the dangerous contributions. In addition, partial cancellations take place in amplitudes with $\lambda = 0$ between elementary ω and $h_1(1170)$ exchanges in $\gamma\gamma \to \pi^0\pi^0$ reaction and between $a_2(1320)$ and $a_1(1260)$ exchanges in $\gamma\gamma \to \pi^+\pi^-$. The contribution of the ρ exchange to $\gamma\gamma \to \pi\pi$ is small (because $g^2_{\rho\pi\gamma} \approx g^2_{\omega\pi\gamma}/9$) and is additionally cancelled by the $b_1(1235)$-exchange contribution.

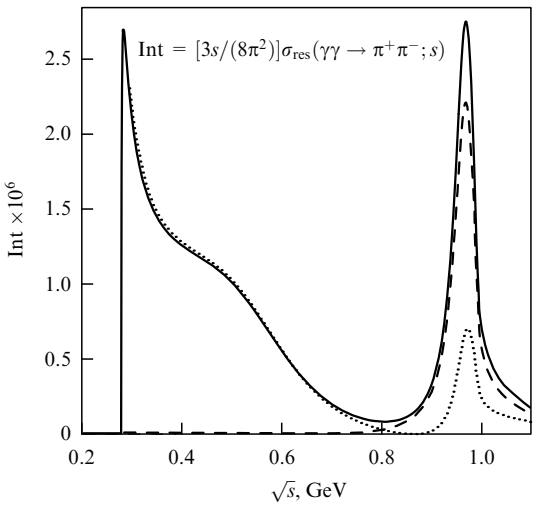

Figure 21. The integrand in formula (35) corresponding to the combined fit (see Fig. 20) of the data on $\gamma\gamma \to \pi^+\pi^-$ and $\gamma\gamma \to \pi^0\pi^0$ reactions is shown by the solid curve. The dotted and dashed curves display the contributions from resonant elastic $\gamma\gamma \to \pi^+\pi^- \to \pi^+\pi^-$ and inelastic $\gamma\gamma \to K^+K^- \to \pi^+\pi^-$ rescatterings, respectively.

[see Eqns (10) and (25)–(27)], where $\tilde{I}^{\pi^+}_{\pi^+\pi^-}(s; x_1)$ and $\tilde{I}^{K^+}_{K^+K^-}(s; x_2)$ are analogs of functions $\tilde{I}^{\pi^+}_{\pi^+\pi^-}(s)$ and $\tilde{I}^{K^+}_{K^+K^-}(s)$, constructed taking into account the form factors (see Appendices A.1 and A.3). Figure 21 depicts the energy dependence of the $\sigma_{\rm res}(\gamma\gamma \to \pi^+\pi^-; s)$ cross section multiplied by factor $3s/(8\pi^2)$. In an energy range close to 1 GeV, there is a quite apparent peak from $f_0(980)$ resonance mainly due to the contribution of inelastic $\gamma\gamma \to K^+K^- \to \pi^+\pi^-$ rescattering. Let us determine, following Refs [102, 105, 107], the $f_0(980) \to \gamma\gamma$ decay width averaged over the resonance mass distribution in the $\pi\pi$ channel:

$$\langle\Gamma_{f_0\to\gamma\gamma}\rangle_{\pi\pi} = \int_{0.8\ {\rm GeV}}^{1.1\ {\rm GeV}} \frac{3s}{8\pi^2}\,\sigma_{\rm res}(\gamma\gamma \to \pi^+\pi^-; s)\,{\rm d}\sqrt{s}\,. \qquad (35)$$

This quantity is an adequate working characteristic of the coupling between $f_0(980)$ and $\gamma\gamma$. For the presented combined fit, $\langle\Gamma_{f_0\to\gamma\gamma}\rangle_{\pi\pi} \approx 0.19$ keV [107]. Taking into account that the $2m_\pi < \sqrt{s} < 0.8$ GeV region is dominated by the wide $\sigma(600)$ resonance, we obtain $\langle\Gamma_{\sigma\to\gamma\gamma}\rangle_{\pi\pi} \approx 0.45$ keV by analogy with formula (35) [107]. Note that the cusp near the $\pi\pi$ threshold in the expression $[3s/(8\pi^2)]\sigma_{\rm res}(\gamma\gamma \to \pi^+\pi^-; s)$ (see Fig. 21) is a manifestation of the corrections for the finite width in the propagator of scalar resonance. A simple explanation of this phenomenon is presented in Appendix A.1.

Such a threshold enhancement is absent in the total S-wave amplitude of the $\gamma\gamma \to \pi\pi$ event due to the shielding of the resonance contribution to the $T^0_0(s)$ amplitude by the chiral background (see, for example, Fig. 20b).

The above examples clearly demonstrate the nontriviality of obtaining information about two-photon decays of $\sigma(600)$ and $f_0(980)$ resonances. For example, it is impossible to determine $\Gamma_{\sigma\to\gamma\gamma}(m^2_\sigma)$ directly from the data, because the cross section in the σ region is formed by both the resonance and the compensating background. A concrete dynamic model of the total amplitude is needed to separate them, the simple Breit–Wigner formula being insufficient here.

As for the $f_0(980)$ resonance, experimentalists have begun to take into consideration already two of the three important circumstances [90–92] (see also Refs [10, 11]) that we pointed out in paper [105]. One is that account is taken of the

corrections for the finite width due to the coupling of $f_0(980)$ resonance with the $K\bar{K}$ channel in the $f_0(980)$-resonance propagator, which essentially influence the shape of the $f_0(980)$ peak in the $\pi\pi$ channel. The other is that interference of the $f_0(980)$ resonance with the background is taken into consideration even if in the simplest form. But no model was constructed for the $f_0(980) \to \gamma\gamma$ decay amplitude itself, which was simply assumed to be constant [90–92]. Fitting data in this way, the Belle Collaboration extracted the values for $\Gamma_{f_0\to\gamma\gamma}(m_{f_0}^2)$ presented in Table 4. However, they should not be perceived literally. To begin with, they cannot be used to determine the coupling constant $g_{f_0\gamma\gamma}$ in the effective interaction Lagrangian, i.e., the constant of the direct $f_0(980) \to \gamma\gamma$ transition, because such a constant is small and does not define the $f_0(980) \to \gamma\gamma$ decay, as shown above. While the model of the $f_0(980) \to \gamma\gamma$ decay amplitude remains unspecified, the meaning of $\Gamma_{f_0\to\gamma\gamma}(m_{f_0}^2)$ values obtained by simplified parametrization is rather vague.[23] In principle, the values of $\Gamma_{f_0\to\gamma\gamma}(m_{f_0}^2)$ collated in Table 4 can be regarded as the preliminary estimates of $\langle\Gamma_{f_0\to\gamma\gamma}\rangle$, i.e., as the $f_0(980) \to \gamma\gamma$ decay width averaged over the hadron mass distribution [102, 105, 107].

In the framework of the dispersion approach, the so-called pole two-photon widths $\Gamma_{R\to\gamma\gamma}(pole)$, $R = \sigma, f_0$ are usually introduced to characterize the coupling of $\sigma(600)$ and $f_0(980)$ resonances with photons (see, for example, Refs [194, 208, 222, 239, 247]). These widths are determined through the moduli of the complex pole residues of the $\gamma\gamma \to \pi\pi$ and $\pi\pi \to \pi\pi$ amplitudes constructed theoretically. Based on the analysis in paper [9], it should be noted that the residues of the above amplitudes are essentially complex and cannot be used as coupling constants in a Hermitian effective Lagrangian. Naturally, these residues are 'dressed' by the background because they relate to the total amplitudes. Our analysis in the framework of the $SU(2)_L \times SU(2)_R$-linear σ model [9] indicated that the background essentially influences the values and phases of the residues. Thus, the focus on quantities like $\Gamma_{R\to\gamma\gamma}(pole)$ obtained in the dispersion approach does not help to elucidate the mechanism governing the two-photon decays of scalar mesons and does not shed light on the nature of light scalars.

5. Production of $a_0(980)$ resonance in the $\gamma\gamma \to \pi^0\eta$ reaction

Our conclusions about the important role of the K^+K^- loop mechanism in the two-photon production of the $a_0(980)$ resonance and its putative four-quark nature, made in the late 1980s and the early 1990s [48, 102, 103]), were based on an analysis of the results of the first Crystal Ball [189] (see Fig. 5) and JADE [96] experiments on the $\gamma\gamma \to \pi^0\eta$ reaction. Unfortunately, large statistical errors in these data and a rather rough step in the invariant mass of $\pi^0\eta$ system (40 MeV and 60 MeV in the Crystal Ball and JADE experiments, respectively) left many uncertainties.

As mentioned in Section 3.1, the Belle Collaboration obtained new data on the $\gamma\gamma \to \pi^0\eta$ reaction at the KEK B-factory in 2009 [93] with statistics three orders of magnitude higher than those in the previous Crystal Ball and JADE experiments (336 and 291 events, respectively).

The experiments revealed a sizable $\gamma\gamma \to \pi^0\eta$ cross section in the region between $a_0(980)$ and $a_2(1320)$ resonances

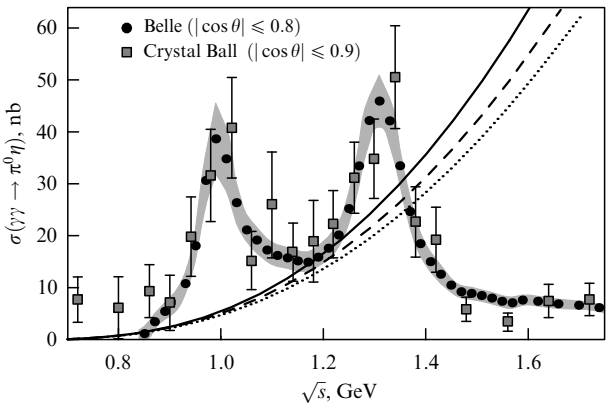

Figure 22. Belle [93] and Crystal Ball [189] data on the $\gamma\gamma \to \pi^0\eta$ reaction cross section. The shaded band shows the size of the systemic error in the Belle data (mean statistical error is roughly ± 0.4 nb). The solid, dashed, and dotted lines demonstrate the total, helicity 0, and S-wave cross sections of $\gamma\gamma \to \pi^0\eta$ (for $|\cos\theta| \leqslant 0.8$) corresponding to elementary ρ and ω exchanges.

(Fig. 22)[24], which suggests the presence of additional contributions that must be coherent with the resonance ones because only the two lowest partial S and D_2 waves dominate in the $\gamma\gamma \to \pi^0\eta$ amplitude in the case of the $\pi^0\eta$-system invariant mass $\sqrt{s} < 1.4$ GeV [93]. Phenomenological fitting of the data on the $\gamma\gamma \to \pi^0\eta$ reaction taking account of interference between resonance and background contributions was performed in Ref. [93]. It turned out that a description of the S-wave requires the knowledge not only of the contributions from both the $a_0(980)$ resonance and the putative heavy $a_0(Y)$ resonance, but also of the smooth background whose amplitude is comparable with the amplitude of $a_0(980)$ resonance at the maximum and has a large imaginary part [93]. As a result, the background leads to a fourfold increase in the cross section in the $a_0(980)$-peak region and to the filling of the dip between $a_0(980)$- and $a_2(1320)$-resonances. The origin of such a large background in the S-wave remains to be elucidated, while the imaginary part of the background amplitude is due to contributions from the real intermediate states: $\pi\eta$, $K\bar{K}$, and $\pi\eta'$; naturally, dynamic decoding is needed here.

We revealed in Refs [109, 110] that the experimentally observed pattern results from the interplay of many dynamic factors. In order to analyze the data, we further developed the model discussed earlier in papers [102, 103, 108]. This model is based on the concept of $a_0(980)$ resonance as a possible candidate for the four-quark state, supported by a number of weighty facts [1, 4, 34, 36, 45, 48, 85, 86, 133, 169]. We found a solution for the $\gamma\gamma \to \pi^0\eta$ amplitude that agrees with predictions of the chiral theory for the $\pi\eta$ scattering length, with the strong coupling of $a_0(980)$ resonance to the $\pi\eta$, $K\bar{K}$, and $\pi\eta'$ channels and the key role of the $a_0(980) \to (K\bar{K} + \pi^0\eta + \pi^0\eta') \to \gamma\gamma$ rescattering mechanisms in the $a_0(980) \to \gamma\gamma$ decay. Such a picture is consistent with the $q^2\bar{q}^2$-nature of $a_0(980)$ and agrees with the properties of its partners, $\sigma_0(600)$ and $f_0(980)$, specifically with those manifested in $\gamma\gamma \to \pi\pi$ reactions (see above). In recent papers [109, 110], we also demonstrated the important role of vector exchanges in the formation of the nonresonant background

[23] The above considerations also hold for the case of $\sigma(600)$ resonance.

[24] The JADE [96] data for $\gamma\gamma \to \pi^0\eta$ are not normalized and are therefore omitted in Fig. 22.

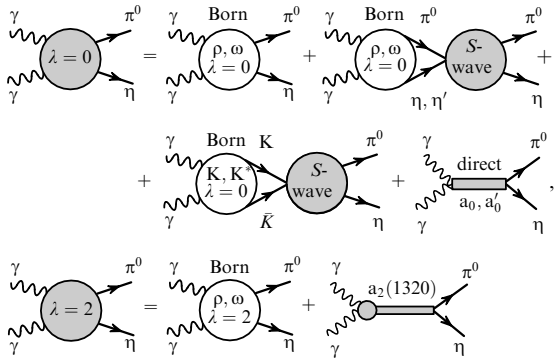

Figure 23. Diagrams corresponding to helicity amplitudes (36) and (37) for the $\gamma\gamma \to \pi^0\eta$ reaction.

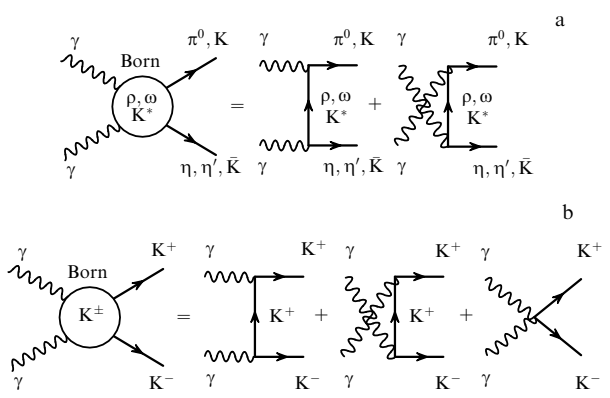

Figure 24. The Born ρ-, ω-, K*-, and K-exchange diagrams for $\gamma\gamma \to \pi^0\eta$, $\gamma\gamma \to \pi^0\eta'$, and $\gamma\gamma \to K\bar{K}$ reactions.

in the $\gamma\gamma \to \pi^0\eta$ reaction and obtained preliminary information on the $\pi^0\eta \to \pi^0\eta$ reaction.

The Belle data were analyzed using the specially constructed helicity (M_λ) and the corresponding partial ($M_{\lambda J}$) amplitudes of the $\gamma\gamma \to \pi^0\eta$ reaction, taking account of the electromagnetic Born contributions from ρ, ω, K*, and K exchanges modified by the form factors and strong elastic and inelastic final-state interactions in the $\pi^0\eta$, $\pi^0\eta'$, K^+K^-, and $K^0\bar{K}^0$ channels, and of the contributions from direct resonance–photon interactions:

$$M_0(\gamma\gamma \to \pi^0\eta; s, \theta) = M_0^{\text{Born V}}(\gamma\gamma \to \pi^0\eta; s, \theta) + \tilde{I}^{\text{V}}_{\pi^0\eta}(s)\, T_{\pi^0\eta\to\pi^0\eta}(s) + \tilde{I}^{\text{V}}_{\pi^0\eta'}(s)\, T_{\pi^0\eta'\to\pi^0\eta}(s) + \left(\tilde{I}^{\text{K}^{*+}}_{\text{K}^+\text{K}^-}(s) - \tilde{I}^{\text{K}^{*0}}_{\text{K}^0\bar{\text{K}}^0}(s) + \tilde{I}^{\text{K}^+}_{\text{K}^+\text{K}^-}(s; x_2)\right) \times\ T_{\text{K}^+\text{K}^-\to\pi^0\eta}(s) + \tilde{M}^{\text{direct}}_{\text{res}}(s)\,, \quad (36)$$

$$M_2(\gamma\gamma \to \pi^0\eta; s, \theta) = M_2^{\text{Born V}}(\gamma\gamma \to \pi^0\eta; s, \theta) + 80\pi d^2_{20}(\theta) M_{\gamma\gamma\to a_2(1320)\to\pi^0\eta}(s)\,, \quad (37)$$

where θ is the polar take-off angle of π^0 (or η) in the γγ center-of-mass system. The diagrams corresponding to the amplitudes (36), (37) are presented in Figs 23 and 24.

The first terms on the right-hand sides of expressions (36) and (37) are the real Born helicity amplitudes represented by the sum of equal contributions from ρ and ω exchanges:

$$M_0^{\text{Born V}}(\gamma\gamma \to \pi^0\eta; s, \theta) = 2g_{\omega\pi\gamma}g_{\omega\eta\gamma}\,\frac{s}{4}\left[\frac{tG_\omega(s,t)}{t-m_\omega^2} + \frac{uG_\omega(s,u)}{u-m_\omega^2}\right], \quad (38)$$

$$M_2^{\text{Born V}}(\gamma\gamma \to \pi^0\eta; s, \theta) = 2g_{\omega\pi\gamma}g_{\omega\eta\gamma}\,\frac{m_\pi^2 m_\eta^2 - tu}{4}\left[\frac{G_\omega(s,t)}{t-m_\omega^2} + \frac{G_\omega(s,u)}{u-m_\omega^2}\right], \quad (39)$$

where

$$g_{\omega\eta\gamma} = \frac{1}{3}\, g_{\omega\pi\gamma}\sin(\theta_{\text{i}} - \theta_{\text{P}})\,,$$

$$g^2_{\omega\pi\gamma} = 12\pi\Gamma_{\omega\to\pi\gamma}\left[\frac{m_\omega^2 - m_\pi^2}{2m_\omega}\right]^{-3} \approx 0.519\ \text{GeV}^{-2}\ [10, 11]\,,$$

$\theta_{\text{i}} = 35.3^\circ$ is the 'ideal' mixing angle, θ_{P} is the mixing angle in the pseudoscalar nonet, t and u are the Mandelstam variables for the $\gamma\gamma \to \pi^0\eta$ reaction, and $G_\omega(s,t)$ and $G_\omega(s,u)$ are t- and u-channel form factors; for elementary ρ and ω exchanges $G_\omega(s,t) = G_\omega(s,u) = 1$. In the corresponding Born amplitudes for $\gamma\gamma \to \pi^0\eta'$, one finds $g_{\omega\eta'\gamma} = (1/3)g_{\omega\pi\gamma}\cos(\theta_{\text{i}} - \theta_{\text{P}})$, and for $\gamma\gamma \to K\bar{K}$ with the K* exchange, $g^2_{\text{K}^{*+}\text{K}^+\gamma} \approx 0.064\ \text{GeV}^{-2}$ and $g^2_{\text{K}^{*0}\text{K}^0\gamma} \approx 0.151\ \text{GeV}^{-2}$ [10, 11].

Note that information on the start-up Born sources of the $\gamma\gamma \to \pi^0\eta$ reaction corresponding to exchanges with the quantum numbers of ρ- and ω-mesons [also $b_1(1235)$- and $h_1(1170)$-mesons] is very scarce in the nonasymptotic energy range of interest. What is clear is that there are no experimental observations of elementary ρ and ω exchanges whose contributions to the $\gamma\gamma \to \pi^0\eta$ cross section (mostly to the S-wave) rapidly increase with energy (see Fig. 22).[25] This fact was explained in paper [103] by the Reggeization of elementary exchanges that suppresses dangerous contributions even in the energy range from 1 to1.5 GeV. Therefore, we employ the Regge type form factors $G_\omega(s,t) = \exp[(t - m_\omega^2)b_\omega(s)]$, $G_\omega(s,u) = \exp[(u - m_\omega^2)b_\omega(s)]$, where

$$b_\omega(s) = b_\omega^0 + \frac{\alpha'_\omega}{4}\ln\left[1 + \left(\frac{s}{s_0}\right)^4\right],$$

$b_\omega^0 = 0$, $\alpha'_\omega = 0.8\ \text{GeV}^{-2}$, and $s_0 = 1\ \text{GeV}^2$ (and, by analogy, for the K* exchange).

As regards $b_1(1235)$ and $h_1(1170)$ exchanges, their amplitudes have shapes analogous to those defined by formulas (38) and (39), except for the common sign in the helicity 0 amplitude. Proper estimation suggests that the axial-vector exchanges amplitudes are at least five times smaller than the corresponding vector exchange amplitudes; for this reason, their contributions are neglected.[26]

The terms in formula (36) proportional to S-wave hadron amplitudes $T_{\pi^0\eta\to\pi^0\eta}(s)$, $T_{\pi^0\eta'\to\pi^0\eta}(s)$, and $T_{\text{K}^+\text{K}^-\to\pi^0\eta}(s)$ are attributed to the rescattering mechanisms. In these amplitudes, we take into account the contribution from the mixed $a_0(980)$ resonance and heavy $a_0(\text{Y})$ resonance (denoted for brevity as a_0 and a_0', respectively), as well as the background

[25] These contributions are weakly sensitive to the usually discussed magnitudes of θ_{P} [11]. The reference curves in Fig. 22 correspond to $\theta_{\text{P}} = -22^\circ$.

[26] The high-spin exchanges in the $\gamma\gamma \to \pi^0\eta$ reaction are the correction against the background of the K-exchange contribution. This correction is needed to describe the data on the said reaction (see below). As far as $\gamma\gamma \to \pi\pi$ reactions are concerned, the corrections from the high-spin exchanges prove to be less significant against the background of the summarized contribution from π and K exchanges, and it is impossible to take them into account at the current level of knowledge.

contributions:

$$T_{\pi^0\eta\to\pi^0\eta}(s)=T_0^1(s)=\frac{\eta_0^1(s)\exp\bigl(2\mathrm{i}\delta_0^1(s)\bigr)-1}{2\mathrm{i}\rho_{\pi\eta}(s)}$$
$$=T_{\pi\eta}^{\mathrm{bg}}(s)+\exp\bigl(2\mathrm{i}\delta_{\pi\eta}^{\mathrm{bg}}(s)\bigr)T_{\pi^0\eta\to\pi^0\eta}^{\mathrm{res}}(s)\,, \qquad (40)$$

$$T_{\pi^0\eta'\to\pi^0\eta}(s)=T_{\pi^0\eta'\to\pi^0\eta}^{\mathrm{res}}(s)\exp\bigl[\mathrm{i}\bigl(\delta_{\pi\eta'}^{\mathrm{bg}}(s)+\delta_{\pi\eta}^{\mathrm{bg}}(s)\bigr)\bigr]\,, \qquad (41)$$

$$T_{\mathrm{K^+K^-}\to\pi^0\eta}(s)=T_{\mathrm{K^+K^-}\to\pi^0\eta}^{\mathrm{res}}(s)\exp\bigl[\mathrm{i}\bigl(\delta_{\mathrm{K\bar K}}^{\mathrm{bg}}(s)+\delta_{\pi\eta}^{\mathrm{bg}}(s)\bigr)\bigr]\,, \qquad (42)$$

where

$$T_{\pi\eta}^{\mathrm{bg}}(s)=\frac{\exp\bigl(2\mathrm{i}\delta_{\pi\eta}^{\mathrm{bg}}(s)\bigr)-1}{2\mathrm{i}\rho_{\pi\eta}(s)}\,,$$

$$T_{\pi^0\eta\to\pi^0\eta}^{\mathrm{res}}(s)=\frac{\eta_0^1(s)\exp\bigl(2\mathrm{i}\delta_{\pi\eta}^{\mathrm{res}}(s)\bigr)-1}{2\mathrm{i}\rho_{\pi\eta}(s)}\,,$$

$$\delta_0^1(s)=\delta_{\pi\eta}^{\mathrm{bg}}(s)+\delta_{\pi\eta}^{\mathrm{res}}(s)\,,\quad \rho_{ab}(s)=\frac{\sqrt{s-m_{ab}^{(+)2}}\,\sqrt{s-m_{ab}^{(-)2}}}{s}\,,$$

$m_{ab}^{(\pm)}=m_b\pm m_a$, $ab=\pi\eta$, $\mathrm{K^+K^-}$, $\mathrm{K^0\bar K^0}$, $\pi\eta'$, and $\delta_{\pi\eta}^{\mathrm{bg}}(s)$, $\delta_{\pi\eta'}^{\mathrm{bg}}(s)$, and $\delta_{\mathrm{K\bar K}}^{\mathrm{bg}}(s)$ are the phases of elastic background contributions in the $\pi\eta$, $\pi\eta'$, and $\mathrm{K\bar K}$ channels with isospin $I=1$, respectively (see Appendix A.2).

The amplitudes of the $\mathrm{a_0}-\mathrm{a_0'}$-resonance complex in Eqns (40)–(42) have a form analogous to that described by formulas (25), (26) [109, 110, 171, 275]:

$$T_{ab\to\pi^0\eta}^{\mathrm{res}}(s)=\frac{g_{\mathrm{a_0}ab}\Delta_{\mathrm{a_0'}}(s)+g_{\mathrm{a_0'}ab}\Delta_{\mathrm{a_0}}(s)}{16\pi\bigl[D_{\mathrm{a_0}}(s)D_{\mathrm{a_0'}}(s)-\Pi_{\mathrm{a_0a_0'}}^2(s)\bigr]}\,, \qquad (43)$$

where

$$\Delta_{\mathrm{a_0'}}(s)=D_{\mathrm{a_0'}}(s)g_{\mathrm{a_0}\pi^0\eta}+\Pi_{\mathrm{a_0a_0'}}(s)g_{\mathrm{a_0'}\pi^0\eta}\,,$$

$$\Delta_{\mathrm{a_0}}(s)=D_{\mathrm{a_0}}(s)g_{\mathrm{a_0'}\pi^0\eta}+\Pi_{\mathrm{a_0a_0'}}(s)g_{\mathrm{a_0}\pi^0\eta}\,,$$

$g_{\mathrm{a_0}ab}$ and $g_{\mathrm{a_0'}ab}$ are the coupling constants, and the propagator for the $\mathrm{a_0}$ resonance (and, by analogy, for $\mathrm{a_0'}$) is given by

$$\frac{1}{D_{\mathrm{a_0}}(s)}=\frac{1}{m_{\mathrm{a_0}}^2-s+\sum_{ab}\bigl[\mathrm{Re}\,\Pi_{\mathrm{a_0}}^{ab}(m_{\mathrm{a_0}}^2)-\Pi_{\mathrm{a_0}}^{ab}(s)\bigr]}\,,$$

where $\mathrm{Re}\,\Pi_{\mathrm{a_0}}^{ab}(s)$ is defined by the singly residual dispersion integral of $\mathrm{Im}\,\Pi_{\mathrm{a_0}}^{ab}(s)=\sqrt{s}\,\Gamma_{\mathrm{a_0}\to ab}(s)=g_{\mathrm{a_0}ab}^2\,\rho_{ab}(s)/(16\pi)$, with

$$\Pi_{\mathrm{a_0a_0'}}(s)=C_{\mathrm{a_0a_0'}}+\sum_{ab}\frac{g_{\mathrm{a_0'}ab}}{g_{\mathrm{a_0}ab}}\,\Pi_{\mathrm{a_0}}^{ab}(s)\,,$$

and $C_{\mathrm{a_0a_0'}}$ being the resonance mixing parameter (see Appendix A.2 for the explicit form of polarization operators $\Pi_{\mathrm{a_0}}^{ab}(s)$ [108, 132, 169, 170]). The amplitude

$$\tilde M_{\mathrm{res}}^{\mathrm{direct}}(s)=s\,\frac{g_{\mathrm{a_0}\gamma\gamma}^{(0)}\Delta_{\mathrm{a_0'}}(s)+g_{\mathrm{a_0'}\gamma\gamma}^{(0)}\Delta_{\mathrm{a_0}}(s)}{D_{\mathrm{a_0}}(s)D_{\mathrm{a_0'}}(s)-\Pi_{\mathrm{a_0a_0'}}^2(s)}\exp\bigl(\mathrm{i}\delta_{\pi\eta}^{\mathrm{bg}}(s)\bigr) \qquad (44)$$

in formula (36) describes the $\gamma\gamma\to\pi^0\eta$ transition caused by direct coupling constants $g_{\mathrm{a_0}\gamma\gamma}^{(0)}$ and $g_{\mathrm{a_0'}\gamma\gamma}^{(0)}$ of $\mathrm{a_0}$- and $\mathrm{a_0'}$-resonances with photons; factor s appears due to gauge invariance.

Expression (36) implies that the $T_{ab\to\pi^0\eta}(s)$ amplitudes in the $\gamma\gamma\to ab\to\pi^0\eta$ rescattering loops (see Fig. 23) lie on the mass shell. Functions $\tilde I_{\pi^0\eta}^{\mathrm{V}}(s)$, $\tilde I_{\pi^0\eta'}^{\mathrm{V}}(s)$, $\tilde I_{\mathrm{K\bar K}}^{\mathrm{K^*}}(s)$, and the previously introduced $\tilde I_{\mathrm{K^+K^-}}^{\mathrm{K^+K^-}}(s;x_2)$ are the amplitudes of the triangle loop diagrams describing transitions $\gamma\gamma\to ab\to$ (*scalar state with a mass equaling* $\sqrt{s}$) in which the meson pairs $\pi^0\eta$, $\pi^0\eta'$, and $\mathrm{K\bar K}$ are produced by electromagnetic Born sources (see Fig. 24) (the corresponding formulas are presented in Appendices A.2 and A.3). The constructed amplitude $M_0(\gamma\gamma\to\pi^0\eta;s,\theta)$ satisfies the Watson theorem in the elastic region.

For the $\mathrm{a_2}(1320)$-resonance production amplitude in formula (37), we use parametrization analogous to Eqns (28) and (29):

$$M_{\gamma\gamma\to\mathrm{a_2}(1320)\to\pi^0\eta}(s)$$
$$=\frac{\sqrt{s\Gamma_{\mathrm{a_2}\to\gamma\gamma}(s)\Gamma_{\mathrm{a_2}}^{\mathrm{tot}}(s)\,B(\mathrm{a_2}\to\pi\eta)/\rho_{\pi\eta}(s)}}{m_{\mathrm{a_2}}^2-s-\mathrm{i}\sqrt{s}\,\Gamma_{\mathrm{a_2}}^{\mathrm{tot}}(s)}\,, \qquad (45)$$

where

$$\Gamma_{\mathrm{a_2}}^{\mathrm{tot}}(s)=\Gamma_{\mathrm{a_2}}^{\mathrm{tot}}\,\frac{m_{\mathrm{a_2}}^2}{s}\,\frac{q_{\pi\eta}^5(s)}{q_{\pi\eta}^5(m_{\mathrm{a_2}}^2)}\,\frac{D_2\bigl(q_{\pi\eta}(m_{\mathrm{a_2}}^2)r_{\mathrm{a_2}}\bigr)}{D_2\bigl(q_{\pi\eta}(s)r_{\mathrm{a_2}}\bigr)}\,, \qquad (46)$$

$q_{\pi\eta}(s)=\sqrt{s}\,\rho_{\pi\eta}(s)/2$, $D_2(x)=9+3x^2+x^4$, $r_{\mathrm{a_2}}$ is the interaction radius, and $\Gamma_{\mathrm{a_2}\to\gamma\gamma}(s)=(\sqrt{s}/m_{\mathrm{a_2}})^3\Gamma_{\mathrm{a_2}\to\gamma\gamma}$. To recall, the $\mathrm{f_2}(1270)\to\gamma\gamma$ and $\mathrm{a_2}(1320)\to\gamma\gamma$ decay widths are in excellent agreement with the relation $\Gamma_{\mathrm{f_2}\to\gamma\gamma}/\Gamma_{\mathrm{a_2}\to\gamma\gamma}=25/9$ [10, 11, 197] that is valid in the naive $\mathrm{q\bar q}$ model, for direct $\mathrm{q\bar q}\to\gamma\gamma$ transitions.

The results of our fitting the Belle data on the $\gamma\gamma\to\pi^0\eta$ reaction cross section are demonstrated in Figs 25 and 26. The corresponding values of model parameters are presented in Appendix A.2. The excellent agreement with the experimental results (see Fig. 25) allows for definitive conclusions about the main dynamic components of the $\gamma\gamma\to\pi^0\eta$ reaction mechanism, whose contributions are illustrated in detail by Fig. 26a, b.

Let us start from the contribution of inelastic $\gamma\gamma\to\mathrm{K^+K^-}\to\pi^0\eta$ rescattering in which the intermediate $\mathrm{K^+K^-}$

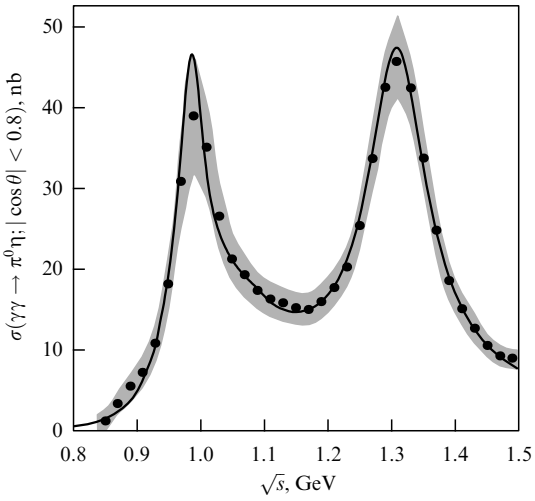

Figure 25. The fit to the Belle data on the $\gamma\gamma\to\pi^0\eta$ reaction cross section. The resulting solid line corresponds to solid line *1* in Figs 26a or 26b weighted with the Gaussian $\sigma=10$ MeV mass resolution. The shaded band shows the size of the systematic error in data.

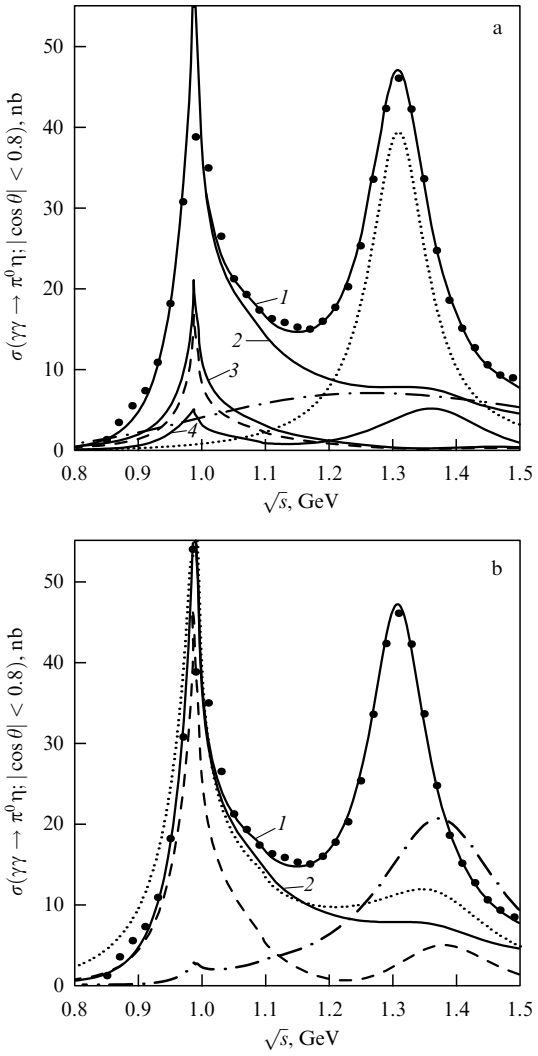

Figure 26. The fit to the Belle data. (a) The total $\gamma\gamma \to \pi^0\eta$ cross section (solid line *1*), its portions with helicities 0 (solid line *2*) and 2 (dotted line), the contribution from $\gamma\gamma \to K^+K^- \to \pi^0\eta$ rescattering with the intermediate K^+K^- pair resulting from the Born K exchange (solid line *3*), the contribution from $\gamma\gamma \to K\bar{K} \to \pi^0\eta$ rescattering with intermediate $K\bar{K}$-pairs resulting from Born K and K^* exchanges (dashed line), the contribution from the amplitude of Born ρ and ω exchanges with $\lambda = 0$ (dashed-dot line), and the joint contribution from this amplitude and *S*-wave $\gamma\gamma \to (\pi^0\eta + \pi^0\eta') \to \pi^0\eta$ rescattering (solid line *4*). (b) Solid lines *1* and *2* are the same as in plot (a), the dashed-dot line corresponds to the contribution of the $\tilde{M}^{\text{direct}}_{\text{res}}(s)$ amplitude caused by direct transitions of a_0 and a_0' into photons, the dotted line traces the total contribution from the $a_0 - a_0'$-resonance complex, and the dashed line shows the cross section with helicity 0 and without the contribution from the direct transition amplitude $\tilde{M}^{\text{direct}}_{\text{res}}(s)$.

pair is produced as a result of a charged one-kaon exchange (Fig. 24b). Similar to the case of $f_0(980)$ production in $\gamma\gamma \to \pi\pi$ reactions [106, 107], this mechanism specifies the natural scale for the $a_0(980)$-production cross section in the $\gamma\gamma \to \pi^0\eta$ reaction and also leads to the narrowing of the $a_0(980)$-peak in this channel [102, 108]. The maximum of the cross section $\sigma(\gamma\gamma \to K^+K^- \to a_0(980) \to \pi^0\eta)$ is controlled by the product of the ratio of the square of coupling constants $R_{a_0} = g^2_{a_0K^+K^-}/g^2_{a_0\pi\eta}$ and the quantity $|\tilde{I}^{K^+}_{K^+K^-}(4m^2_{K^+}; x_2)|^2$. The estimation of this cross section (neglecting the effect of the heavy a_0' resonance) gives $\sigma(\gamma\gamma \to K^+K^- \to a_0(980) \to \pi^0\eta; |\cos\theta| \leqslant 0.8) \approx 0.8 \times 1.4\alpha^2 R_{a_0}/m^2_{a_0} \approx 24\ [\text{nb}] \times R_{a_0}$. The narrowing of the $a_0(980)$-peak in the $\sigma(\gamma\gamma \to K^+K^- \to a_0(980) \to \pi^0\eta)$ cross section results from the sharp reduction of function $|\tilde{I}^{K^+}_{K^+K^-}(s; x_2)|^2$ below the K^+K^- threshold [102, 108]. The $\gamma\gamma \to K^+K^- \to \pi^0\eta$ rescattering contribution to the $\gamma\gamma \to \pi^0\eta$ cross section is shown by solid curve *3* in Fig. 26a. The K^* exchange further narrows slightly the $a_0(980)$-peak (see the dashed curve under curve *3* in Fig. 26a).

Evidently, the $\gamma\gamma \to K\bar{K} \to \pi^0\eta$ rescattering mechanism alone is not enough to describe the data in the $a_0(980)$-resonance region. The addition of the Born contribution from ρ and ω exchanges, modified by *S*-wave $\gamma\gamma \to (\pi^0\eta + \pi^0\eta') \to \pi^0\eta$ rescattering, and the $\tilde{M}^{\text{direct}}_{\text{res}}(s)$ amplitude, which is due to direct transitions of a_0 and a_0' into photons, makes it possible to obtain the observed cross section value. The contributions of these two mechanisms themselves are rather small in the region of $a_0(980)$ resonance (see solid curve *4* in Fig. 26a for the former, and the dashed-dot curve in Fig. 26b for the latter), but their coherent sum with the contribution from inelastic $\gamma\gamma \to K\bar{K} \to \pi^0\eta$ rescattering (see diagrams for the amplitude with $\lambda = 0$ in Fig. 23) results in significant enhancement of the $a_0(980)$ resonance (solid curve *2* in Fig. 26a). To recall, all *S*-wave contributions to the $\gamma\gamma \to \pi^0\eta$ amplitude have the same phase up to the K^+K^- threshold, in agreement with the Watson theorem.

It should be noted that we deduced from the fit of the $\gamma\gamma \to \pi^0\eta$ data (as a by-product) preliminary information on the *S*-wave amplitude of the $\pi^0\eta \to \pi^0\eta$ reaction, which is important for pseudoscalar meson physics. All characteristics of this amplitude are presented in Fig. 27. The important role of the background $\pi^0\eta$ elastic rescattering amplitude, $T^{\text{bg}}_{\pi\eta}(s)$, should be noted here [see formula (40)]. First, the choice of the negative background phase $\delta^{\text{bg}}_{\pi\eta}(s)$ (Fig. 27b) in $T^{\text{bg}}_{\pi\eta}(s)$ makes it possible to correlate the πη scattering length in the model being considered with the estimates based on the current algebra [276, 277] and chiral perturbation theory [278, 279], according to which $a_0^1 \approx 0.005 - 0.01$ (in units of m_π^{-1}). The resonance contribution to a_0^1 (≈ 0.3) is compensated for by the background contribution. Second, the large negative value of $\delta^{\text{bg}}_{\pi\eta}(s)$ in an energy range around 1 GeV accounts for the resonance-like behavior of the reaction cross section shown by solid curve *4* in Fig. 26a.

Let us turn to Fig. 26b and discuss the contribution from the supposedly existing heavy a_0' resonance [11] with the mass $m_{a_0'} \approx 1.4$ GeV. The cross section corresponding to the $\tilde{M}^{\text{direct}}_{\text{res}}(s)$ amplitude (dashed-dot curve) exhibits a marked enhancement in the energy range around 1.4 GeV. This enhancement transforms into a shoulder in the cross section corresponding to the total resonance contribution (dotted curve), i.e., to the joint contribution from the $\tilde{M}^{\text{direct}}_{\text{res}}(s)$ amplitude and rescattering amplitudes proportional to the amplitudes of resonance transitions $ab \to \pi^0\eta$ ($ab = \pi\eta$, K^+K^-, $K^0\bar{K}^0$, $\pi\eta'$). Finally, there are no signs of resonance near 1.4 GeV in the total cross section σ_0 (solid curve *2*) which additionally includes the Born $\gamma\gamma \to \pi^0\eta$ contribution and the $\gamma\gamma \to \pi^0\eta \to \pi^0\eta$ rescattering caused by the background $\pi^0\eta \to \pi^0\eta$ elastic amplitude. Thus, we are dealing with strong destructive interference between different contributions, masking the a_0' resonance in the $\gamma\gamma \to \pi^0\eta$ cross section. Nevertheless, it is owing to a_0' that one can simulate a significant smooth *S*-wave background beneath $a_2(1320)$ resonance and between $a_0(980)$- and $a_2(1320)$-resonances, as required by the Belle data [93]. Also, a wide range of energies,

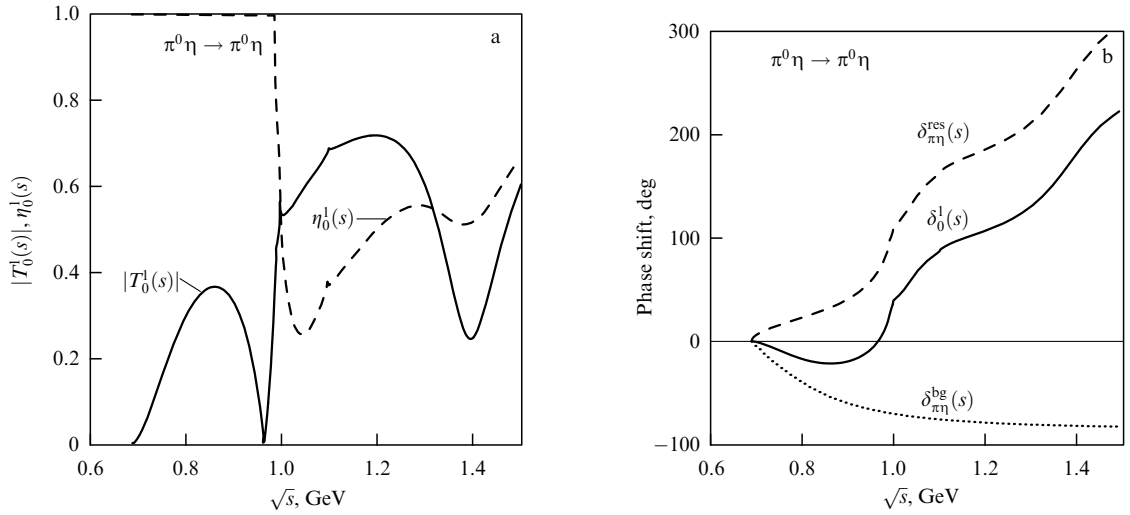

Figure 27. The *S*-wave $\pi^0\eta \to \pi^0\eta$ transition amplitude: (a) $|T_0^1(s)|$ and inelasticity $\eta_0^1(s)$, and (b) phase shifts ($a_0^1 = 0.0098$).

1.28–1.42 GeV, is admissible for the mass of a_0' due to the resulting cancellations (see Ref. [109] for details).[27]

Let us now consider the $\gamma\gamma \to \pi^0\eta$ reaction cross section determined by resonance contributions alone and find, by analogy with formula (35), the $a_0(980) \to \gamma\gamma$ decay width averaged over the resonance mass distribution in the $\pi\eta$ channel [102, 108]:

$$\langle \Gamma_{a_0\to\gamma\gamma}\rangle_{\pi\eta} = \int_{0.9\ \mathrm{GeV}}^{1.1\ \mathrm{GeV}} \frac{s}{4\pi^2}\,\sigma_{\rm res}(\gamma\gamma \to \pi^0\eta; s)\,\mathrm{d}\sqrt{s}\,, \qquad (47)$$

where the integral is calculated over the region of the $a_0(980)$-resonance responsibility. Taking into account the contribution from all rescatterings and direct transitions to $\gamma\gamma$ in $\sigma_{\rm res}$ gives

$$\langle \Gamma_{a_0\to(K\bar{K}+\pi\eta+\pi\eta'+\mathrm{direct})\to\gamma\gamma}\rangle_{\pi\eta} \approx 0.4\ \mathrm{keV}\,.$$

Taking into account only the rescatterings leads to

$$\langle \Gamma_{a_0\to(K\bar{K}+\pi\eta+\pi\eta')\to\gamma\gamma}\rangle_{\pi\eta} \approx 0.23\ \mathrm{keV}\,,$$

while account of the direct transitions alone yields

$$\langle \Gamma^{\rm direct}_{a_0\to\gamma\gamma}\rangle_{\pi\eta} \approx 0.028\ \mathrm{keV}\,.$$

This analysis points to the dominant role of $a_0(980) \to (K\bar{K} + \pi^0\eta + \pi^0\eta') \to \gamma\gamma$ rescattering mechanisms, i.e., four-quark transitions, in the $a_0(980) \to \gamma\gamma$ decay. Such a picture suggests the $q^2\bar{q}^2$-nature of $a_0(980)$ resonance and is consistent with the properties of its partners — $\sigma_0(600)$- and $f_0(980)$-resonances. As concerns the prediction of the ideal $q\bar{q}$ model for the two-photon decay widths of $f_0(980)$- and $a_0(980)$-mesons, $\Gamma_{f_0\to\gamma\gamma}/\Gamma_{a_0\to\gamma\gamma} = 25/9$, it is excluded by experiment.[28]

6. Preliminary results

The results of a theoretical analysis of experimental attainments in the region of relatively low (up to 1 GeV) energies can be formulated as follows.

(1) Naive consideration of the mass spectrum of the light scalar mesons $\sigma(600)$, $\kappa(800)$, $a_0(980)$, and $f_0(980)$ reveals their four-quark, $q^2\bar{q}^2$, structure.

(2) Both intensities and mechanisms of $a_0(980)$- and $f_0(980)$-resonance production in $\phi(1020)$-meson radiative decays, the four-quark transitions $\phi(1020) \to K^+K^- \to \gamma[a_0(980)/f_0(980)]$, suggest the $q^2\bar{q}^2$-nature of light scalars.

(3) The intensities and mechanisms of two-photon production of light scalars, four-quark transitions $\gamma\gamma \to \pi^+\pi^- \to \sigma(600)$, $\gamma\gamma \to \pi^0\eta \to a_0(980)$, and $\gamma\gamma \to K^+K^- \to f_0(980)/a_0(980)$, also suggest their $q^2\bar{q}^2$-nature.

(4) Moreover, the absence of $J/\psi \to \gamma f_0(980)$, $\rho a_0(980)$, $\omega f_0(980)$ decays in the presence of intense $J/\psi \to \gamma f_2(1270)$, $\gamma f_2'(1525)$, $\rho a_2(1320)$, $\omega f_2(1270)$ decays is at variance with the *P*-wave two-quark, $q\bar{q}$, structure of $a_0(980)$ and $f_0(980)$ resonances.

(5) Note also that $a_0(980)$- and $f_0(980)$-mesons look like 'outsiders' among the well established $b_1(1235)$, $h_1(1170)$, $a_1(1260)$, $f_1(1285)$, $a_2(1320)$, and $f_2(1270)$ mesons representing the members of the lowest *P*-wave $q\bar{q}$ multiplet.

[27] To recall, we did not need to introduce a heavy isoscalar resonance for the theoretical description of the $\gamma\gamma \to \pi^+\pi^-$ and $\gamma\gamma \to \pi^0\pi^0$ processes in Section 4, nor had the Belle group to do the same for the phenomenological treatment of their experimental data [91, 92]. In principle, $f_0(1370)$ might be such a resonance [11]. Generally speaking, the situation with heavy scalar resonances with masses $\gtrsim 1.3$ GeV has long been confusing. Suffice it to say that the authors of Ref. [75] question the very existence of such a state as $f_0(1370)$ (see also Refs [280, 281]). It appears that the wish to see scalar resonances with masses 1.3–1.4 GeV as the partners of the well-established $b_1(1235)$, $h_1(1170)$, $a_1(1260)$, $f_1(1285)$, $a_2(1320)$, and $f_2(1270)$ states belonging to the lowest *P*-wave $q\bar{q}$-multiplet cannot be realized in a naïve manner. Anyway, the question remains open and awaits further experimental and theoretical studies to be resolved.

[28] As mentioned in paper [108], there are no grounds for a model of nonrelativistic $K\bar{K}$ molecules due to the large momenta in the kaon loops describing $\phi \to K^+K^- \to \gamma(f_0/a_0)$ and $f_0/a_0 \to K^+K^- \to \gamma\gamma$ decays [45, 214, 215]. Our analysis provides an additional argument against the molecular model. The fact is that the $a_0(980)$ resonance is strongly coupled to the $K\bar{K}$ and $\pi\eta$ channels that are equivalent, in accordance with the $q^2\bar{q}^2$ model. We find it impossible to construct a weakly bound $K\bar{K} + \pi\eta$ molecule. Moreover, the widths of the two-photon decays of scalar resonances are calculated in the molecular model at the resonance point [282, 283], which is insufficient to describe the $\gamma\gamma \to \pi^+\pi^-$, $\gamma\gamma \to \pi^0\pi^0$, and $\gamma\gamma \to \pi^0\eta$ reactions. No attempts to describe the data on these processes in the framework of the molecular model have been reported thus far; therefore, the results obtained are only of academic interest.

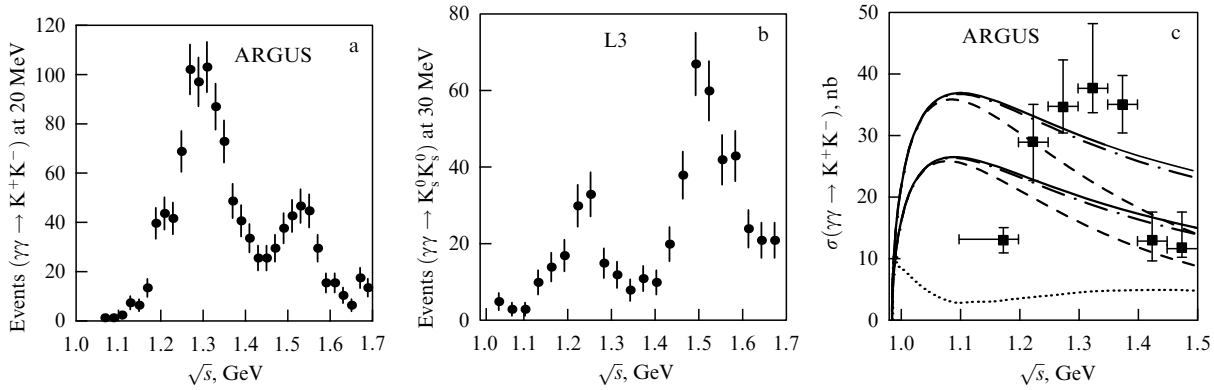

Figure 28. Mass distributions for the reactions $\gamma\gamma \to K^+K^-$ (a) and $\gamma\gamma \to K^0_S K^0_S$ (b) measured by ARGUS [269] and L3 [290], respectively. (c) Illustration of the scale of the $K\bar{K}$-production cross sections in $\gamma\gamma$ collisions. Experimental points correspond to the sum of partial $\gamma\gamma \to K^+K^-$-production cross sections with $\lambda J = [22, 02, 00]$ (ARGUS [269]). The upper dashed, dashed-dot, and solid curves correspond to the Born $\gamma\gamma \to K^+K^-$ cross sections for the elementary one-kaon exchange with $\lambda J = 00$, $\lambda J = [00, 22]$ and to the total cross section (the contribution with $\lambda J = 02$ is negligible). The lower dashed, dashed-dot, and solid curves show the same cross sections modified by the form factor (see Section 4 and Appendix A3). The dotted curve is the estimate of the S-wave $\gamma\gamma \to K^+K^-$ cross section in our model.

7. Future research

7.1 $f_0(980)$ and $a_0(980)$ resonances near $\gamma\gamma \to K^+K^-$ and $\gamma\gamma \to K^0\bar{K}^0$ reaction thresholds

The Belle Collaboration studied the $\gamma\gamma \to \pi^+\pi^-$, $\gamma\gamma \to \pi^0\pi^0$, and $\gamma\gamma \to \pi^0\eta$ reactions at a high-statistics level.[29] In July 2010, it also published the data on the $\gamma\gamma \to \eta\eta$ reaction [285]. The $\gamma\gamma \to \eta\eta$ cross section for $\sqrt{s} > 1.2$ GeV is dominated by the contributions from tensor $f_2(1270)$, $a_2(1320)$, and $f_2'(1525)$ resonances. But an appreciable S-wave contribution of $\approx (1.5 \pm 0.15 \pm 0.7)$ nb near the threshold, $2m_\eta = 1.0957\ \text{GeV} < \sqrt{s} < 1.2$ GeV, points to the presence of a subthreshold resonance strongly coupled to the $\eta\eta$ channel. Such resonance in the $q^2\bar{q}^2$ model is $f_0(980)$. Unfortunately, $\gamma\gamma \to \eta\eta$ is not the best reaction for its investigation because it allows only the end of the tail of this resonance to be seen.

Moreover, high-statistics information is still lacking for the $\gamma\gamma \to K^+K^-$ and $\gamma\gamma \to K^0\bar{K}^0$ processes in the energy range around 1 GeV. It is believed that $a_0(980)$ and $f_0(980)$ resonances exhibit their four-quark structure in these processes in a very peculiar way [103, 104].

Experiments reported in Refs [100, 190, 269, 286–291] have demonstrated that the cross sections of $\gamma\gamma \to K^+K^-$ and $\gamma\gamma \to K^0_S K^0_S$ reactions in an energy range of $1 < \sqrt{s} < 1.7$ GeV are actually saturated with the contributions from classical tensor $f_2(1270)$, $a_2(1320)$, and $f_2'(1525)$ resonances (Fig. 28) produced in helicity states with $\lambda = 2$. The $q\bar{q}$ model [292] predicts constructive and destructive interference between $f_2(1270)$- and $a_2(1320)$-resonance contributions in $\gamma\gamma \to K^+K^-$ and $\gamma\gamma \to K^0\bar{K}^0$ reactions, respectively. Note that the region near the $K\bar{K}$ thresholds, $2m_K < \sqrt{s} < 1.1$ GeV, sensitive to the S-wave contributions, remains virtually unexplored. In the ARGUS experiment [269] (Fig. 28a), the efficacy of recording K^+K^- events for $2m_{K^+} < \sqrt{s} < 1.1$ GeV was negligible, while the overall statistics in the L3 [290] (Fig. 28b) and CLEO [100] experiments on the $\gamma\gamma \to K^0_S K^0_S$ reaction for $2m_{K^0} < \sqrt{s} < 1.1$ GeV did not exceed 60 events.

The absence of an appreciable nonresonant background in the $\gamma\gamma \to K^+K^-$ cross section seems at first sight rather surprising, since the Born contribution mediated through the charged one-kaon exchange mechanism and comparable with the tensor resonance contributions must be present in this channel (Fig. 28c). As seen from this figure, the Born cross section is dominated by the S-wave contribution for $\sqrt{s} < 1.5$ GeV. For this reason, a large noncoherent background could be expected under tensor meson peaks in the K^+K^- channel. However, taking account of the resonant interaction between K^+- and K^--mesons in the final state results in the compensation of a considerable part of this background [103, 104].

To recall, the compensation arises in the following way. Due to the contribution from the $\gamma\gamma \to K^+K^- \to K^+K^-$ rescattering amplitude with real kaons in the intermediate state, the Born S-wave $\gamma\gamma \to K^+K^-$ amplitude acquires the factor

$$\xi(s) = 1 + i\rho_{K^+}(s) T_{K^+K^- \to K^+K^-}(s)\,.$$

Near the K^+K^- threshold, the $T_{K^+K^- \to K^+K^-}(s)$ amplitude is dominated by contributions from $a_0(980)$ and $f_0(980)$ resonances. Given their strong coupling to $K\bar{K}$-channels, naturally realized in the four-quark scheme, the $T_{K^+K^- \to K^+K^-}(s)$ amplitude possesses an appreciable imaginary part. As a result, factor $|\xi(s)|^2$ just above the K^+K^- threshold is much smaller than unity and the seed S-wave Born contribution is compensated for over a wide $\sqrt{s}$ range. The dotted curve in Fig. 28c represents our estimate of the S-wave $\gamma\gamma \to K^+K^-$ cross section (see Appendix A.3 for details), which fairly well agrees with the ones obtained in earlier studies [103, 104].

Thus, one can hope to detect scalar contributions at the level of 5–10 nb in the $\gamma\gamma \to K^+K^-$ cross section for

[29] Worthy of note are the plans to measure with a high degree of accuracy the cross section of the $\gamma\gamma \to \pi^+\pi^-$ reaction in the near-threshold region of $\sqrt{s}$ from 0.28 to 0.45 GeV at the renovated Frascati DAΦNE φ-factory using the KLOE-2 detector [175, 284]. Thus far, only very inaccurate MARK II data for this reaction are available [95] (Fig. 6a). It is also planned to measure the integral and differential cross sections of $\gamma\gamma \to \pi^+\pi^-$ and $\gamma\gamma \to \pi^0\pi^0$ reactions in the $\sqrt{s}$ range from 0.45 to 1.1 GeV [175, 284] and thereby replenish prior experimental information on the production of $\sigma(600)$ and $f_0(980)$. One of the objectives is to reduce statistical errors in the $\gamma\gamma \to \pi^0\pi^0$ cross section in the vicinity of $\sigma(600)$ resonance to 2% (Fig. 6b).

$2m_{K^+} < \sqrt{s} < 1.1$ GeV. As regards the $\gamma\gamma \to K^0\bar{K}^0$ reaction, its amplitude does not contain the Born contribution, while the $a_0(980)$-resonance contribution has the sign opposite to that in the $\gamma\gamma \to K^+K^-$ channel. As a result, the contributions of S-wave rescattering amplitudes with isospin $I = 0$ and 1 in the $\gamma\gamma \to K^0\bar{K}^0$ reaction practically cancel each other and the corresponding cross section should be at the level of $\lesssim 1$ nb.

7.2 σ(600), $f_0(980)$, and $a_0(980)$ resonances in γγ* collisions

Studies of light scalars produced in $\gamma\gamma^*(Q^2)$ collisions have good prospects. Given that σ(600), $f_0(980)$, and $a_0(980)$ resonances are the four-quark states, their contributions to the $\gamma\gamma^*(Q^2) \to \pi^0\pi^0$ and $\gamma\gamma^*(Q^2) \to \pi^0\eta$ reaction cross sections must decrease with increasing Q^2 faster than the contributions from classical tensor $q\bar{q}$-mesons $f_2(1270)$ and $a_2(1320)$. Such a behavior of the contribution from the resonance exotic $q^2\bar{q}^2$-state with $I^G(J^{PC}) = 2^+(2^{++})$ [48, 85, 86] to the $\gamma\gamma^* \to \rho^0\rho^0$ and $\gamma\gamma^* \to \rho^+\rho^-$ cross sections have recently been observed by the L3 Collaboration [293–296].

7.3 The search for $J/\psi \to \omega f_0(980)$ and $J/\psi \to \rho a_0(980)$ decays

These decays are important for the elucidation of the nature of $f_0(980)$ and $a_0(980)$ resonances [36, 38, 41]. The $J/\psi \to \rho a_0(980)$ decay remains to be demonstrated, while $B(J/\psi \to \rho a_0(980)) < 4.4 \times 10^{-4}$ [36]. Information concerning $B(J/\psi \to \omega f_0(980)) = (1.4 \pm 0.5) \times 10^{-4}$ [11] needs to be substituted by the appropriate upper limit [38, 41].

7.4 Inelasticity of ππ scattering and $f_0(980) - a_0(980)$ mixing

Considerable progress has been achieved in experimental studies of various reactions with the participation of $f_0(980)$- and $a_0(980)$-mesons. Nevertheless, it turns out that an equally good description of the available data can be obtained for substantially different sets of interaction constants $g_{f_0K^+K^-}$, $g_{f_0\pi^+\pi^-}$, etc. (see, e.g., Refs [34, 132, 136, 171, 172]). Certainly, it would be highly desirable to fix their values. As far as $g_{f_0K^+K^-}$ and $g_{f_0\pi^+\pi^-}$ constants are concerned, this issue could be addressed using precise data on the inelasticity of ππ scattering near the $K\bar{K}$ threshold, which have not been updated since 1975 [112–115]. In all probability, the VES Collaboration that conducted experiments on the $\pi^-p \to \pi^+\pi^-n$ reaction at the Institute of High-Energy Physics (Protvino) may have possession of such unprocessed data.

Moreover, the product of $g_{a_0K^+K^-}g_{f_0K^+K^-}$ constants can be fixed from the data on $f_0(980) - a_0(980)$ mixing expected from the BES III experiments [131].

Exclusive information on $g_{a_0K^+K^-}g_{f_0K^+K^-}$ could be obtained from studies on the spin asymmetry jump due to $f_0(980) - a_0(980)$ mixing in the $\pi^-p \to f_0(980)n \to a_0(980)n \to \pi^0\eta n$ reaction [124].

The present work was supported in part by RFBR grant No. 10-02-00016.

8. Appendices

A.1 γγ → ππ

This Appendix comprises explicit expressions for the Born helicity amplitudes corresponding to the charged one-pion exchange mechanism and for the triangle loop integrals $\tilde{I}^{\pi^+}_{\pi^+\pi^-}(s)$ and $\tilde{I}^{\pi^+}_{\pi^+\pi^-}(s; x_1)$ used in Section 4. In addition, a few useful auxiliary formulas for the solitary scalar resonance are presented.

The Born helicity amplitudes for an elementary one-pion exchange in the $\gamma\gamma \to \pi^+\pi^-$ reaction have the form

$$M_0^{\text{Born}\,\pi^+}(s,\theta) = \frac{4m_{\pi^+}^2}{s}\,\frac{8\pi\alpha}{1-\rho_{\pi^+}^2(s)\cos^2\theta}\,, \tag{48}$$

$$M_2^{\text{Born}\,\pi^+}(s,\theta) = \frac{8\pi\alpha\rho_{\pi^+}^2(s)\sin^2\theta}{1-\rho_{\pi^+}^2(s)\cos^2\theta}\,, \tag{49}$$

where $\rho_{\pi^+}(s) = (1 - 4m_{\pi^+}^2/s)^{1/2}$. Their partial-wave expansions are as follows:

$$M_\lambda^{\text{Born}\,\pi^+}(s,\theta) = \sum_{J\geqslant\lambda}(2J+1)M_{\lambda J}^{\text{Born}\,\pi^+}(s)\,d^J_{\lambda 0}(\theta)\,, \tag{50}$$

where $d^J_{\lambda 0}(\theta)$ are usual d-functions (see, e.g., Refs [10, 11]). The three lowest partial waves take the form

$$M_{00}^{\text{Born}\,\pi^+}(s) = 4\pi\alpha\,\frac{1-\rho_{\pi^+}^2(s)}{\rho_{\pi^+}(s)}\ln\frac{1+\rho_{\pi^+}(s)}{1-\rho_{\pi^+}(s)}\,, \tag{51}$$

$$M_{02}^{\text{Born}\,\pi^+}(s) = 4\pi\alpha\,\frac{1-\rho_{\pi^+}^2(s)}{\rho_{\pi^+}^2(s)}\left[\frac{3-\rho_{\pi^+}^2(s)}{2\rho_{\pi^+}(s)}\ln\frac{1+\rho_{\pi^+}(s)}{1-\rho_{\pi^+}(s)} - 3\right], \tag{52}$$

$$M_{22}^{\text{Born}\,\pi^+}(s) = 4\pi\alpha\sqrt{\frac{3}{2}}\left[\frac{\left(1-\rho_{\pi^+}^2(s)\right)^2}{2\rho_{\pi^+}^3(s)}\ln\frac{1+\rho_{\pi^+}(s)}{1-\rho_{\pi^+}(s)} - \frac{1}{\rho_{\pi^+}^2(s)} + \frac{5}{3}\right]. \tag{53}$$

The amplitude of the triangle loop diagram describing the $\gamma\gamma \to \pi^+\pi^- \to$ (*scalar state with a mass equaling* $\sqrt{s}$) transition is given by

$$\tilde{I}^{\pi^+}_{\pi^+\pi^-}(s) = \frac{s}{\pi}\int_{4m_{\pi^+}^2}^{\infty}\frac{\rho_{\pi^+}(s')M_{00}^{\text{Born}\,\pi^+}(s')}{s'(s'-s-i\varepsilon)}\,ds'\,. \tag{54}$$

The fact that $\tilde{I}^{\pi^+}_{\pi^+\pi^-}(s) \propto s$ as $s \to 0$ is a consequence of gauge invariance. For $0 < s < 4m_{\pi^+}^2$, one has

$$\tilde{I}^{\pi^+}_{\pi^+\pi^-}(s) = 8\alpha\left(\frac{m_{\pi^+}^2}{s}\left[\pi - 2\arctan\left|\rho_{\pi^+}(s)\right|\right]^2 - 1\right), \tag{55}$$

and for $s \geqslant 4m_{\pi^+}^2$, the desired amplitude is

$$\tilde{I}^{\pi^+}_{\pi^+\pi^-}(s) = 8\alpha\left\{\frac{m_{\pi^+}^2}{s}\left[\pi + i\ln\frac{1+\rho_{\pi^+}(s)}{1-\rho_{\pi^+}(s)}\right]^2 - 1\right\}. \tag{56}$$

The form factor introduced in formula (33), viz.

$$G_{\pi^+}(t,u) = \frac{1}{s}\left[\frac{m_{\pi^+}^2 - t}{1-(u-m_{\pi^+}^2)/x_1^2} + \frac{m_{\pi^+}^2 - u}{1-(t-m_{\pi^+}^2)/x_1^2}\right]$$

(here, Mandelstam variables $t = m_{\pi^+}^2 - s[1 - \rho_{\pi^+}(s)\cos\theta]/2$ and $u = m_{\pi^+}^2 - s[1 + \rho_{\pi^+}(s)\cos\theta]/2$), modifies the Born partial amplitudes. Let us introduce the notations

$$M_{0J}^{\text{Born}\,\pi^+}(s) = \frac{1-\rho_{\pi^+}^2(s)}{\rho_{\pi^+}(s)}\,F_{0J}^{\text{Born}\,\pi^+}\left(\rho_{\pi^+}(s)\right), \tag{57}$$

$$M_{2J}^{\text{Born}\,\pi^+}(s) = \rho_{\pi^+}(s)F_{2J}^{\text{Born}\,\pi^+}\left(\rho_{\pi^+}(s)\right). \tag{58}$$

Then, the corresponding amplitudes taking account of the form factor can be represented in the form

$$M_{0J}^{\text{Born}\,\pi^+}(s;x_1)=\frac{1-\rho_{\pi^+}^2(s)}{\rho_{\pi^+}(s)}\times\left[F_{0J}^{\text{Born}\,\pi^+}\left(\rho_{\pi^+}(s)\right)-F_{0J}^{\text{Born}\,\pi^+}\left(\rho_{\pi^+}(s;x_1)\right)\right], \quad (59)$$

$$M_{2J}^{\text{Born}\,\pi^+}(s;x_1)=\rho_{\pi^+}(s)\times\left[F_{2J}^{\text{Born}\,\pi^+}\left(\rho_{\pi^+}(s)\right)-F_{2J}^{\text{Born}\,\pi^+}\left(\rho_{\pi^+}(s;x_1)\right)\right], \quad (60)$$

where

$$\rho_{\pi^+}(s;x_1)=\frac{\rho_{\pi^+}(s)}{1+2x_1^2/s}\,. \quad (61)$$

Function $\tilde{I}^{\pi^+}_{\pi^+\pi^-}(s)$ [see formulas (54)–(56)] is replaced, taking into account the form factor, by the following expression

$$\tilde{I}^{\pi^+}_{\pi^+\pi^-}(s;x_1)=\frac{s}{\pi}\int_{4m_{\pi^+}^2}^{\infty}\frac{\rho_{\pi^+}(s')M_{00}^{\text{Born}\,\pi^+}(s';x_1)}{s'(s'-s-\mathrm{i}\varepsilon)}\,\mathrm{d}s'\,. \quad (62)$$

In this case, numerical integration is needed.

To facilitate understanding the structure and normalization of the rather complicated expressions used in data fitting, we will present here formulas for the production cross section of σ resonance and its two-photon decay width due to the $\gamma\gamma\to\pi^+\pi^-\to\sigma\to\pi^+\pi^-$ rescattering mechanism in the imaginary case of a solitary σ resonance coupled only to the ππ channel.

The corresponding resonance cross section has the familiar form

$$\sigma_{\text{res}}(\gamma\gamma\to\pi^+\pi^-;s)=\frac{8\pi}{s}\,\frac{\sqrt{s}\,\Gamma_{\sigma\to\pi^+\pi^-\to\gamma\gamma}(s)\,\sqrt{s}\,\Gamma_{\sigma\to\pi^+\pi^-}(s)}{\left|D_\sigma(s)\right|^2}\,, \quad (63)$$

where

$$\Gamma_{\sigma\to\pi^+\pi^-\to\gamma\gamma}(s)=\frac{1}{16\pi\sqrt{s}}\left|M_{\sigma\to\pi^+\pi^-\to\gamma\gamma}(s)\right|^2=\left|\frac{1}{16\pi}\,\tilde{I}^{\pi^+}_{\pi^+\pi^-}(s)\right|^2\frac{g^2_{\sigma\pi^+\pi^-}}{16\pi\sqrt{s}}\,. \quad (64)$$

If σ resonance is additionally direct-coupled to γγ collisions, with the coupling described by the $sg^{(0)}_{\sigma\gamma\gamma}$ amplitude, then the width $\Gamma_{\sigma\to\pi^+\pi^-\to\gamma\gamma}(s)$ in formula (63) should be replaced by

$$\Gamma_{\sigma\to\gamma\gamma}(s)=\frac{1}{16\pi\sqrt{s}}\left|M_{\sigma\to\gamma\gamma}(s)\right|^2, \quad (65)$$

where

$$M_{\sigma\to\gamma\gamma}(s)=M_{\sigma\to\pi^+\pi^-\to\gamma\gamma}(s)+sg^{(0)}_{\sigma\gamma\gamma}\,. \quad (66)$$

The propagator of the σ resonance with the mass m_σ in formula (63) has the form

$$\frac{1}{D_\sigma(s)}=\frac{1}{m_\sigma^2-s+\text{Re}\,\Pi_\sigma^{\pi\pi}(m_\sigma^2)-\Pi_\sigma^{\pi\pi}(s)}\,, \quad (67)$$

where $\Pi_\sigma^{\pi\pi}(s)$ is the polarization operator of σ corresponding to the contribution of the $\pi^+\pi^-$ and $\pi^0\pi^0$ intermediate states.

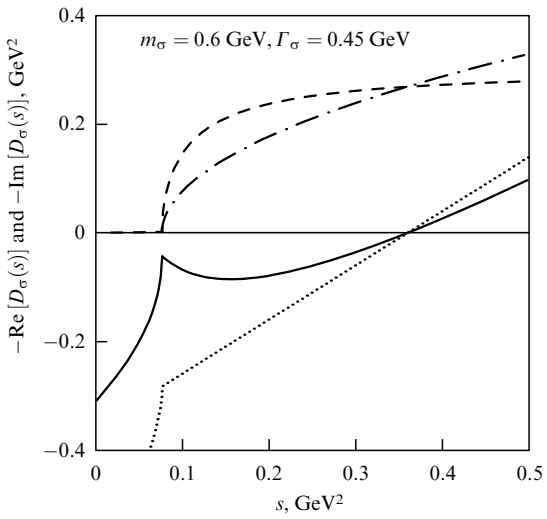

Figure 29. Demonstration of the correction for the finite width in the solitary σ-resonance propagator (the curves are described in the text).

For $s\geqslant 4m_{\pi^+}^2\,(=4m_{\pi^0}^2)$, one obtains

$$\Pi_\sigma^{\pi\pi}(s)=\frac{3}{2}\,\frac{g^2_{\sigma\pi^+\pi^-}}{16\pi}\,\rho_{\pi^+}(s)\left[\mathrm{i}-\frac{1}{\pi}\ln\frac{1+\rho_{\pi^+}(s)}{1-\rho_{\pi^+}(s)}\right]. \quad (68)$$

If $0<s<4m_{\pi^+}^2$, then $\rho_{\pi^+}(s)\to\mathrm{i}|\rho_{\pi^+}(s)|$ and

$$\Pi_\sigma^{\pi\pi}(s)=-\frac{3}{2}\,\frac{g^2_{\sigma\pi^+\pi^-}}{16\pi}\left|\rho_{\pi^+}(s)\right|\left[1-\frac{2}{\pi}\arctan\left|\rho_{\pi^+}(s)\right|\right]. \quad (69)$$

The $\sigma\to\pi\pi$ decay width is expressed as

$$\Gamma_{\sigma\to\pi\pi}(s)=\frac{1}{\sqrt{s}}\,\text{Im}\,\Pi_\sigma^{\pi\pi}(s)=\frac{3}{2}\,\frac{g^2_{\sigma\pi^+\pi^-}}{16\pi}\,\frac{\rho_{\pi^+}(s)}{\sqrt{s}}\,. \quad (70)$$

The quantity $\text{Re}\,[\Pi_\sigma^{\pi\pi}(m_\sigma^2)-\Pi_\sigma^{\pi\pi}(s)]$ in the denominator of the right-hand side of Eqn (67) is the correction for the finite width of a resonance decay. In Fig. 29, the solid and dashed curves depict the real and imaginary parts of the inverse propagator $D_\sigma(s)$ (taken with the minus sign) for the case of resonance with the mass $m_\sigma=0.6$ GeV and the width $\Gamma_\sigma=\Gamma_{\sigma\to\pi\pi}(m_\sigma^2)=0.45$ GeV. It is evidenced that $\text{Re}\,[D_\sigma(s)]$ can be close to zero at $s=4m_{\pi^+}^2$ due to the correction for the large finite width (coupling constant). As a result, a threshold cusp appears in the amplitudes proportional to $|1/D_\sigma(s)|$.[30] For comparison, dotted and dashed-dot curves in Fig. 29 show for the same values of m_σ and Γ_σ the real and imaginary parts of the inverse propagator $D_\sigma(s)=m_\sigma^2-s-\mathrm{i}m_\sigma\Gamma_\sigma[(s-4m_{\pi^+}^2)/(m_\sigma^2-4m_{\pi^+}^2)]^{1/2}$ (taken with the minus sign) in which the correction for the finite width is absent [118].

A.2 $\gamma\gamma\to\pi^0\eta$

Polarization operators $\Pi^{ab}_{a_0}(s)$ ($ab=\pi\eta,\,K^+K^-,\,K^0\bar{K}^0,\,\pi\eta'$) of a_0 resonance introduced in Section 5 [see the paragraph with formulas (43) and (44)] have the following form for

[30] References to the papers in which corrections for the finite widths and analytic properties of the propagators for the real $f_0(980)$, $a_0(980)$, and σ(600) resonances were investigated are presented in Section 2. In connection with the $\gamma\gamma\to\pi^0\eta$ and $\gamma\gamma\to\pi\pi$ reactions, these corrections were discussed also in Refs [102, 105].

$s \geqslant m_{ab}^{(+)2}$ (where $m_{ab}^{(\pm)} = m_b \pm m_a$, $m_b \geqslant m_a$):

$$\Pi_{a_0}^{ab}(s) = \frac{g_{a_0\to ab}^2}{16\pi}\left[\frac{m_{ab}^{(+)}m_{ab}^{(-)}}{\pi s}\ln\frac{m_a}{m_b} + \rho_{ab}(s)\left(i - \frac{1}{\pi}\ln\frac{\sqrt{s-m_{ab}^{(-)2}}+\sqrt{s-m_{ab}^{(+)2}}}{\sqrt{s-m_{ab}^{(-)2}}-\sqrt{s-m_{ab}^{(+)2}}}\right)\right], \quad (71)$$

where

$$\rho_{ab}(s) = \frac{\sqrt{s-m_{ab}^{(+)2}}\sqrt{s-m_{ab}^{(-)2}}}{s};$$

for $m_{ab}^{(-)2} < s < m_{ab}^{(+)2}$:

$$\Pi_{a_0}^{ab}(s) = \frac{g_{a_0\to ab}^2}{16\pi}\left[\frac{m_{ab}^{(+)}m_{ab}^{(-)}}{\pi s}\ln\frac{m_a}{m_b} - \rho_{ab}(s)\left(1 - \frac{2}{\pi}\arctan\frac{\sqrt{m_{ab}^{(+)2}-s}}{\sqrt{s-m_{ab}^{(-)2}}}\right)\right], \quad (72)$$

where

$$\rho_{ab}(s) = \frac{\sqrt{m_{ab}^{(+)2}-s}\sqrt{s-m_{ab}^{(-)2}}}{s},$$

and for $s \leqslant m_{ab}^{(-)2}$:

$$\Pi_{a_0}^{ab}(s) = \frac{g_{a_0\to ab}^2}{16\pi}\left[\frac{m_{ab}^{(+)}m_{ab}^{(-)}}{\pi s}\ln\frac{m_a}{m_b} - \rho_{ab}(s)\,\frac{1}{\pi}\ln\frac{\sqrt{m_{ab}^{(+)2}-s}+\sqrt{m_{ab}^{(-)2}-s}}{\sqrt{m_{ab}^{(+)2}-s}-\sqrt{m_{ab}^{(-)2}-s}}\right], \quad (73)$$

where

$$\rho_{ab}(s) = \frac{\sqrt{m_{ab}^{(+)2}-s}\sqrt{m_{ab}^{(-)2}-s}}{s}.$$

The triangle loop integral in formula (36) takes the form

$$\tilde I_{\pi\eta}^{V}(s) = \frac{s}{\pi}\int_{(m_\pi+m_\eta)^2}^{\infty}\frac{\rho_{\pi\eta}(s')M_{00}^{\text{Born V}}(\gamma\gamma\to\pi^0\eta;s')}{s'(s'-s-i\varepsilon)}\,ds', \quad (74)$$

the Born S-wave amplitude

$$M_{00}^{\text{Born V}}(\gamma\gamma\to\pi^0\eta;s) = \frac{1}{2}\int_{-1}^{1}M_0^{\text{Born V}}(\gamma\gamma\to\pi^0\eta;s,\theta)\,d\cos\theta, \quad (75)$$

and $M_0^{\text{Born V}}(\gamma\gamma\to\pi^0\eta;s,\theta)$ is defined in formula (38). Functions $\tilde I_{\pi^0\eta'}^{V}(s)$ and $\tilde I_{K\bar K}^{K^*}(s)$ entering formula (36) are calculated in a similar way, while function $\tilde I_{K^+K^-}^{K^+}(s;x_2)$ is found from formula (92) in Appendix A.3.

For the background phase shifts, we utilized the simplest parametrizations quite satisfactorily in the physical region of the $\gamma\gamma\to\pi^0\eta$ reaction:

$$\exp\left(i\delta_{ab}^{bg}(s)\right) = \left(\frac{1+iF_{ab}(s)}{1-iF_{ab}(s)}\right)^{1/2}, \quad (76)$$

$$F_{\pi\eta}(s) = \frac{\sqrt{1-m_{\pi\eta}^{(+)2}/s}\left[c_0 + c_1(s-m_{\pi\eta}^{(+)2})\right]}{1+c_2(s-m_{\pi\eta}^{(+)2})^2}, \quad (77)$$

$$F_{K\bar K}(s) = \frac{f_{K\bar K}\sqrt{s}\left(\rho_{K^+K^-}(s)+\rho_{K^0\bar K^0}(s)\right)}{2}, \quad (78)$$

$$F_{\pi\eta'}(s) = f_{\pi\eta'}\sqrt{s-m_{\pi\eta'}^{(+)2}}. \quad (79)$$

The curves in Figs 25–27 correspond to the following model parameters:

$(m_{a_0}, g_{a_0\pi\eta}, g_{a_0K^+K^-}, g_{a_0\pi\eta'}) = (0.9845, 4.23, 3.79, -2.13)$ GeV;

$(m_{a_0'}, g_{a_0'\pi\eta}, g_{a_0'K^+K^-}, g_{a_0'\pi\eta'}) = (1.4,\ 3.3,\ 0.28,\ 2.91)$ GeV;

$(g_{a_0\gamma\gamma}, g_{a_0\gamma\gamma}) = (1.77, -11.5)\times 10^{-3}$ GeV^{-1};

$C_{a_0a_0'} = 0.06$ GeV^2, $c_0 = -0.603$,

$c_1 = -6.48$ GeV^{-2}, $c_2 = 0.121$ GeV^{-4};

$(f_{K\bar K}, f_{\pi\eta'}) = (-0.37,\ 0.28)$ GeV^{-1};

$(m_{a_2}, \Gamma_{a_2}^{\text{tot}}) = (1.322,\ 0.116)$ GeV;

$\Gamma_{a_2\to\gamma\gamma}^{(0)} = 1.053$ keV, $r_{a_2} = 1.9$ GeV^{-1}, $\theta_P = -24^\circ$

(see paper [109] for details).

A.3 $\gamma\gamma \to K\bar K$

Born amplitudes of the $\gamma\gamma\to K^+K^-$ reaction, determined by an elementary K exchange, $M_\lambda^{\text{Born K}^+}(s,\theta)$, and $M_{\lambda J}^{\text{Born K}^+}(s)$, result from the corresponding Born $\gamma\gamma\to\pi^+\pi^-$ amplitudes $M_\lambda^{\text{Born }\pi^+}(s,\theta)$ and $M_{\lambda J}^{\text{Born }\pi^+}(s)$ by the substitutions $m_{\pi^+}\to m_{K^+}$ and $\rho_{\pi^+}(s)\to\rho_{K^+}(s) = (1-4m_{K^+}^2/s)^{1/2}$ in formulas (48), (49), and (51)–(53); they have the following form

$$M_0^{\text{Born K}^+}(s,\theta) = \frac{4m_{K^+}^2}{s}\frac{8\pi\alpha}{1-\rho_{K^+}^2(s)\cos^2\theta}, \quad (80)$$

$$M_2^{\text{Born K}^+}(s,\theta) = \frac{8\pi\alpha\rho_{K^+}^2(s)\sin^2\theta}{1-\rho_{K^+}^2(s)\cos^2\theta}, \quad (81)$$

$$M_{00}^{\text{Born K}^+}(s) = 4\pi\alpha\,\frac{1-\rho_{K^+}^2(s)}{\rho_{K^+}(s)}\ln\frac{1+\rho_{K^+}(s)}{1-\rho_{K^+}(s)}, \quad (82)$$

$$M_{02}^{\text{Born K}^+}(s) = 4\pi\alpha\,\frac{1-\rho_{K^+}^2(s)}{\rho_{K^+}^2(s)}\left[\frac{3-\rho_{K^+}^2(s)}{2\rho_{K^+}(s)}\ln\frac{1+\rho_{K^+}(s)}{1-\rho_{K^+}(s)} - 3\right], \quad (83)$$

$$M_{22}^{\text{Born K}^+}(s) = 4\pi\alpha\sqrt{\frac{3}{2}}\left[\frac{\left(1-\rho_{K^+}^2(s)\right)^2}{2\rho_{K^+}^3(s)}\ln\frac{1+\rho_{K^+}(s)}{1-\rho_{K^+}(s)} - \frac{1}{\rho_{K^+}^2(s)} + \frac{5}{3}\right]. \quad (84)$$

Function $\tilde I_{K^+K^-}^{K^+}(s)$ is obtained from $\tilde I_{\pi^+\pi^-}^{\pi^+}(s)$ by the substitutions $m_{\pi^+}\to m_{K^+}$ and $\rho_{\pi^+}(s)\to\rho_{K^+}(s)$ in expressions (55) and (56); therefore, for $0 < s < 4m_{K^+}^2$, one finds

$$\tilde I_{K^+K^-}^{K^+}(s) = 8\alpha\left\{\frac{m_{K^+}^2}{s}\left[\pi - 2\arctan\left|\rho_{K^+}(s)\right|\right]^2 - 1\right\}, \quad (85)$$

and for $s \geqslant 4m_{K^+}^2$, the desired function is

$$\tilde I_{K^+K^-}^{K^+}(s) = 8\alpha\left\{\frac{m_{K^+}^2}{s}\left[\pi + i\ln\frac{1+\rho_{K^+}(s)}{1-\rho_{K^+}(s)}\right]^2 - 1\right\}. \quad (86)$$

Taking account of the form factor

$$G_{\mathrm{K}^+}(t,u)=\frac{1}{s}\left[\frac{m^2_{\mathrm{K}^+}-t}{1-(u-m^2_{\mathrm{K}^+})/x_2^2}+\frac{m^2_{\mathrm{K}^+}-u}{1-(t-m^2_{\mathrm{K}^+})/x_2^2}\right] \quad (87)$$

(here, $t=m^2_{\mathrm{K}^+}-s[1-\rho_{\mathrm{K}^+}(s)\cos\theta]/2$ and $u=m^2_{\mathrm{K}^+}-s[1+\rho_{\mathrm{K}^+}(s)\cos\theta]/2$), the partial $M_{\lambda J}^{\mathrm{Born}\,\mathrm{K}^+}(s)$ amplitudes are replaced by $M_{\lambda J}^{\mathrm{Born}\,\mathrm{K}^+}(s;x_2)$. Substituting $\rho_{\mathrm{K}^+}(s)$ and $\rho_{\mathrm{K}^+}(s;x_2)=\rho_{\mathrm{K}^+}(s)/(1+2x_2^2/s)$ instead of $\rho_{\pi^+}(s)$ and $\rho_{\pi^+}(s;x_1)$, respectively, into formulas (57)–(60), one obtains

$$M_{0J}^{\mathrm{Born}\,\mathrm{K}^+}(s)=\frac{1-\rho^2_{\mathrm{K}^+}(s)}{\rho_{\mathrm{K}^+}(s)}\,F_{0J}^{\mathrm{Born}\,\mathrm{K}^+}\bigl(\rho_{\mathrm{K}^+}(s)\bigr)\,, \quad (88)$$

$$M_{2J}^{\mathrm{Born}\,\mathrm{K}^+}(s)=\rho_{\mathrm{K}^+}(s)F_{2J}^{\mathrm{Born}\,\mathrm{K}^+}\bigl(\rho_{\mathrm{K}^+}(s)\bigr)\,, \quad (89)$$

$$M_{0J}^{\mathrm{Born}\,\mathrm{K}^+}(s;x_2)=\frac{1-\rho^2_{\mathrm{K}^+}(s)}{\rho_{\mathrm{K}^+}(s)}\Bigl[F_{0J}^{\mathrm{Born}\,\mathrm{K}^+}\bigl(\rho_{\mathrm{K}^+}(s)\bigr)-F_{0J}^{\mathrm{Born}\,\mathrm{K}^+}\bigl(\rho_{\mathrm{K}^+}(s;x_2)\bigr)\Bigr]\,, \quad (90)$$

$$M_{2J}^{\mathrm{Born}\,\mathrm{K}^+}(s;x_2)=\rho_{\mathrm{K}^+}(s)\Bigl[F_{2J}^{\mathrm{Born}\,\mathrm{K}^+}\bigl(\rho_{\mathrm{K}^+}(s)\bigr)-F_{2J}^{\mathrm{Born}\,\mathrm{K}^+}\bigl(\rho_{\mathrm{K}^+}(s;x_2)\bigr)\Bigr]\,. \quad (91)$$

Accordingly, taking into consideration the form factor, $\tilde{I}^{\mathrm{K}^+}_{\mathrm{K}^+\mathrm{K}^-}(s)$ is replaced by the function

$$\tilde{I}^{\mathrm{K}^+}_{\mathrm{K}^+\mathrm{K}^-}(s;x_2)=\frac{s}{\pi}\int_{4m^2_{\mathrm{K}^+}}^{\infty}\frac{\rho_{\mathrm{K}^+}(s')M_{00}^{\mathrm{Born}\,\mathrm{K}^+}(s';x_2)}{s'(s'-s-\mathrm{i}\varepsilon)}\,\mathrm{d}s'. \quad (92)$$

It should be noted that multiplication of the explicitly known function $|\tilde{I}^{\mathrm{K}^+}_{\mathrm{K}^+\mathrm{K}^-}(s)|^2$ [see formulas (85), (86), and Fig. 17] corresponding to the elementary one-kaon exchange by coefficient 0.68 gives a result for the $0.8<\sqrt{s}<1.2$ GeV region that coincides (with an accuracy higher than 3%) with the result of numerical calculation of function $|\tilde{I}^{\mathrm{K}^+}_{\mathrm{K}^+\mathrm{K}^-}(s;x_2)|^2$, taking account of the form factor at the value of $x_2=1.75$ GeV found from data fitting.

The S-wave amplitudes of the $\gamma\gamma\to\mathrm{K}^+\mathrm{K}^-$ and $\gamma\gamma\to\mathrm{K}^0\bar{\mathrm{K}}^0$ reactions used for the purpose of estimation in the $\mathrm{K}\bar{\mathrm{K}}$-threshold region have the form

$$M_{00}(\gamma\gamma\to\mathrm{K}^+\mathrm{K}^-;s)=M_{00}^{\mathrm{Born}\,\mathrm{K}^+}(s;x_2)+\tilde{I}^{\pi+}_{\pi^+\pi^-}(s;x_1)T_{\pi^+\pi^-\to\mathrm{K}^+\mathrm{K}^-}(s)+\tilde{I}^{\mathrm{K}^+}_{\mathrm{K}^+\mathrm{K}^-}(s;x_2)\times T_{\mathrm{K}^+\mathrm{K}^-\to\mathrm{K}^+\mathrm{K}^-}(s)+M^{\mathrm{direct}}_{\mathrm{res};+}(s)\,, \quad (93)$$

$$M_{00}(\gamma\gamma\to\mathrm{K}^0\bar{\mathrm{K}}^0;s)=\tilde{I}^{\pi+}_{\pi^+\pi^-}(s;x_1)\,T_{\pi^+\pi^-\to\mathrm{K}^0\bar{\mathrm{K}}^0}(s)+\tilde{I}^{\mathrm{K}^+}_{\mathrm{K}^+\mathrm{K}^-}(s;x_2)\,T_{\mathrm{K}^+\mathrm{K}^-\to\mathrm{K}^0\bar{\mathrm{K}}^0}(s)+M^{\mathrm{direct}}_{\mathrm{res};-}(s)\,. \quad (94)$$

The corresponding cross sections are as follows:

$$\sigma_{00}(\gamma\gamma\to\mathrm{K}^+\mathrm{K}^-)=\frac{\rho_{\mathrm{K}^+}(s)}{32\pi s}\bigl|M_{00}(\gamma\gamma\to\mathrm{K}^+\mathrm{K}^-;s)\bigr|^2\,, \quad (95)$$

$$\sigma_{00}(\gamma\gamma\to\mathrm{K}^0_{\mathrm{S}}\mathrm{K}^0_{\mathrm{S}})=\frac{\rho_{\mathrm{K}^0}(s)}{64\pi s}\bigl|M_{00}(\gamma\gamma\to\mathrm{K}^0\bar{\mathrm{K}}^0;s)\bigr|^2\,. \quad (96)$$

The amplitudes of $\pi\pi\to\mathrm{K}\bar{\mathrm{K}}$ reactions, $T_{\pi^+\pi^-\to\mathrm{K}^+\mathrm{K}^-}(s)=T_{\pi^+\pi^-\to\mathrm{K}^0\bar{\mathrm{K}}^0}(s)=T_{\mathrm{K}^+\mathrm{K}^-\to\pi^+\pi^-}(s)$, are defined by formulas (23), (26). The amplitudes of $\mathrm{K}^+\mathrm{K}^-\to\mathrm{K}^+\mathrm{K}^-$ and $\mathrm{K}^+\mathrm{K}^-\to\mathrm{K}^0\bar{\mathrm{K}}^0$ reactions take the form

$$T_{\mathrm{K}^+\mathrm{K}^-\to\mathrm{K}^+\mathrm{K}^-}(s)=\frac{t_0^0(s)+t_0^1(s)}{2}\,, \quad (97)$$

$$T_{\mathrm{K}^+\mathrm{K}^-\to\mathrm{K}^0\bar{\mathrm{K}}^0}(s)=\frac{t_0^0(s)-t_0^1(s)}{2}\,, \quad (98)$$

where $t_0^I(s)$ are the S-wave amplitudes of $\mathrm{K}\bar{\mathrm{K}}\to\mathrm{K}\bar{\mathrm{K}}$ reactions with isospin $I=0$ and 1:

$$t_0^0(s)=\frac{\exp\bigl(2\mathrm{i}\delta_{\mathrm{B}}^{\mathrm{K}\bar{\mathrm{K}}}(s)\bigr)-1}{2\mathrm{i}\rho_{\mathrm{K}^+}(s)}+\exp\bigl(2\mathrm{i}\delta_{\mathrm{B}}^{\mathrm{K}\bar{\mathrm{K}}}(s)\bigr)T^{\mathrm{K}\bar{\mathrm{K}}}_{\mathrm{res};0}(s)\,, \quad (99)$$

$$t_0^1(s)=\frac{\exp\bigl(2\mathrm{i}\delta_{\mathrm{K}\bar{\mathrm{K}}}^{\mathrm{bg}}(s)\bigr)-1}{2\mathrm{i}\rho_{\mathrm{K}^+}(s)}+\exp\bigl(2\mathrm{i}\delta_{\mathrm{K}\bar{\mathrm{K}}}^{\mathrm{bg}}(s)\bigr)T^{\mathrm{K}\bar{\mathrm{K}}}_{\mathrm{res};1}(s)\,, \quad (100)$$

where $\delta_{\mathrm{B}}^{\mathrm{K}\bar{\mathrm{K}}}(s)$ and $\delta_{\mathrm{K}\bar{\mathrm{K}}}^{\mathrm{bg}}(s)$ are the phases in the channels with $I=0$ and 1, respectively, and

$$T^{\mathrm{K}\bar{\mathrm{K}}}_{\mathrm{res};0}(s)=\frac{g_{\sigma\mathrm{K}^+\mathrm{K}^-}\bar{\Delta}^0_{\mathrm{f}_0}(s)+g_{\mathrm{f}_0\mathrm{K}^+\mathrm{K}^-}\bar{\Delta}^0_{\sigma}(s)}{8\pi\bigl[D_{\sigma}(s)D_{\mathrm{f}_0}(s)-\Pi^2_{\mathrm{f}_0\sigma}(s)\bigr]}\,, \quad (101)$$

$$T^{\mathrm{K}\bar{\mathrm{K}}}_{\mathrm{res};1}(s)=\frac{g_{\mathrm{a}_0\mathrm{K}^+\mathrm{K}^-}\bar{\Delta}^1_{\mathrm{a}_0'}(s)+g_{\mathrm{a}_0'\mathrm{K}^+\mathrm{K}^-}\bar{\Delta}^1_{\mathrm{a}_0}(s)}{8\pi\bigl[D_{\mathrm{a}_0}(s)D_{\mathrm{a}_0'}(s)-\Pi^2_{\mathrm{a}_0\mathrm{a}_0'}(s)\bigr]}\,, \quad (102)$$

where

$$\bar{\Delta}^0_{\mathrm{f}_0}(s)=D_{\mathrm{f}_0}(s)g_{\sigma\mathrm{K}^+\mathrm{K}^-}+\Pi_{\mathrm{f}_0\sigma}(s)g_{\mathrm{f}_0\mathrm{K}^+\mathrm{K}^-}\,,$$

$$\bar{\Delta}^0_{\sigma}(s)=D_{\sigma}(s)g_{\mathrm{f}_0\mathrm{K}^+\mathrm{K}^-}+\Pi_{\mathrm{f}_0\sigma}(s)g_{\sigma\mathrm{K}^+\mathrm{K}^-}\,,$$

$$\bar{\Delta}^1_{\mathrm{a}_0'}(s)=D_{\mathrm{a}_0'}(s)g_{\mathrm{a}_0\mathrm{K}^+\mathrm{K}^-}+\Pi_{\mathrm{a}_0\mathrm{a}_0'}(s)g_{\mathrm{a}_0'\mathrm{K}^+\mathrm{K}^-}\,,$$

$$\bar{\Delta}^1_{\mathrm{a}_0}(s)=D_{\mathrm{a}_0}(s)g_{\mathrm{a}_0'\mathrm{K}^+\mathrm{K}^-}+\Pi_{\mathrm{a}_0a_0'}(s)g_{\mathrm{a}_0\mathrm{K}^+\mathrm{K}^-}\,.$$

The amplitudes of direct resonance–photon transitions assume the form

$$M^{\mathrm{direct}}_{\mathrm{res};\pm}(s)=s\exp\bigl(\mathrm{i}\delta_{\mathrm{B}}^{\mathrm{K}\bar{\mathrm{K}}}(s)\bigr)\frac{g^{(0)}_{\sigma\gamma\gamma}\bar{\Delta}^0_{\mathrm{f}_0}(s)+g^{(0)}_{\mathrm{f}_0\gamma\gamma}\bar{\Delta}^0_{\sigma}(s)}{D_{\sigma}(s)D_{\mathrm{f}_0}(s)-\Pi^2_{\mathrm{f}_0\sigma}(s)}\pm s\exp\bigl(\mathrm{i}\delta_{\mathrm{K}\bar{\mathrm{K}}}^{\mathrm{bg}}(s)\bigr)\frac{g^{(0)}_{\mathrm{a}_0\gamma\gamma}\bar{\Delta}^1_{\mathrm{a}_0'}(s)+g^{(0)}_{\mathrm{a}_0'\gamma\gamma}\bar{\Delta}^1_{\mathrm{a}_0}(s)}{D_{\mathrm{a}_0}(s)D_{\mathrm{a}_0'}(s)-\Pi^2_{\mathrm{a}_0\mathrm{a}_0'}(s)}\,. \quad (103)$$

References

1. Achasov N N, Ivanchenko V N *Nucl. Phys. B* **315** 465 (1989)
2. Achasov N N, Gubin V V *Phys. Rev. D* **63** 094007 (2001)
3. Achasov N N, Gubin V V *Yad. Fiz.* **65** 1566 (2002) [*Phys. Atom. Nucl.* **65** 1528 (2002)]
4. Achasov N N *Nucl. Phys. A* **728** 425 (2003)
5. Achasov N N *Yad. Fiz.* **67** 1552 (2004) [*Phys. Atom. Nucl.* **67** 1529 (2004)]
6. Achasov N N, Shestakov G N *Phys. Rev. D* **49** 5779 (1994)
7. Achasov N N, Shestakov G N *Yad. Fiz.* **56** (9) 206 (1993) [*Phys. Atom. Nucl.* **56** 1270 (1993)]
8. Achasov N N, Shestakov G N *Int. J. Mod. Phys. A* **9** 3669 (1994)
9. Achasov N N, Shestakov G N *Phys. Rev. Lett.* **99** 072001 (2007)
10. Amsler C et al. (Particle Data Group) *Phys. Lett. B* **667** 1 (2008)
11. Nakamura K et al. (Particle Data Group) *J. Phys. G Nucl. Part. Phys.* **37** 075021 (2010)
12. Rosenfeld A H et al. (Particle Data Group) *Rev. Mod. Phys.* **37** 633 (1965)
13. Rosenfeld A H et al. (Particle Data Group) *Rev. Mod. Phys.* **39** 1 (1967)
14. Barash-Schmidt N et al. (Particle Data Group) *Rev. Mod. Phys.* **41** 109 (1969)
15. Gell-Mann M, Lévy M *Nuovo Cimento* **16** 705 (1960)

16. Gell-Mann M *Physics* **1** 63 (1964)
17. Lévy M *Nuovo Cimento A* **52** 23 (1967)
18. Rittenberg A et al. (Particle Data Group) *Rev. Mod. Phys.* **43** S1 (1971)
19. Lasinski T A et al. (Particle Data Group) *Rev. Mod. Phys.* **45** S1 (1973)
20. Jaffe R L *Phys. Rev. D* **15** 267, 281 (1977)
21. Sannino F, Schechter J *Phys. Rev. D* **52** 96 (1995)
22. Törnqvist N A *Z. Phys. C* **68** 647 (1995)
23. Ishida S et al. *Prog. Theor. Phys.* **95** 745 (1996)
24. Harada M, Sannino F, Schechter J *Phys. Rev. D* **54** 1991 (1996)
25. Ishida S *AIP Conf. Proc.* **432** 705 (1998)
26. Black D et al. *Phys. Rev. D* **58** 054012 (1998)
27. Black D et al. *Phys. Rev. D* **59** 074026 (1999)
28. Ishida M, in *Proc. of the Possible Existence of σ-Meson and Its Implication to Hadron Physics* (KEK Proc., 2000-4, Eds S Ishida et al.) (Tsukuba: KEK, 2000); *Soryushiron Kenkyu* **102** (5) E58 (2001); hep-ph/0012325
29. Barnett R M et al. (Particle Data Group) *Phys. Rev. D* **54** 1 (1996)
30. Eidelman S et al. (Particle Data Group) *Phys. Lett. B* **592** 1 (2004)
31. Spanier S, Törnqvist N A, Amsler C *Phys. Lett. B* **667** 594 (2008)
32. Amsler C et al. "Note on scalar mesons" *J. Phys. G Nucl. Part. Phys.* **37** 075021 (2010)
33. Montanet L *Rep. Prog. Phys.* **46** 337 (1983)
34. Achasov N N, Devyanin S A, Shestakov G N *Usp. Fiz. Nauk* **142** 361 (1984) [*Sov. Phys. Usp.* **27** 161 (1984)]
35. Achasov N N *Nucl. Phys. B Proc. Suppl.* **21** 189 (1991)
36. Achasov N N *Usp. Fiz. Nauk* **168** 1257 (1998) [*Phys. Usp.* **41** 1149 (1998)]
37. Achasov N N *Nucl. Phys. A* **675** 279 (2000)
38. Achasov N N *Yad. Fiz.* **65** 573 (2002) [*Phys. Atom. Nucl.* **65** 546 (2002)]
39. Achasov N N *AIP Conf. Proc.* **619** 112 (2002)
40. Achasov N N, in *Proc. of the Intern. Symp. on Hadron Spectroscopy, Chiral Symmetry and Relativistic Description of Bound Systems* (KEK Proc., 2003-7, Eds S Ishida et al.) (Tsukuba: KEK, 2003) p. 151
41. Achasov N N, in *Proc. of the KEK Workshop on Hadron Spectroscopy and Chiral Particle Search in J/Ψ Decay Data at BES* (KEK Proc., 2003-10, Eds K Takamatsu et al.) (Tsukuba: KEK) p. 66
42. Achasov N N, in *Proc. of the 13th Intern. Seminar on High Energy Physics*: *QUARKS'2004, Pushkinskie Gory, Russia, 24–30 May 2004* (Eds D G Levkov, V A Matveev, V A Rubakov) (Moscow: INR RAS, 2004) p. 110
43. Achasov N N *Phys. Part. Nucl.* **36** (Suppl. 2) 146 (2005); in *Proc. of the Intern. Bogoliubov Conf. "Problems of Theoretical and Mathematical Physics"* (Eds V G Kadyshevsky, A N Sissakian) (Dubna: JINR, 2004)
44. Achasov N N, in *Proc. of the 14th Intern. Seminar on High Energy Physics*: *QUARKS'2006, St. Petersburg, Russia, 19–25 May 2006* Vol. 1 (Eds S V Demidov et al.) (Moscow: INR RAS, 2007) p. 29
45. Achasov N N, in *Proc. of the 15th Intern. Seminar on High Energy Physics*: *QUARKS'2008, Sergiev Posad, Russia, 23–29 May 2008* Vol. 1 (Eds V A Duk, V A Matveev, V A Rubakov) (Moscow: INR RAS, 2010) p. 3; arXiv:0810.2601
46. Achasov N N *Nucl. Phys. B Proc. Suppl.* **186** 283 (2009)
47. Achasov N N *Fiz. Elem. Chastits At. Yadra* **41** 1663 (2010) [*Phys. Part. Nucl.* **41** 891 (2010)]; arXiv:1001.3468
48. Achasov N N, Shestakov G N *Usp. Fiz. Nauk* **161** (6) 53 (1991) [*Sov. Phys. Usp.* **34** 471 (1991)]
49. Achasov N N, Shestakov G N, in *Proc. of the Intern. Workshop on e^+e^- Collisions from ϕ to ψ* (Eds G V Fedotovich, S I Redin) (Novosibirsk: BINP, 2000) p. 294
50. Delbourgo R, Scadron M D *Int. J. Mod. Phys. A* **13** 657 (1998)
51. Godfrey S, Napolitano J *Rev. Mod. Phys.* **71** 1411 (1999)
52. Tuan S F *AIP Conf. Proc.* **619** 495 (2002)
53. Tuan S F, in *Proc. of the Intern. Symp. on Hadron Spectroscopy, Chiral Symmetry and Relativistic Description of Bound Systems* (KEK Proc., 2003-7, Eds S Ishida et al.) (Tsukuba: KEK, 2003) p. 319
54. Close F E, Törnqvist N A *J. Phys. G Nucl. Part. Phys.* **28** R249 (2002)
55. Alford M, Jaffe R L *AIP Conf. Proc.* **688** 208 (2003)
56. Jaffe R, Wilczek F *Phys. Rev. Lett.* **91** 232003 (2003)
57. Amsler C, Törnqvist N A *Phys. Rep.* **389** 61 (2004)
58. Maiani L et al. *Phys. Rev. Lett.* **93** 212002 (2004)
59. Jaffe R L *Phys. Rep.* **409** 1 (2005)
60. Jaffe R L *Prog. Theor. Phys. Suppl.* **168** 127 (2007)
61. Kalashnikova Yu S et al. *Eur. Phys. J. A* **24** 437 (2005)
62. Caprini I, Colangelo G, Leutwyler H *Phys. Rev. Lett.* **96** 132001 (2006)
63. Bugg D V *Eur. Phys. J. C* **47** 57 (2006)
64. Achasov N N, Kiselev A V, Shestakov G N *Nucl. Phys. B Proc. Suppl.* **162** 127 (2006)
65. Achasov N N, Kiselev A V, Shestakov G N *Nucl. Phys. B Proc. Suppl.* **181–182** 169 (2008)
66. Achasov N N, Shestakov G N *Chinese Phys. C* **34** 807 (2010)
67. Achasov N N, Shestakov G N, in *the 16th Intern. Seminar on High Energy Physics*: *QUARKS-2010, Kolomna, Russia, June 2010*
68. Fariborz A H, Jora R, Schechter J *Phys. Rev. D* **76** 014011 (2007)
69. Fariborz A H, Jora R, Schechter J *Phys. Rev. D* **77** 094004 (2008)
70. Fariborz A H, Jora R, Schechter J *Nucl. Phys. B Proc. Suppl.* **186** 298 (2009)
71. Fariborz A H, Jora R, Schechter J *Phys. Rev. D* **79** 074014 (2009)
72. Narison S *Phys. Rev. D* **73** 114024 (2006)
73. Narison S *Nucl. Phys. B Proc. Suppl.* **186** 306 (2009); arXiv:0811.0563
74. Törnqvist N A *Acta Phys. Polon. B* **38** 2831 (2007)
75. Klempt E, Zaitsev A *Phys. Rep.* **454** 1 (2007)
76. Maiani L, Polosa A D, Riquer V *Phys. Lett. B* **651** 129 (2007)
77. Pennington M *Prog. Theor. Phys. Suppl.* (168) 143 (2007)
78. Pennington M R, in *Proc. of the 11th Intern. Conf. on Meson-Nucleon Physics and the Structure of the Nucleon, Julich, Germany, 2007*, p. 106
79. van Beveren E, Rupp G, in *Proc. of the 11th Intern. Conf. on Meson-Nucleon Physics and the Structure of the Nucleon, September 10–14, 2007, Germany* (Eds H Machner, S Krewald) (Menlo Park, CA: SLAC, 2007) p. 130
80. Bystritsky Yu M et al. *Phys. Rev. D* **77** 054008 (2008)
81. Leutwyler H *AIP Conf. Proc.* **1030** 46 (2008)
82. 't Hooft G et al. *Phys. Lett. B* **662** 424 (2008)
83. Ivashyn S A, Korchin A Y *Eur. Phys. J. C* **54** 89 (2008)
84. Ebert D, Faustov R N, Galkin V O *Eur. Phys. J. C* **60** 273 (2009)
85. Achasov N N, Devyanin S A, Shestakov G N *Phys. Lett. B* **108** 134 (1982)
86. Achasov N N, Devyanin S A, Shestakov G N *Z. Phys. C* **16** 55 (1982)
87. Budnev V M et al. *Phys. Rep.* **15** 181 (1975)
88. Kolanoski H *Two-Photon Physics at e^+e^- Storage Rings* (Berlin: Springer-Verlag, 1984)
89. Mori T et al. (Belle Collab.), in *Proc. of the Intern. Symp. on Hadron Spectroscopy, Chiral Symmetry and Relativistic Description of Bound Systems* (KEK Proc., 2003-7, Eds S Ishida et al.) (Tsukuba: KEK, 2003) p. 159
90. Mori T et al. (Belle Collab.) *Phys. Rev. D* **75** 051101(R) (2007)
91. Mori T et al. (Belle Collab.) *J. Phys. Soc. Jpn.* **76** 074102 (2007)
92. Uehara S et al. (Belle Collab.) *Phys. Rev. D* **78** 052004 (2008)
93. Uehara S et al. (Belle Collab.) *Phys. Rev. D* **80** 032001 (2009)
94. Marsiske H et al. (Crystal Ball Collab.) *Phys. Rev. D* **41** 3324 (1990)
95. Boyer J et al. (MARK II Collab.) *Phys. Rev. D* **42** 1350 (1990)
96. Oest T et al. (JADE Collab.) *Z. Phys. C* **47** 343 (1990)
97. Behrend H-J et al. (CELLO Collab.) *Z. Phys. C* **56** 381 (1992)
98. Bienlein J K, in *Proc. of the 9th Intern. Workshop on Photon-Photon Collisions, La Jolla, CA, USA, 22–26 March 1992* (Eds D O Caldwell, H P Paar) (Singapore: World Scientific, 1992) p. 241
99. Barate R et al. (ALEPH Collab.) *Phys. Lett. B* **472** 189 (2000)
100. Braccini S *Acta Phys. Polon. B* **31** 2143 (2000)
101. Achasov N N, Devyanin S A, Shestakov G N *Z. Phys. C* **27** 99 (1985)
102. Achasov N N, Shestakov G N *Z. Phys. C* **41** 309 (1988)
103. Achasov N N, Shestakov G N *Yad. Fiz.* **55** 2999 (1992) [*Sov. J. Nucl. Phys.* **55** 1677 (1992)]
104. Achasov N N, Shestakov G N *Mod. Phys. Lett. A* **9** 1351 (1994)
105. Achasov N N, Shestakov G N *Phys. Rev. D* **72** 013006 (2005)
106. Achasov N N, Shestakov G N *Phys. Rev. D* **77** 074020 (2008)

107. Achasov N N, Shestakov G N *Pis'ma Zh. Eksp. Teor. Fiz.* **88** 345 (2008) [*JETP Lett.* **88** 295 (2008)]
108. Achasov N N, Shestakov G N *Pis'ma Zh. Eksp. Teor. Fiz.* **90** 355 (2009) [*JETP Lett.* **90** 313 (2009)]
109. Achasov N N, Shestakov G N *Phys. Rev. D* **81** 094029 (2010)
110. Achasov N N, Shestakov G N *Pis'ma Zh. Eksp. Teor. Fiz.* **92** 3 (2010) [*JETP Lett.* **92** 1 (2010)]
111. Flatté S M et al. *Phys. Lett. B* **38** 232 (1972)
112. Protopopescu S D et al. *Phys. Rev. D* **7** 1279 (1973)
113. Hyams B et al. *Nucl. Phys. B* **64** 134 (1973)
114. Grayer G et al. *Nucl. Phys. B* **75** 189 (1974)
115. Hyams B et al. *Nucl. Phys. B* **100** 205 (1975)
116. Gay J et al. *Phys. Lett. B* **63** 220 (1976)
117. Morgan D *Phys. Lett. B* **51** 71 (1974)
118. Flatté S M *Phys. Lett. B* **63** 224, 228 (1976)
119. Martin A D, Ozmutlu E N, Squires E J *Nucl. Phys. B* **121** 514 (1977)
120. Petersen J L "The $\pi\pi$ interaction", Yellow CERN Preprint 77-04 (Geneva: CERN, 1977)
121. Estabrooks P *Phys. Rev. D* **19** 2678 (1979)
122. Achasov N N, Devyanin S A, Shestakov G N *Phys. Lett. B* **88** 367 (1979)
123. Achasov N N, Devyanin S A, Shestakov G N *Yad. Fiz.* **33** 1337 (1981) [*Sov. J. Nucl. Phys.* **33** 715 (1981)]
124. Achasov N N, Shestakov G N *Phys. Rev. Lett.* **92** 182001 (2004)
125. Achasov N N, Shestakov G N *Phys. Rev. D* **70** 074015 (2004)
126. Wu J-J, Zhao Q, Zou B S *Phys. Rev. D* **75** 114012 (2007)
127. Wu J-J, Zou B S *Phys. Rev. D* **78** 074017 (2008)
128. Dorofeev V et al., in *Proc. of the 12th Intern. Conf. on Hadron Spectroscopy, Frascati, Italy, 8–13 October 2007* (Frascati Physics Series, Vol. 46, Eds L Benussi et al.) (Frascati, Italy: INFN, 2007); arXiv:0712.2512
129. Dorofeev V et al. *Eur. Phys. J. A* **38** 149 (2008)
130. Nikolaenko V et al. *Int. J. Mod. Phys. A* **24** 295 (2009)
131. Harris F *Int. J. Mod. Phys. A* **26** 347 (2011); arXiv:1008.3569
132. Achasov N N, Devyanin S A, Shestakov G N *Yad. Fiz.* **32** 1098 (1980) [*Sov. J. Nucl. Phys.* **32** 566 (1980)]
133. Achasov N N, Devyanin S A, Shestakov G N *Phys. Lett. B* **96** 168 (1980)
134. Achasov N N, Devyanin S A, Shestakov G N *Phys. Lett. B* **102** 196 (1981)
135. Achasov N N, Devyanin S A, Shestakov G N "On four-quark nature of scalar $S^*(980)$ and $\delta(980)$ resonances", Preprint TP-121 (Novosibirsk: Institute for Mathematics, 1981)
136. Achasov N N, Devyanin S A, Shestakov G N *Z. Phys. C* **22** 53 (1984)
137. Achasov M N et al. (SND Collab.) *Phys. Lett. B* **438** 441 (1998)
138. Achasov M N et al. (SND Collab.) *Phys. Lett. B* **440** 442 (1998)
139. Achasov M N et al. (SND Collab.) *Phys. Lett. B* **479** 53 (2000)
140. Achasov M N et al. (SND Collab.) *Phys. Lett. B* **485** 349 (2000)
141. Akhmetshin R R et al. (CMD-2 Collab.) *Phys. Lett. B* **462** 371 (1999)
142. Akhmetshin R R et al. (CMD-2 Collab.) *Phys. Lett. B* **462** 380 (1999)
143. Aloisio A et al. (KLOE Collab.) *Phys. Lett. B* **536** 209 (2002)
144. Aloisio A et al. (KLOE Collab.) *Phys. Lett. B* **537** 21 (2002)
145. Dubrovin M *AIP Conf. Proc.* **688** 231 (2003)
146. Ambrosino F et al. (KLOE Collab.) *Phys. Lett. B* **634** 148 (2006)
147. Ambrosino F et al. (KLOE Collab.) *Eur. Phys. J. C* **49** 473 (2007)
148. Ambrosino F et al. (KLOE Collab.), in *The 23rd Intern. Symp. on Lepton-Photon Interactions at High Energy, Daegu, Korea, 2007*; arXiv: 0707.4609
149. Bonvicini G et al. (CLEO Collab.) *Phys. Rev. D* **76** 012001 (2007)
150. Cavoto G, in *Proc. of the 5th Flavor Physics and CP Violation Conf., Bled, Slovenia, 2007*, p. 22; arXiv:0707.1242
151. Bossi F et al. (KLOE Collab.) *Riv. Nuovo Cimento* **031** 531 (2008); arXiv:0811.1929
152. Achasov N N, Kiselev A V *Phys. Rev. D* **70** 111901(R) (2004)
153. Bramon A, Grau A, Pancheri G *Phys. Lett. B* **289** 97 (1992)
154. Close F E, Isgur N, Kumano S *Nucl. Phys. B* **389** 513 (1993)
155. Lucio J L M, Napsuciale M *Phys. Lett. B* **331** 418 (1994)
156. Achasov N N, in *The Second DAΦNE Physics Handbook* Vol. 2 (Eds L Maiani, G Pancheri, N Paver) (Frascati: INFN, 1995) p. 671
157. Achasov N N, Gubin V V, Solodov E P *Phys. Rev. D* **55** 2672 (1997)
158. Achasov N N, Gubin V V, Solodov E P *Yad. Fiz.* **60** 1279 (1997) [*Phys. Atom. Nucl.* **60** 1152 (1997)]
159. Achasov N N, Gubin V V, Shevchenko V I *Phys. Rev. D* **56** 203 (1997)
160. Achasov N N, Gubin V V, Shevchenko V I *Int. J. Mod. Phys. A* **12** 5019 (1997)
161. Achasov N N, Gubin V V, Shevchenko V I *Yad. Fiz.* **60** 89 (1997) [*Phys. Atom. Nucl.* **60** 81 (1997)]
162. Achasov N N, Gubin V V *Phys. Rev. D* **56** 4084 (1997)
163. Achasov N N, Gubin V V *Yad. Fiz.* **61** 274 (1998) [*Phys. Atom. Nucl.* **61** 224 (1998)]
164. Achasov N N, Gubin V V *Phys. Rev. D* **57** 1987 (1998)
165. Achasov N N, Gubin V V *Yad. Fiz.* **61** 1473 (1998) [*Phys. Atom. Nucl.* **61** 1367 (1998)]
166. Ambrosino F et al. (KLOE Collab.) *Phys. Lett. B* **679** 10 (2009)
167. Ambrosino F et al. (KLOE Collab.) *Phys. Lett. B* **681** 5 (2009)
168. Bini C (and KLOE Collab.), in *The 34th Intern. Conf. on High Energy Physics*: *ICHEP 2008, July 29 – August 5, 2008, Philadelphia, Pennsylvania*; arXiv:0809.5004
169. Achasov N N, Kiselev A V *Phys. Rev. D* **68** 014006 (2003)
170. Achasov N N, Kiselev A V *Yad. Fiz.* **67** 653 (2004) [*Phys. Atom. Nucl.* **67** 633 (2004)]
171. Achasov N N, Kiselev A V *Phys. Rev. D* **73** 054029 (2006)
172. Achasov N N, Kiselev A V *Yad. Fiz.* **70** 2005 (2007) [*Phys. Atom. Nucl.* **70** 1956 (2007)]
173. Di Micco B (and KLOE Collab.) *Nucl. Phys. B Proc. Suppl.* **181–182** 215 (2008)
174. Shekhovtsova O, Venanzoni G, Pancheri G *Comput. Phys. Commun.* **180** 1206 (2009)
175. Amelino-Camelia G et al. *Eur. Phys. J. C* **68** 619 (2010); arXiv:1003.3868
176. Field J H, in *Proc. of the 4th Intern. Colloquium on Photon-Photon Interactions, Paris, France, 1981* (Ed. G W London) (Singapore: World Scientific, 1981) p. 447
177. Hilger E, in *Proc. of the 4th Intern. Colloquium on Photon-Photon Interactions, Paris, France, 1981* (Ed. G W London) (Singapore: World Scientific, 1981) p. 149
178. Wedemeyer R J, in *Proc. of the 10th Intern. Symp. on Lepton and Photon Interactions at High Energies* (Ed. W Pfeil) (Bonn: Physikalisches Institut, Univ. Bonn, 1981) p. 410
179. Edwards C et al. (Crystal Ball Collab.) *Phys. Lett. B* **110** 82 (1982)
180. Olsson J E *Lecture Notes Phys.* **191** 45 (1983)
181. Mennessier G *Z. Phys. C* **16** 241 (1983)
182. Kolanoski H, 1985, in *Proc. of the 12th Intern. Symp. on Lepton and Photon Interactions at High Energies* (Eds M Konuma, K Takahashi) (Kyoto: Kyoto Univ., Research Inst. Fund. Phys., 1986) p. 90
183. Kolanoski H, Zerwas P, in *High Energy Electron-Positron Physics* (Eds A Ali, P Söding) (Singapore: World Scientific, 1988) p. 695
184. Kolanoski H *Nucl. Phys. B Proc. Suppl.* **8** 41 (1989)
185. Cordier A, in *Proc. of the 6th Intern. Workshop on Photon-Photon Collisions, Granlibakken, Lake Tahoe, Calif., September 10–13, 1984* (Ed. R L Lander) (Singapore: World Scientific, 1985) p. 122
186. Erne F C, in *Proc. of the 6th Intern. Workshop on Photon-Photon Collisions, Granlibakken, Lake Tahoe, Calif., September 10–13, 1984* (Ed. R L Lander) (Singapore: World Scientific, 1985) p. 151
187. Barnes T *Phys. Lett. B* **165** 434 (1985)
188. Kaloshin A E, Serebryakov V V *Z. Phys. C* **32** 279 (1986)
189. Antreasyan D et al. *Phys. Rev. D* **33** 1847 (1986)
190. Johnson R P, Ph.D. Thesis (Stanford, Calif.: SLAC Stanford Univ., 1986); SLAC-Report-294 (Stanford, Calif.: SLAC Stanford Univ., 1986)
191. Poppe M *Int. J. Mod. Phys. A* **1** 545 (1986)
192. Berger Ch, Wagner W *Phys. Rep. C* **146** 1 (1987)
193. Morgan D, Pennington M R *Phys. Lett. B* **192** 207 (1987)
194. Morgan D, Pennington M R *Z. Phys. C* **37** 431 (1988)
195. Chanowitz M S, in *Proc. of the 8th Intern. Workshop on Photon-Photon Collisions, April 24–28, 1988, Jerusalem, Israel* (Ed. U Karshon) (Singapore: World Scientific, 1988) p. 205
196. Hikasa K et al. (Particle Data Group) *Phys. Rev. D* **45** S1 (1992)
197. Morgan D, Pennington M R, Whalley M R *J. Phys. G Nucl. Part. Phys.* **20** A1 (1994)

198. Barnes T, in *Proc. of the 9th Intern. Workshop on Photon-Photon Collisions, La Jolla, Calif., March 22–26, 1992* (Eds D O Caldwell, H P Paar) (Singapore: World Scientific, 1992) pp. 263, 275
199. Kolanoski H, in *Proc. of the 4th Intern. Conf. on Hadron Spectroscopy, Univ. of Maryland, College Park, 12–16 August 1991* (Eds S Oneda, D C Peaslee) (Singapore: World Scientific, 1992) p. 377
200. Karch K-H, in *Proc. of the 26th Rencontre de Moriond: High Energy Hadronic Interactions, Les Arcs, France, 17–23 March 1991* (Ed. J Tran Thanh Van) (Gif-sur-Yvette: Editions Frontieres, 1991) p. 423
201. Cahn R N, in *Proc. of the 14th Intern. Symp. on Lepton and Photon Interactions at High Energies, August 7–12, 1989, Stanford, Calif.* (Ed. M Riordan) (Singapore: World Scientific, 1990) p. 60
202. Feindt M, Harjes J *Nucl. Phys. B Proc. Suppl.* **21** 61 (1991)
203. Berger S B, Feld B T *Phys. Rev. D* **8** 3875 (1973)
204. Barbieri R, Gatto R, Kögerler R *Phys. Lett. B* **60** 183 (1976)
205. Jackson J D, in *Proc. of the SLAC Summer Institute on Particle Physics: Weak Interactions at High Energy and the Production of New Particles, Stanford, Calif., August 2–13, 1976* (SLAC Rep., No. 198, Ed. M C Zipf) (Stanford, Calif.: SLAC, 1976) p. 147
206. Budnev V M, Kaloshin A E *Phys. Lett. B* **86** 351 (1979)
207. Bergström L, Hulth G, Snellman H *Z. Phys. C* **16** 263 (1983)
208. Morgan D, Pennington M R *Z. Phys. C* **48** 623 (1990)
209. Li Z P, Close F E, Barnes T *Phys. Rev. D* **43** 2161 (1991)
210. Münz C R *Nucl. Phys. A* **609** 364 (1996)
211. Pennington M R *Mod. Phys. Lett. A* **22** 1439 (2007)
212. Weinstein J, Isgur N *Phys. Rev. Lett.* **48** 659 (1982)
213. Weinstein J, Isgur N *Phys. Rev. D* **41** 2236 (1990)
214. Achasov N N, Kiselev A V *Phys. Rev. D* **76** 077501 (2007)
215. Achasov N N, Kiselev A V *Phys. Rev. D* **78** 058502 (2008)
216. Dzierba A R, in *Proc. of the Second Workshop on Physics and Detectors for DAΦNE'95* Vol. 4 (Frascati Physics Series, Eds R Baldini et al.) (Frascati: INFN, 1996) p. 99
217. Alde D et al. *Z. Phys. C* **66** 375 (1995)
218. Alde D et al. *Eur. Phys. J. A* **3** 361 (1998)
219. Alde D et al. *Yad. Fiz.* **62** 462 (1999) [*Phys. Atom. Nucl.* **62** 421 (1999)]
220. Gunter J et al. (E852 Collab.) *Phys. Rev. D* **64** 072003 (2001)
221. Branz T, Gutsche T, Lyubovitskij V *Eur. Phys. J. A* **37** 303 (2007)
222. Boglione M, Pennington M R *Eur. Phys. J. C* **9** 11 (1999)
223. Pennington M R *Nucl. Phys. B Proc. Suppl.* **82** 291 (2000)
224. Groom D E et al. (Particle Data Group) *Eur. Phys. J. C* **15** 1 (2000)
225. Yao W-M et al. (Particle Data Group) *J. Phys. G Nucl. Part. Phys.* **33** 1 (2006)
226. Abe K et al. (Belle Collab.), arXiv:0711.1926
227. Nakazawa N *Nucl. Phys. B Proc. Suppl.* **181–182** 233 (2008)
228. Adachi I et al. (Belle Collab.), arXiv:0810.0334
229. Low F E *Phys. Rev.* **96** 1428 (1954)
230. Gell-Mann M, Goldberger M L *Phys. Rev.* **96** 1433 (1954)
231. Abarbanel H D I, Goldberger M L *Phys. Rev.* **165** 1594 (1968)
232. Lyth D H *J. Phys. G Nucl. Phys.* **10** 39 (1984)
233. Lyth D H *J. Phys. G Nucl. Phys.* **11** 459 (1985)
234. Bijnens J, Cornet F *Nucl. Phys. B* **296** 557 (1988)
235. Donoghue J F, Holstein B R, Lin Y C *Phys. Rev. D* **37** 2423 (1988)
236. Donoghue J F, Holstein B R *Phys. Rev. D* **48** 137 (1993)
237. Morgan D, Pennington M R *Phys. Lett. B* **272** 134 (1991)
238. Oller J A, Oset E *AIP Conf. Proc.* **432** 413 (1998)
239. Pennington M R *Phys. Rev. Lett.* **97** 011601 (2006)
240. Krammer M, Krasemann H *Phys. Lett. B* **73** 58 (1978)
241. Krammer M *Phys. Lett. B* **74** 361 (1978)
242. Krasemann H, Vermaseren J A M *Nucl. Phys. B* **184** 269 (1981)
243. Gersten A *Nucl. Phys. B* **12** 537 (1969)
244. Barrelet E *Nuovo Cimento A* **8** 331 (1972)
245. Sadovsky S A *Yad. Fiz.* **62** 562 (1999) [*Phys. Atom. Nucl.* **62** 519 (1999)]
246. Pennington M R *Nucl. Phys. B Proc. Suppl.* **181–182** 251 (2008)
247. Pennington M R et al. *Eur. Phys. J. C* **56** 1 (2008)
248. Mennessier G et al., arXiv:0707.4511
249. Mennessier G, Narison S, Ochs W *Phys. Lett. B* **665** 205 (2008)
250. Mennessier G, Narison S, Ochs W *Nucl. Phys. B Proc. Suppl.* **181–182** 238 (2008)
251. Mennessier G *Nucl. Phys. B Proc. Suppl.* **186** 287 (2009); arXiv:0811.1589
252. Oller J A, Roca L, Schat C *Phys. Lett. B* **659** 201 (2008)
253. Oller J A, Roca L *Eur. Phys. J. A* **37** 15 (2008)
254. van Beveren E et al. *Phys. Rev. D* **79** 098501 (2009)
255. Kalinovsky Yu L, Volkov M K, arXiv:0809.1795
256. Mao Y at al. *Phys. Rev. D* **79** 116008 (2009)
257. Mennessier G, Narison S, Wang X-G *Phys. Lett. B* **696** 40 (2011); arXiv:1009.2773
258. Garsía-Martín R, Moussallam B *Eur. Phys. J. C* **70** 155 (2010)
259. Adler S L *Phys. Rev.* **177** 2426 (1969)
260. Bell J S, Jackiw R *Nuovo Cimento A* **60** 47 (1969)
261. Bardeen W A, Fritzsch H, Gell-Mann M, in *Proc. of the Meeting on Scale and Conformal Symmetry in Hadron Physics* (Ed. R Gatto) (New York: Wiley, 1973) p. 139; hep-ph/0211388
262. Leutwyler H *Nucl. Phys. B Proc. Suppl.* **64** 223 (1998)
263. Ioffe B L, Oganesian A G *Phys. Lett. B* **647** 389 (2007)
264. Bernstein A M, arXiv:0707.4250
265. Feldmann T *Int. J. Mod. Phys. A* **15** 159 (2000)
266. Babcock J, Rosner J L *Phys. Rev. D* **14** 1286 (1976)
267. Rosner J L *Phys. Rev. D* **23** 1127 (1981)
268. Berger Ch *Lecture Notes Phys.* **134** 82 (1980)
269. Albrecht H et al. (ARGUS Collab.) *Z. Phys. C* **48** 183 (1990)
270. Li D M, Yu H, Shen Q-X *J. Phys. G Nucl. Part. Phys.* **27** 807 (2001)
271. Durusoy N B et al. *Phys. Lett. B* **45** 517 (1973)
272. Hoogland W et al. *Nucl. Phys. B* **126** 109 (1977)
273. Watson K M *Phys. Rev.* **88** 1163 (1952)
274. Achasov N N, Shestakov G N *Phys. Rev. D* **67** 114018 (2003)
275. Achasov N N, Shestakov G N *Phys. Rev. D* **58** 054011 (1998)
276. Osborn H *Nucl. Phys. B* **15** 501 (1970)
277. Petersen J L *Phys. Rep.* **2** 155 (1971)
278. Bernard V, Kaiser N, Meissner U-G *Phys. Rev. D* **44** 3698 (1991)
279. Black D, Fariborz A H, Schechter J *Phys. Rev. D* **61** 074030 (2000)
280. Achasov N N, Shestakov G N *Phys. Rev. D* **53** 3559 (1996)
281. Ochs W *AIP Conf. Proc.* **1257** 252 (2010)
282. Kalashnikova Yu et al. *Phys. Rev. C* **73** 45203 (2006)
283. Hanhart C et al. *Phys. Rev. D* **75** 074015 (2007)
284. Czerwiński E (and KLOE-2 Collab.) *Nucl. Phys. B Proc. Suppl.* **207–208** 137 (2010); arXiv:1009.0113
285. Uehara S et al. (and Belle Collab.) *Phys. Rev. D* **82** 114031 (2010); arXiv:1007.3779
286. Althoff M et al. (TASSO Collab.) *Z. Phys. C* **29** 189 (1985)
287. Althoff M et al. (TASSO Collab.) *Phys. Lett. B* **121** 216 (1983)
288. Berger Ch et al. (PLUTO Collab.) *Z. Phys. C* **37** 329 (1988)
289. Behrend H J et al. (CELLO Collab.) *Z. Phys. C* **43** 91 (1989)
290. Acciarri M et al. (L3 Collab.) *Phys. Lett. B* **501** 173 (2001)
291. Abe K et al. (Belle Collab.) *Eur. Phys. J. C* **32** 323 (2004)
292. Faiman D, Lipkin H J, Rubinstein H R *Phys. Lett. B* **59** 269 (1975)
293. Achard P et al. (L3 Collab.) *Phys. Lett. B* **568** 11 (2003)
294. Achard P et al. (L3 Collab.) *Phys. Lett. B* **597** 26 (2004)
295. Achard P et al. (L3 Collab.) *Phys. Lett. B* **604** 48 (2004)
296. Achard P et al. (L3 Collab.) *Phys. Lett. B* **615** 19 (2005)